DISSERTATION

CHOLINERGIC SYNAPTIC HOMEOSTASIS IS REGULATED BY DROSOPHILA α7 NICOTINIC ACETYLCHOLINE RECEPTORS AND Kv4 POTASSIUM CHANNELS

Submitted by

Abdunaser Omar Eadaim

Department of Biomedical Sciences

In partial fulfillment of the requirements

For the Degree of Doctor of Philosophy

Colorado State University

Fort Collins, Colorado

Spring 2021

Doctoral Committee:

Advisor: Susan Tsunoda

Michael Tamkun
Gregory Amberg
Gerrit Bouma
Colin Clay
Jennifer DeLuca

ABSTRACT

CHOLINERGIC SYNAPTIC HOMEOSTASIS IS REGULATED BY DROSOPHILA α7 NICOTINIC ACETYLCHOLINE RECEPTORS AND Kv4 POTASSIUM CHANNELS

Homeostatic synaptic plasticity (HSP) is an important mechanism that stabilizes neural activity during changes that occur during development and learning and memory formation, and some pathological conditions. HSP in cholinergic neurons has been implicated in pathological conditions, such as Alzheimer's disease and nicotine addiction. In a previous study in primary *Drosophila* neuron culture, cholinergic activity was blocked using pharmacological tools and this induced a homeostatic response that was mediated by an increase in the Drosophila α7 (Dα7) nAChR, which was subsequently tuned by an increase in the voltage-dependent potassium channel, Kv4/Shal. In this study, we inhibit cholinergic activity in live flies using temperature-sensitive mutant alleles of the choline acetyltransferase gene (Cha^{ts2} mutants). We show that this *in vivo* activity inhibition induces HSP similarly mediated by Dα7 nAChRs followed by an up-regulation of Kv4/Shal. We show that the up-regulation of Dα7 nAChRs alone is sufficient to induce an increase in Kv4/Shal protein, as well as mRNA. Finally, we test the involvement of transcription factors, dCREB2 and nuclear factor of activated T cells (NFAT) in the up-regulation of *Kv4/Shal*. In particular, we find that NFAT is required for the inactivity-induced up-regulation of Kv4/Shal channels. Our studies reveal a novel receptor-ion channel system transcriptionally coupled to prevent over-excitation.

TABLE OF CONTENTS

ABSTRACT ii

CHAPTER 1. INTRODUCTION 1

1. Homeostatic Synaptic Plasticity (HSP) at Mammalian Glutamatergic Synapses 1

1.1 Functions of HSP 1

1.2 Implication of HSP in human disease 3

1.3 Pathways of HSP 7

1.3.1 Homeostatic Intrinsic plasticity 7

1.3.2 Secreted and Cell Adhesion Molecules 9

1.3.3 Presynaptic expression of homeostatic synaptic plasticity 12

1.3.4 Postsynaptic expression of homeostatic synaptic plasticity 12

2. Regulation of HSP at the *Drosophila* Neuromuscular Junction (NMJ) 14

3. Nicotinic Acetylcholine Receptors (nAChRs) 16

4. Cholinergic HSP 18

5. Temperature sensitive Choline acetyltransferase mutants (*Cha*^{ts}) as a tool to inhibit cholinergic activity 20

6. NACHO and nAChRs Biogenesis 23

7. Transcriptional Programming in Synaptic Homeostasis 26

7.1 Nuclear Factor of Activated T-cells (NFAT) 27

8. Overview of This Dissertation 33

CHAPTER 2. MATERIALS AND METHODS 36

1- Fly Stocks 36

2. Heat-Treatment/Shock Protocols 36

3. Immunoblotting 37
3.1 Sample Preparation 37
3.2 Workflow 37
3.3 Data collection and analysis 39
4. RNA Extraction 39
4.1 Sample collection and storage 39
4.2 Workflow (integrity and purity) 39
5. Reverse Transcription 40
6. Quantitative Polymerase Chain Reaction (qPCR) 41
6.1 Primer and Probe design (specificity, sensitivity and efficiency) 41
6.2 Sample preparation and workflow 42
6.3 Data collection and analysis 44
7. Digital Droplet Polymerase Chain Reaction (ddPCR) 44
7.1 Identifying proper starting material concentration 45
7.2 Sample preparation and workflow 45
7.3 Data collection and analysis 46
CHAPTER 3. CHOLINERGIC HOMEOSTATIC SYNAPTIC PLASTICITY 47
3.1 Overview 47
3.2 *Cha*^{ts2}-induced inactivity up-regulates Dα7-nAChRs (Homeostatic response) 48
3.3 *Drosophila* NACHO (dNACHO) Up-regulates Dα7 expression 51
3.4 Dα7-EGFP up-regulation has no affect on dNACHO protein level 52
3.5 *Cha*^{ts2}-induced inactivity up-regulates dNACHO-HA protein level 53
3.6 Conclusion 54

CHAPTER 4. REGULATION OF HSP BY Kv4/Shal CHANNELS 55

4.1 Overview 55

4.2 Cholinergic activity blockade increases Kv4/Shal protein and mRNA levels 56

4.3 Cholinergic activity blockade using tetanus toxin induces Kv4/Shal Protein and mRNA up-regulation 58

4.4 Kv4/Shal protein and mRNA Up-Regulation depends on Dα7-nAChRs 62

4.5 Over-expression of Dα7-EGFP and/or dNACHO-HA results in Shal/Kv4 protein and mRNA Up-Regulation 64

4.6 RNAi knockdown of *dNACHO* block the *Cha^{ts2}*-induced increase in Kv4/Shal protein 69

4.7 Conclusion 70

CHAPTER 5. CA^{+2}-DEPENDENT TRANSCRIPTIONAL ACTIVATORS, INCLUDING DNFAT AND DCREB-2, ARE INVOLVED IN KV4/SHAL UP-REGULATION IN RESPONSE TO *CHA^{TS2}*-ACTIVITY INHIBITION 72

5.1 Overview 72

5.2 *Cha^{ts2}*-Induced Inactivity, or Over-Expression of Dα7, Activates the dNFAT-Based CaLexA Reporter 72

5.3 dNFAT is required for inactivity-induced up-regulation of Kv4/Shal 75

5.4 dCREB2-a over-expression up-regulates Kv4/Shal protein and mRNA 78

5.5 Conclusion 82

CHAPTER 6. DISCUSSION 84

6.1 Overview 84

6.2 Cholinergic activity inhibition induces a homeostatic response and Kv4/Shal protein and mRNA up-regulation 85

6.2.2 *Cha*^{ts2}- induced activity inhibition induces regulatory mechanism 88

6.2.3 *Cha*^{ts2}- induced activity inhibition induces Dα7 chaperon protein up-regulation 89

6.3 Over-expression of Dα7 nAChRs alone is sufficient to up-regulate Kv4/Shal protein and mRNA 90

6.4 dNFAT and dCREB2 are implicated in Kv4/Shal up-regulation 91

6.5 Conclusion 94

REFERENCES 97

LIST OF TABLES

Table 1. Primary and secondary antibodies concentration against different proteins (Kv4, GFP and HA) and their loading controls (Actin and Syntaxin) 38

Table 2. Forward and reverse primers, amplicon size and corresponding probes for *Kv4* and two reference genes (*RpS0A* and *eIF1A*) 42

LIST OF FIGURES

Figure 1. Log of dilution factors plotted against Ct values and slopes were used to estimate primer efficiency 43

Figure 2. Inhibition of Cholinergic Activity in *Cha^{ts2}*/+ Neurons Induces a Homeostatic Increase in Dα7 Protein 50

Figure 3. dNACHO positively regulated Dα7-EGFP 52

Figure 4. Dα7-EGFP over-expression does not affect dNACHO-HA protein level 53

Figure 5.*Cha^{ts2}*-Induced Inactivity Induces dNACHO-HA Up-Regulation 54

Figure 6. Blocking Neural Activity *In Vivo* Results in an Up-Regulation of Kv4/Shal Protein 58

Figure 7. Blocking Neural/Cholinergic Activity Using Pan-neural Driver, *elav-Gal4*, to Drive Tetanus Toxin Expression Up-Regulates Kv4/Shal Protein/mRNA 60

Figure 8. Blocking Neural/Cholinergic Activity Using *Chat* Driver, *Chat-Gal4*, to Drive Tetanus Toxin Expression Up-Regulates Kv4/Shal Protein/mRNA 61

Figure 9. Kv4/Shal protein and mRNA up-Regulation in response to *Cha^{ts2}*-Induced inactivity requires Dα7 nAChRs 63

Figure 10. Constitutive expression of Dα7-EGFP has no effect on Kv4/Shal protein 65

Figure 11. Effect of Dα7-EGFP Over-Expression expression on Kv4/Shal protein 66

Figure12. Over-expression Dα7 alone is sufficient to up-Regulate Kv4/Shal Protein/mRNA 68

Figure 13. *dNACHO* knockdown inhibits Kv4/Shal protein up-regulation in response to *Cha^{ts2}*-Induced inactivity 70

Figure 14. *In vivo* Activity Inhibition, or Dα7 Over-Expression, Activates the NFAT-Based CaLexA Reporter 75

Figure 15. dNFAT does not affect basal levels of Kv4/Shal protein and mRNA levels 76

Figure 16. dNFAT is Required for the *Cha^{ts2}*-induced Increase in Kv4/Shal Protein and mRNA 77

Figure 17. dNFAT Over-Expression Does Not Affect Kv4/Shal protein levels 79

Figure 18. *dCREB-2a* is involved in Kv4/Shal Protein and mRNA up-regulation 82

Figure 19. Working model of homeostatic synaptic plasticity and regulatory mechanism in response to *Cha*^{ts2}**-** induced activity inhibition 96

CHAPTER 1: INTRODUCTION

1. Homeostatic Synaptic Plasticity (HSP) at Mammalian Glutamatergic Synapses

1.1 Functions of HSP

Neurons are capable of changing and adapting their connections in response to perturbations of signaling. Although neurons are exposed to stress or activity perturbation, they are capable of maintaining their structure and function throughout the life of the organism/animal (1,2). Maintaining neural activity within an optimal range is thought to be essential for the nervous system to counter stress or changes in activity (1,3–5). The mechanisms that maintain neural network activity at a desirable set point underlie what is called homeostatic synaptic plasticity (HSP) (4,5). HSP has been suggested to play a neuroprotective role during times of activity change, such as development, learning, memory formation, and neuropathological conditions that alter neural activity, like Alzheimer disease and nicotine addiction (6). Generally, homeostatic synaptic plasticity (HSP) is a negative feedback mechanism to neutralize perturbations of network synaptic signaling, preventing over- or under activity of neural circuits (7–9). Multiple studies have documented that HSP induces presynaptic and postsynaptic compensatory changes to avoid over-excitation (10,11).

Neural circuits experience different types of perturbations that lead to activity change. Extensively studied forms of such activity-dependent changes in synaptic strength are Hebbian plasticity, which include long-term potentiation (LTP) and long-term depression (LTD) (12). LTP is a rapid change in individual synaptic activity in an excitation specific manner that is thought to underlie learning and memory formation mechanisms

(13–16). LTP is a positive feedback mechanism and can reduce a threshold set point to drive further rounds of potentiation. To avoid an epileptogenic state, neurons deploy homeostatic mechanisms to monitor and counteract over-excitation (17,18), and maintain synaptic strength in an optimal range that might enable the storage of information (3,9). An important hallmark feature of the interaction between Hebbian plasticity and HSP is that the first happens in a synapse specific manner in short time course, but sometimes HSP occurs cell-wide and extended for days (19–22).

Despite the distinct functionality of Hebbian plasticity and HSP, the targeted biological parameters that would be adjusted are the same, neural excitability (23,24), synaptic strength (25–27) and change in the number of synaptic contacts (28,29). Notably, neurons can discriminate between Hebbian and non-Hebbian plasticity when they take place at the same time and maintain the overall synaptic strength (10) . Rabinowitch and Segev (2006 and 2008) (30,31) proposed that when specific synapses in a specific dendritic branch are experiencing LTP, the synaptic strength of neighboring synapses weaken, thereby maintaining the overall branch synaptic strength.

The major challenge that faces HSP is maintaining an excitatory- inhibitory balance. Altogether, when excitatory inputs are up-regulated, inhibitory synaptic inputs are required to prevent network over-excitation (32). When intact hippocampi were treated with tetrodotoxin (TTX) to block action potentials, electrophysiological studies found that excitatory inputs were up-regulated, and accompanied by an increase in frequency and amplitude of inhibitory spontaneous currents (33). On the other hand, after blocking glutamatergic receptors, C3 regions of hippocampal slice cultures displayed no

change in the level of the gamma-aminobutyric acid (GABA)-synthetic enzyme glutamate decarboxylase isoform,GAD65, and GABAA receptor α1 subunits (34).

Interestingly, excitation-inhibition balance is developmentally regulated (33,35). For instance, TTX treated hippocampal slices showed an increase in **m**iniature **E**xcitatory **P**ost **S**ynaptic **C**urrent (mEPSC) amplitudes in young animals only, and an increase in mEPSC frequency in both adult and young animals. Moreover, TTX treatment showed an increase in **m**iniature **I**nhibitory **P**ost **S**ynaptic **C**urrent (mIPSC) amplitude in both young and adult animals, but an mIPSC frequency increase was reported in adult animals only (35), suggesting that the balance between excitatory and inhibitory inputs to homeostatic modulation has different responses during development (33,35).

1.2 Implication of HSP in human disease

Multiple studies indicate that alteration in HSP contributes to the pathogenesis of neurological and neuropsychiatric disorders. Homeostatic signaling perturbations have been embroiled in intellectual disability and autism spectrum disorders (36–38) , Epilepsy (39), Schizophrenia (40) and in neurodegenerative disorders such as Alzheimer's disease (41,42) and nicotinic addiction (43–45).

Rett Syndrome is the most widely hereditarily caused form of intellectual disability in females, and it is caused by mutations in the gene encoding the transcription repressor, methylated CpG binding protein 2, MeCP2, which binds to the promoter of target gene and inhibits transcription. Chronic inhibition of GABA receptors in hippocampal cultures triggers synaptic down-regulation and results in an increase in MeCP2, which represses GluA2 expression (37). Inhibition or genetic deletion of MeCP2 prevents synaptic down

regulation (37), indicating that MeCP2 mediates this pathway. Another study showed that MeCP2 plays a critical role in synaptic up-regulation in response to neural activity blockade of neocortical neuron (38). It is interesting that another study has reported lack of up-regulation of synaptic strength in response to visual deprivation *in vivo* in a mouse model of Rett syndrome (38). These studies strongly indicate that perturbation of HSP may be responsible for some of the neurological defects in Rett syndrome.

Fragile-X syndrome is a neuropsychiatric disorder distinguished by developmental abnormalities including intellectual disability, features of autism spectrum disorders such as disabilities in communication and social interaction, and in some cases seizures (46). This genetic condition is caused by a mutation in the Fmr1 gene, which encodes Fragile X mental retardation protein (FMRP), an RNA-binding protein that regulates dendritic protein synthesis. It is interesting that FMRP plays a pivotal role in homeostatic plasticity by increasing synaptic strength induced by RA (36). FMRP is necessary for HSP that is mediated by retinoic acid (RA) and it is required for dendritic protein synthesis (47). In addition, FMRP plays a critical role in RA-dependent synaptic homeostasis and RA-dependent GluA1 local translation (36). In the absence of FMRP or RA, activity blockade with TTX in hippocampal neurons fails to up-regulate synaptic strength or initiate translation of dendritic synaptic proteins (36). These observations suggest that some of the symptoms related to fragile-X syndrome may also be a consequence of homeostatic plasticity perturbation.

Mechanisms that function to balance between excitation and inhibition in the brain are necessary to prevent epilepsy, and defects in these mechanisms may lead to epileptogenic activity (11). Activity change in inhibitory neurons plays an important role in

homeostatic responses to avoid short-term increases in neural activity that may be connected to some pathological conditions, such as seizures (48). The neocortex, part of the cerebral cortex, which maintains firing activity, has been found to be involved in homeostatic plasticity (39). Simulation studies have predicted that prolonged isolation of the neocortex results in burst discharges that are similar to epileptic burst discharges reported in experimental studies of traumatic brain injury *in vivo* (39). It is interesting that epileptic seizure after traumatic brain injury is age-dependent, with elderly people more susceptible to epileptogenic attack than younger people (49). In addition, HSP regulation in response to brain injury is age-dependent, possibly explaining the severity of epileptic seizure in adults after traumatic brain injury as shown in studies examining the properties of traumatic brain injury -induced epileptogenesis (50).

One hallmark of advanced stages of Alzheimer's disease (AD) is the presence of amyloid plaques with an accumulation of amyloid β (Aβ), which is produced by cleavage of the amyloid precursor protein by β- and Ɣ- secretase. In the familial form of AD, mutations in presenilin-1, the catalytic subunit of Ɣ-secretases, have been documented. Hippocampal neuronal cultures derived from *psen1*$^{-/-}$ mice or neurons expressing the *presenilin-1* mutation (*Psen1*^{M146v}) exhibit impairment in synaptic plasticity (42). Another study characterized the impairment of HSP in hippocampal neurons from *Psen1*^{M146V} animals and showed an increase in calcineurin phosphatase activity that diminishes GluA1 Ser845 phosphorylation, which reduces trafficking and recruitment of AMPA receptors to postsynaptic membrane in these neurons (41).

Recently, the Tsunoda lab used direct application of Aβ40/ Aβ42 and a transgenic *Drosophila* line that expresses a secreted form of the human Aβ42 peptide as a model to

examine the effects of Aβ42 on cholinergic synaptic activity. The study showed that expression of Aβ42 resulted in an early increase in cholinergic activity followed by later synaptic inhibition. The early synaptic activity up-regulation is mediated by Dα7 nAChRs, and the later down-regulation of synaptic strength was dependent on a Dα7-mediated HSP mechanism induced by earlier hyper-activity. This study suggests that early Aβ-induced increases in activity trigger endogenous HSP mechanisms that generate the synaptic inhibition associated with cognitive/motor dysfunction (6).

Multiple studies in the literature suggest that other diseases also induce a homeostatic response to balance out the perturbed activity induced by these diseases. For example, Myasthenia gravis is an autoimmune disease initiated by production of auto-antibodies against acetylcholine receptor at the neuromuscular junction (NMJ), results in muscle fatigue and weakness. Human myasthenia gravis patients show an increase in acetylcholine release at the NMJ (51,52), which has been suggested to be a response to disease symptoms. Myasthenia gravis symptoms were induced in mouse after prolonged exposure to α- Bungarotoxin, an acetylcholine receptor antagonist (51), and resulted in an up-regulation of acetylcholine release. These findings suggest that myasthenia gravis induces adaptive HSP to compensate for reduced activity in muscle cells.

Huntington's disease (HD) is another example of a disease that induces HSP. HD is a neurodegenerative disease caused by mutations that result in an increase in CAG repeats (glutamate codon) in the gene encoding huntingtin protein that result in an increase in huntingtin protein levels. HD is characterized by early severe atrophy in the striatum and it is associated with death of medium spiny neurons (MSN) (53). Studies have showed that the density of dendritic spines in a HD transgenic model is decreased

compared to age-matched animal controls. However, intrinsic excitability and AMPA receptors that mediate synaptic transmission in MSN are up-regulated (53), suggesting that these changes are a compensatory response in MSN that modulate HD symptoms.

1.3 Pathways of HSP

Multiple studies have suggested that compensatory changes happen in intrinsic electrical prosperities, pre- and postsynaptic compartments of individual neuron in response to activity perturbation (10,11).

1.3.1 Homeostatic Intrinsic plasticity

Regulation of intrinsic excitability is well-documented in invertebrate and vertebrate neurons (54–57). Multiple studies have found that neurons can adjust their properties in response to their own activity (56). When a specific ion channel is knocked down or deleted or when pharmacological blocker is applied, the neurons can tune themselves and compensate for missed channel activity by expression of another mix of ion channels (58). Neural activity or excitability is associated with changes in intracellular Ca^{+2} (59,60), so that when neural activity is increased, associated intracellular Ca^{+2} is required to induce outward K^+ currents (61). When activity of cortical neurons was blocked by TTX treatment and after washing out the blocker, neural excitation was increased due to an increase Na^+ current density and a decrease in K^+ current densities (62,63), suggesting that neurons are able to monitor their activity and adjust their ion channel conductances to restore pre-perturbation activity (56). Interestingly, this intrinsic plasticity can strengthen synaptic plasticity via local changes in dendritic excitability or reduced

homeostatic response through increase threshold of firing rate to control spike generation (64–66).

Over-expression studies have supported the implication of compensatory mechanisms in the regulation of intrinsic neural excitability. When *Kv4/Shal* mRNA was delivered into pyloric dilator neurons of the lobster somatogastric ganglion (67,68), this resulted in a great increase in the A-type transient K^+ current (I_A), but no change in neural excitability because the increase in I_A was modulated by an increase in hyperpolarization current (I_h). These findings demonstrated that homeostatic mechanisms will adjust values of membrane conductances to maintain overall neural activity (69). In *Drosophila*, two A-type potassium channel genes, *Kv4/shal* and *Kv1/shaker*, are reciprocally transcriptionally coupled to maintain A-type channel expression (70). When *Kv4/Shal* gene is mutated in motorneuron of *Drosophila* larvae, *Kv1/Shaker* expression was up-regulated and *Kv1/Shaker* gene is mutated in motorneuron of *Drosophila* larvae, *Kv4/Shal* expression was up-regulated (71), suggesting that ion channels in the same neuron can balance each other to maintain activity (70). Neural intrinsic excitability is regulated by changes in density, distribution and function of ion channels to modulate synaptic inputs. In response to an increase in synaptic activity, *Xenopus* retinocortical circuits exhibit a decrease in Na^+ currents to reduce intrinsic excitability and maintain overall activity in optimal range (72). On the other hand, inhibiting synaptic activity during development in *Xenopus* tectal neurons and motorneurons in *Drosophila* resulted in an increase in both Na^+ current and intrinsic excitability (72–74).

Localization of voltage gated potassium and sodium channels in the axon initial segment (AIS) plays an important role in intrinsic homeostatic plasticity (4). The AIS is

the site where the neural signal is initiated and it is responsible for regulating neural activity (75,76). In mice, AIS length in pyramidal cortex is shortened after 13-14 days postnatal (77) and this event adjusts ion channel density, distribution and function that consequently affects transcription, translation and posttranslational modification , trafficking processes implemented in intrinsic homeostatic plasticity to keep overall activity at pre-perturbation set point (77). In avian brainstem auditory neurons, deprivation of neural input resulted in an increase in AIS length (77). This increase led to 1.7 fold increase in voltage-gated Na^+ channels to re-establish neural activity (77).

1.3.2 Secreted and Cell Adhesion Molecules

In response to activity blockade, different cellular and molecular mechanisms are implicated in the homeostatic response, ranging from transcription, translation, trophic signaling and cell-cell adhesion molecules (10). Chronic changes in network activity trigger downstream cascades that result in transcriptional activation (78) and newly synthesized mRNA trafficked to dendritic branches for local translation and synaptic strength modulation (79,80).

In response to synaptic stimulation, glutamatergic neurons express Arc/Arg3.1 protein, which plays a critical role in homeostatic synaptic plasticity (81). *Arc/Arg3.1* mRNA is then packaged and transported to dendrites for local translation (80,82). Arc/Arg3.1 protein forms a complex structure with dynamin and endophilin to trigger AMPA receptor endocytosis (83). In addition, local dendritic protein synthesis can be controlled by the phosphorylation of translation effectors. For instance, chronic inhibition of synaptic activity results in dephosphorylation of eukayotic elongation factor-2 (eEF2),

generating an active form, and thereby enhancing dendritic protein synthesis. On the other hand, chronic activation of network activity leads to phosphorylation of the active form of eEF2, which inhibits protein synthesis (84,85).

Many secreted molecules mediate presynaptic and postsynaptic homeostatic responses. For instance, neurotrophin is a cytokine derived from glia cells that targets neurons and plays a critical role in a local homeostatic feedback mechanism (10). Brain-derived neurotrophic factor (BDNF) is produced in excitatory and inhibitory neurons in its precursor form (Pro-BDNF) and then processed and stored intracellularly as BDNF (10) or processed by plasmin, an extracellular protease that converts the precursor proBDNF to the mature BDNF, and stored extracellularly (86). BDNF release mechanisms are mediated by Ca^{+2} (87) and modulated by synaptotagmin-IV (88). When released, BDNF binds to TrKB receptors and triggers downstream signaling involved in the control of homeostatic synaptic plasticity (89,90). Interestingly, BDNF plays a crucial role in the organization of N-type and P/Q type of Ca^{+2} channels and spontaneous neurotransmitter release in the resting state (91).

Earlier studies have documented that tumor necrosis factor (TNFα), secreted by glia cells plays a crucial role in homeostatic mechanisms in inhibitory and excitatory neurons *in vitro* and in *in vivo* (19,92). TNFα positively regulates postsynaptic homeostasis by enhancing GluA2-lacking AMPA receptor delivery and down-regulates GABAA receptors from the cell surface (92,93). TNFα is required for homeostatic synaptic plasticity triggered by neural network inhibition, but not required for homeostatic synaptic plasticity induced by neural network activation (94).

Another essential player in homeostatic synaptic plasticity is retinoic acid (RA). It has been reported that RA is required for gene expression throughout development, LTP and LTD (95). *In vivo* studies have shown that neural activity inhibition with TTX and D-2-amino-5-phosphonopentanoic acid (APV), a selective NMDA receptor antagonist, triggers RA synthesis (47). Adding RA by itself, without neural activity manipulation, up-regulates AMPA receptor expression and enhances GluA1 synthesis in dendrites via the RA receptor, RARα (47,96). RA signaling pathways have been documented in Hebbian and non-Hebbian plasticity and this may explain the diversity of RA receptors: for instance, RARα has been shown to function in HSP (47,96), while and RXR$_{\gamma}$ has been shown to function in LTD (97).

Cell adhesion molecules have also been shown to play crucial roles in HSP. Cell-to-cell adhesion molecules maintain synapse structure and arrange cell-cell or cell-extracellular matrix signaling (10). Integrins are heterodimeric transmembrane adhesion molecules that act as signal mediators between the extracellular matrix and the cell (98). An earlier study reported that β3 integrins up-regulate AMPA receptors in response to network activity inhibition, but expression of the dominant-negative form of β3 integrins in post-synaptic neurons decreases synaptic AMPA currents (99,100). The N-Cadherin/β-catenin complex is another class of adhesion protein. N-cadherin is a Ca^{+2}-dependent hemophilic cell adhesion protein that plays an important role in synapse formation and spine morphology (101,102). N-cadherin is connected to the cytoskeleton through β- and α-catenin, and to a synaptic scaffold protein through its PDZ binding domain. By this connection, N-cadherin can play an important role in modulating presynaptic and

postsynaptic activities (103–105). In addition, N-cadherin can adjust synaptic activity via its direct binding to AMPA receptor subunits (106).

1.3.3 Presynaptic expression of homeostatic synaptic plasticity

The pre-synaptic compartment plays a pivotal role in maintaining synaptic strength. In dissociated hippocampal neuron cultures, blocking action potentials using TTX or adding an AMPA receptor antagonist results in an increase in synapse size and an increase in the number of docked neurotransmitter vesicles at the synaptic cleft (107,108).These observations indicate an increase in the probability of release of neurotransmitter from presynaptic neurons (108). Furthermore, chronic neural activity depletion leads to up-regulation of mEPSC frequency and an increase in neurotransmitter vesicles recycling, as monitored by styryl dyes, vesicle turnover, or synaptotagmin luminal domain antibody uptake assays (107,109–112). On the other hand, chronic stimulation of network activity in dissociated neuronal cultures reduces the number of recruited neurotransmitter vesicles and decreases the probability of release (107,113,114). Additionally, manipulation of the glutamate transporter, v-Glut1, expression has a bidirectional effect on glutamate vesicle content, thereby affecting the efficiency of the presynaptic homeostatic response (115,116).

1.3.4 Postsynaptic expression of homeostatic synaptic plasticity

A hallmark feature of the synaptic response to persistent activity perturbation at excitatory synapses is an increase in AMPA receptors, mediating mEPSC amplitude (61,117). Glutamatergic AMPA receptors are composed of four subunits (GluA1-A4) in

hetero-tetrameric combinations (118). When network activity was altered, the change in subunit combination and availability of synaptic AMPA receptors may be controlled by different processes, such as endocytosis/exocytosis, and lateral diffusion of receptors in/out the synapse (119–122). Newly synthesized AMPA receptors (123,124) locally translated in dendrites (124), are also involved in the postsynaptic homeostatic response to network activity inhibition. Phosphorylation of Ser845 on the GluA1 subunit of AMPA receptors by protein kinase PKA (125,126) facilitates trafficking and recruitment of AMPA receptors to postsynaptic membranes in response to LTP (126,127). On the other hand, dephosphorylation of GluA1-Ser845 by calcium dependent calcineurin triggers AMPA receptors endocytosis, which is required for LTD (128–130). Phosphorylation of GluA1-Ser845 is also increased and decreased to up-regulate and down- regulate AMPA receptors, respectively, in response to activity perturbation (131), suggesting that GluA1-containing receptors mediate synaptic up scaling.

Subunit composition determines channel properties, such as agonist affinity, gating kinetics and calcium permeability, so postsynaptic responses can also be modulated by switching between receptor subunits without a change in the total receptor number (132). Ca^{+2}-permeable -GluA1-containing AMPARs (CP-AMPARs) are implicated in postsynaptic up-scaling (110,133,134) by switching from Ca^{+2}-impermeable GluA2-containing AMPARs (CI-AMPARS) to CP-AMPARs in response to receptor inactivation (132). In an *in vitro* study, chronic TTX- hippocampal treated slices showed a selective increase in CP-AMPARs in CA1 pyramidal neurons (135), and persistent inhibition of AMPA or L-type calcium channels in hippocampal dissociated cultures enhances CP-AMPARs localization at postsynaptic compartments (110).

Synaptic scaffold proteins, such as postsynaptic density protein-95 (PDS-95) and PDS-93 play critical roles in Hebbian plasticity and HSP (136–139). These proteins interact with trans-membrane proteins, including AMPAR regulatory proteins (TARPs), and play an important role in AMPAR trafficking and cell surface insertion in response to network activity perturbation (140,141). Other scaffold proteins like PICK1,GRIP and AKAP150 may also be involved in Hebbian and HSP (129,142,143). These scaffold proteins recruit kinases (PKA) and phosphatases (calcineurin) to dendrites and post-synaptic densities and have been implicated in the up-regulation and down-regulation of synaptic strength in response to circuit activity change (144,145).

2. Regulation of HSP at the *Drosophila* Neuromuscular Junction (NMJ)

Many experimental studies have documented that the central and peripheral nervous systems in vertebrate and invertebrate organisms deploy homeostatic synaptic plasticity to control cellular activity and counterbalance the experimental perturbations that increase or decrease cellular excitability. These changes have been reported to be bidirectional in neurons and muscle excitation (4,146–148). Experimental evidence has shown that perturbing the activity at the NMJ results in many changes, including the number of ion channels in motorneurons (149,150), the probability of release of neurotransmitter vesicles from motorneurons (151,152) and the increased sensitivity of postsynaptic receptors(148).

HSP has been extensively studied at the *Drosophila* NMJ. Synaptic activity at the *Drosophila* NMJ is regulated by PKA that modulates change in receptors' cell surface expression and retrograde signaling that induces presynaptic release. Two glutamate

receptors, DGluRIIA (153) and DGluRIIB (154) have been identified in *Drosophila* muscle .Sequence analysis has shown that only DGluRIIA has PKA phosphorylation site (155) and mutations that delete DGluRIIA are homozygous viable (154). PKA-dependent modulation requires the muscle-specific glutamate receptor DGluRIIA (148). Homozygous DGluRIIA mutation or in transgenic line with over-expression of constitutively active protein kinase A have shown an increase in neurotransmitter release, suggesting there is retrograde signaling induces presynaptic homeostatic response (155).

Chronic impairment of postsynaptic neurotransmitter receptors resulted in an increase in neurotransmitter release to restore activity (155). Presynaptic homeostasis has been shown to be mediated by Ca^{+2} entry through P/Q type Ca^{+2} channels (100,156,157). Likewise, in the vertebrate CNS, presynaptic homeostatic responses depend on Ca^{+2} influx (158). Upon neural activity blockade, the Ca^{+2} sensor synaptotagmin, the synaptic vesicle protein SV2B, and the pore forming subunit Cav2.1 of P/Q type Ca^{+2} channels became highly expressed in the presynaptic compartment, resulting in an increase in probability of neurotransmitter release (159). Other studies have showed that transgenic expression of the delayed rectifier potassium channel, Kir2.1, resulted in hyperpolarization of the muscle and a delay in muscle synaptic depolarization (151). Muscle membrane excitability was re-established by an up-regulation of the probability release of neurotransmitter vesicles(160).

Chronic post-synaptic inhibition triggers a presynaptic change, suggesting trans-synaptic communication to induce presynaptic homeostasis (161). Retrograde Bone Morphogenic Protein (BMP) signaling plays a critical role in homeostatic control of muscle excitation in *Drosophila* (162,163). At the *Drosophila* NMJ, Ephrin/Eph receptor signaling

in motor neurons is required for the retrograde homeostatic response (161). Eph is a muscle derived signal that binds to Eph receptors on motor neurons and subsequently activates Rho-GEF ephexin and Rho-GTPase Cdc42 downstream cascades (161). Prolonged post synaptic inactivation induces presynaptic neurotransmitter release by acting on $Ca_V2.1$ channels (100,156). It has been suggested that Ephexin/Cdc42 couples synaptic Eph signaling to modulation of presynaptic $Ca_V2.1$ channels to induce the presynaptic homeostatic response (156).

3. Nicotinic Acetylcholine Receptors (nAChRs)

nAChRs are ligand- activated neurotransmitter receptors. There are two subtypes of acetylcholine receptors: the metabotropic muscarinic receptors (mAChRs) and ionotropic nicotinic receptors (nAChRs). Both groups are activated by acetylcholine and, expressed in neural and, non-neural cells, such as skin, pancreas and lung (164–167). nAChRs are widely distributed and abundant in the mammalian central nervous system (168). Structurally, each ionotropic receptor is composed of five subunits that form a water-filled, cation-permeable pore (169,170). Each subunit of a nAChR possesses a large extracellular N-terminal domain, which binds the ligand, three hydrophobic trans-membrane regions (M1-M3) followed by a large intracellular loop that connects to the fourth trans-membrane domain, M4, and a short intracellular C-terminal tail (171). Although the N-terminus and some trans-membrane domains are conserved among all nAChRs subunits, the M3-M4 cytoplasmic loop is distinct in length and amino acid sequences (173). It has conserved sequences required for receptor export from the endoplasmic reticulum and trafficking to the cell surface. In addition, other sequences are

important for postsynaptic scaffold protein interaction and for different serine/threonine phosphorylation sites (174,175). Interestingly, the C- terminus of the α7 subunit has a binding site for a G-coupled protein that mediates downstream signaling pathways (176,177), suggesting that α7 receptors may act as a metabotropic receptor and activate second messenger pathways (176).

In mammalian systems, neuronal nAChRs can be homopentamers or heteropentamers. They are composed of diverse combination of seven α subunits, α2-α9, α10 (α8 was identified in chicken) and, 3 β subunits, β2-β4 (178). Different nAChR subunit combinations have different biophysical properties and expression pattern that suggest different physiological functions (179). For instance, homopentameric α7 nAChRs are widespread and abundant in the mammalian CNS and display high Ca^{+2} permeability and faster desensitization than other subtypes (180,181). The α4β2 combination is plentiful in the brain and up-regulated as a consequence of nicotine exposure (182). Channel permeability depends on receptor composition. For example, β2 homomeric receptors are highly permeable to Na^{+} and α7 homomeric receptors are highly permeable to Ca^{+2} (181,183–186). More distinct hetero-multimeric nAChRs combinations are reported, such as α4α6β2 nAChRs that are located in midbrain dopaminergic areas. α-7 containing and β2-containing nAChRs are localized at preterminal, axonal, somatic and dendritic sites (181,186–192). Homo-multimeric nAChRs are formed by α7, α8, α9, but only α7 nAChRs exhibit widespread and abundant expression in brain (189,193,194).

Genetic studies and sequence analysis of the *Drosophila* genome have revealed that nAChRs subunits are encoded by ten genes: seven genes encode α subtypes, Dα1-

7, and three genes encode β subtypes, Dβ1-3. *Drosophila* Dα5-7 share high sequence identity (~ 60%) with mammalian α7, suggesting that Dα5-7 are orthologs of mammalian α7 (195–197). Selective permeability of α7 nAChRs to Ca^{+2} makes it an important player in postsynaptic transmission and plasticity (198).

nAChRs are localize to pre- and post-synaptic compartments and play an essential role in mediating synaptic homeostasis. α7 nAChRs are located in presynaptic terminals and can induce membrane depolarization and increase intracellular Ca^{+2} and therefore positively up-regulate neurotransmitter release (199,200). Additionally, nAChRs are located in postsynaptic compartments (201), and mediate postsynaptic homeostasis (178). nAChRs have been implicated in synaptic plasticity and membrane properties change (202). In CA1 pyramidal cells backpropagation of AP into the dendrites and play a role in synaptic plasticity (203,204). When CA1 pyramidal cells in culture were inhibited with Na+ channel blockers, depolarizing influence of back warded AP may decrease A-type K^+ channels through inactivation and increase activation other channels linked to AP propagation, such as Na^+ and Ca^{+2} (202). In some cell, in response to expression Ca^{+2}-activated K+ Channels, nAChRs could mediated Ca^{+2} influx to stabilize or hyperpolarize the membrane potential (202). nAChRs may therefore mediate presynaptic as well as postsynaptic homeostatic response.

4. Cholinergic HSP

Although most HSP studies have focused on glutamatergic receptors, Ping and Tsunoda (2011) suggested that other excitatory receptors could mediate HSP (205). When nAChRs, the major excitatory neurotransmitter receptors in *Drosophila,* were

pharmacologically blocked *in vitro* using curare, a nAChRs antagonist, Ping and Tsunoda found pre- and postsynaptic homeostatic changes in response to this activity blockade. After 24 hrs of curare treatment, there was a selective increase in Dα7 nAChR proteins concurrent with an increase in frequency and amplitude of miniature excitatory postsynaptic currents (mEPSCs) (205). Newly synthesized Dα7 nAChRs were suggested to be translationally up-regulated (205).

Although HSP studies have focused on pathways mediating pre- and postsynaptic responses, less is known about regulatory mechanisms that might prevent over-compensation by HSP mechanisms (179). One earlier study reported that the monomeric G-protein, Rab3, binds a repressor that negatively regulates the presynaptic response to activity blockade (206). Ping and Tsunoda (2011) showed that cholinergic receptor blockade induced an increase in Kv4/Shal channels, as a regulatory mechanism for tuning the homeostatic response, and preventing over-compensation (205).

After prolonged curare treatment, immunoblots analysis showed an increase in Kv4/Shal protein and electrophysiological studies revealed an up-regulation of the rapidly inactivating A-type K^+ current mediated by Kv4/Shal channels. This up-regulation of Kv4/Shal was shown to stabilize the Dα7 nAChR-mediated homeostatic response to prevent over-excitation (205). Interestingly, Kv4/Shal protein/current up-regulation required the Dα7 nAChRs and synaptic transmission recovery (205). Adding transcription inhibitor, actinomycin D, blocks increase in Kv4/Shal protein (205), suggesting that Kv4/Shal protein up-regulation is transcriptionally regulated. Additionally, Ca^{+2} influx has been found to be essential for an increase in Kv4/Shal channel (205) and when Ca^{+2}/calmodulain-dependent protein kinase kinase (CaMKII) activity was inhibited during

recovery time resulted in inhibition of Kv4/Shal up-regulation. Similar to mammalian α7 nAChRs, the selective increase Dα7 subunits could form highly Ca^{+2}-permeable receptors to activate CaMKII and downstream transcription cascades (205).

In mammals, cholinergic receptors have been implicated in HSP mechanisms. Chronic exposure to nicotine has been documented to up-regulate nicotinic acetylcholine receptors (nAChRs) (44,207), suggesting that this up-regulation may be due to desensitization of nAChRs that trigger HSP mechanisms (179). Cholinergic activity during Alzheimer disease showed early increase in cholinergic activity followed by inhibition in later stage that involve endogenous HSP mechanisms (208,209). In Myasthenia Garvis disease, the human NMJ endplates are affected, showing an increase in neurotransmitter release (52), suggesting that this up-regulation is a homeostatic response mediated by nAChRs.

In this work, we use genetic mutants to reduce cholinergic activity *in vivo* to study HSP and investigate the mechanisms underlying the inactivity-induced up-regulation of Kv4/Shal expression.

5. Temperature sensitive Choline acetyltransferase mutants (*Cha^{ts}*) as a tool to inhibit cholinergic activity

Cholinergic HSP studies have been conducted previously in our lab *in vitro* (*Drosophila* neurons in culture) (205). In this study, we used genetic tools to reduce cholinergic activity *in vivo* and examine if this triggers a similar pathway. We used

temperature sensitive mutant alleles that affect the choline acetyltransferase enzyme and reduce cholinergic activity.

Choline acetyltransferase (ChAT) catalyzes the synthesis of the major excitatory neurotransmitter, acetylcholine, in the *Drosophila* CNS and it has been used as marker for cholinergic synapses (210,211). ChAT plays a crucial role in development and maintenance of cholinergic receptor activity, and reduction in ChAT activity has been reported in many pathological conditions such as memory malfunction and Alzheimer disease (354,355).Greenspan (1980) identified the *Drosophila* ChAT locus on the third chromosome (212). He also identified two temperature sensitive mutations, Cha^{ts1} and Cha^{ts2}. Mutant proteins were found to function at the permissive temperature of 18˚C, but displayed reduced ChAT activity (49-65%) at the restrictive temperature of 30˚C. In a later study, a third temperature sensitive mutant allele, Cha^{ts3}, was identified (213)

Temperature sensitive mutations of ChAT have been shown to be due to point mutations in the *Cha* structural gene, as confirmed by alteration in isoelectric point profile (214). Salvaterra *et. al* 1999 (215) used the single nucleotide primer extension (SNuPE) assay to detect single nucleotide differences that cause thermolability in each Cha^{ts} mutants allele. They found that Cha^{ts1} displays a change in adenine (212) at position 1614 and Cha^{ts2} exhibits a change in A at position 1596. These changes led to a change in a methionine (Met) to lysine (Lys) at amino acid 403 for Cha^{ts1}, and arginine (Arg) to histidine (His) at position 397 for Cha^{ts2} (215).

We planned to use heat-treatment of Cha^{ts} alleles as an approach to alter synaptic transmission in the central nervous system *in vivo*. Heat treatment negatively affects ChAT activity and acetylcholine levels in Cha^{ts} mutants compared to wild-type flies. HT of

wild-type flies at 32˚C for 12hrs was shown to increase ChAT activity, while homozygous *Cha*^{ts1} and *Cha*^{ts2} mutants both displayed a decrease in ChAT activity when compared to the same genotype raised at 18˚C (214). Moreover, the enzyme activity gradually decreased over days until it was undetectable after 71hrs for *Cha*^{ts2} and 95 hours for *Cha*^{ts1} (212) while no changes have been reported with wild-type activity under the same experiment conditions. Instead, ChAT activity in wild-type increased after 120 hrs of heat treatment. When ChAT activity was measured in different *Cha*^{ts} mutant allele combinations at 18˚C, ChAT activity was reduced, compared to wild-type ChAT activity at 18˚C. For instance, *Cha*$^{+}$/*Cha*^{ts1} (16%), *Cha*^{ts1}/*Cha*^{ts1} (32%), *Cha*$^{+}$/*Cha*^{ts2} (42%), *Cha*^{ts1}/*Cha*^{ts2} (58%) (356), and *Cha*^{ts2}/*Cha*^{ts2} (75%) (214); note that these numbers are reduction percentage. In individual fly heads, acetylcholine (ACh) and Choline levels were examined in homozygous. ACh levels and ChAT activity were decreased at 30˚C, while choline levels were not affected by heat treatment (214). Heat treatment showed no effect on acetylcholinesterase in wild-type and *Cha*^{ts1}, but the *Cha*^{ts2} mutant allele showed a 30% decrease in acetylcholinesterase activity after 24hr heat treatment at 32˚C (214) suggesting the heat treatment is specific for ChAT.

ChAT mRNA levels were also decreased in homozygous *Cha*^{ts} mutants at the restrictive temperature (30˚C) (215). At the permissive temperature (18˚C), *ChAT* mRNA levels in wild-type and homozygous *Cha*^{ts} mutants were approximately equal, but when mutant flies were shifted to 30˚C for 48hrs, *ChAT* mRNA levels were increased by 23% in wild-type. On the other hand, *Cha*^{ts1} mRNA levels dropped to 70% and *Cha*^{ts2} mRNA level to 60% after heat treatment, while no change was observed for β-tubulin mRNA levels which was used as a control, suggesting that the change was specific for ChAT

(215). Interestingly, HT at 30˚C does not affect *ChAT* mRNA in heterozygous Cha^{ts} mutants (215).

Alteration of acetylcholine synthesis also has a negative impact on the physiology and behavior of *Drosophila* flies (212). Cha^{ts1} and Cha^{ts2} were identified based on their lethality or inability to reach adulthood stage at 30˚C (212). Both mutants at 30˚C were shown to exhibit behavioral abnormalities. For example, males neglected to court female, and some alleles showed paralysis followed by death (212). Cha^{ts1} and Cha^{ts2} mutants raised at 30˚C have shown death in late embryogenesis, indicating the importance of acetylcholine for normal development (212). Severity of the Cha^{ts3} allele compare to Cha^{ts1} and Cha^{ts2} was demonstrated by the temperature sensitive response after heat treatment. When Cha^{ts} mutants flies were raised at 18˚C and shifted to 30˚C for different periods, Cha^{ts3} mutant flies were more sensitive to heat treatment, expressing a paralytic phenotype faster than Cha^{ts2} and Cha^{ts1} (213).

Because heterozygous Cha^{ts2} exhibits ChAT activity more similar to wild-type when grown at 18°C, and induce ~35% reduction in ChAT activity at 30˚C compare to wild-type (Greenspan et al., 1980), we chose to use Cha^{ts2} as a major tool to inhibit cholinergic activity, then examined if Cha^{ts2}-induced activity inhibition induces homeostatic response.

6. **NACHO and nAChRs Biogenesis**

nAChR homeostasis is required for efficient CNS and peripheral nervous system physiological function (216). This process involves the proper folding, assembly, degradation, and trafficking of nAChRs (216). nAChR folding and assembly happens in

the endoplasmic reticulum (ER) and requires many biochemical steps, including cleavage of the peptide signal, oxidation of disulfide bonds and N-glycosylation of some residues. Because of the sensitivity of this biological process, checkpoints are required to differentiate between correctly folded and misfolded proteins. Essential players include chaperone proteins that reside in the ER and prevent trafficking of non-functional subunits to the cell surface (216). NACHO is recently identified as a transmembrane chaperone protein, located in the ER, which plays an important role in the folding and trafficking nAChRs (175). ER localization of NACHO is mediated by the NACHO C-terminus, which contains an ER-retention signal (KxKxx) known in other proteins to bind β'-COP subunits for Golgi-to-ER retrieval (217).

NACHO mediates cell surface expression of nAChRs, especially α7 nAChRs in non-permissive cells, such as HEK-293 cells, in which expressed nAChR subunits are retained in the ER membrane and are not able to reach the cell surface (218). When nAChR subunits are co-expressed with NACHO, they are successfully recruited to the cell surface and exhibit an induced acetylcholine current (218). α- bungarotoxin is known to selectively bind to α7 nAChRs (219). Genetic deletion of NACHO in hippocampal neurons diminishes receptor trafficking and led to a reduction in α-bungarotoxin binding affinity (218), suggesting reduced trafficking of α7 receptors

NACHO is specific for nAChRs. For example, when NACHO co-expressed with α4+β2 nAChRs in non-permissive cells, an acetylcholine current could be induced (218), but NACHO showed no effect on GluA1or 5-HT3A/B receptors (220). NACHO also plays an essential role in the assembly of α7-, α4β2- and α6-containing nAChRs (220). The *Drosophila* NACHO homolog, dNACHO, shares about 37% sequence identity with human

NACHO (218). When NACHO was suppressed by shRNA, hippocampal neurons were unable to sustain α7 nAChRs mediated current after adding ACh (218). Additionally, NACHO knockdown hippocampal neurons failed to express HA-tagged α7 on cell surface, as indicated by absence of α-bungarotoxin binding sites (218), suggesting that NACHO plays a role in nAChRs, especially α7 nAChR, folding and trafficking.

Previously, resistant to inhibitors of cholinesterase-3, RIC-3 (216) was found to play a pivotal role in nAChRs trafficking in *C.elagans* (221). The mammalian homolog RIC-3 has a weak effect on α7 nAChR biogenesis and it has different effects on other nAChRs and 5-HT_3 receptors. RIC-3 can both enhance and reduce levels of α4β2 and α3β4 nAChRs functional expression, and it can the modulate maturation of 5-HT_3 receptors (222,223), suggesting that mammalian RIC-3 is neither required (224) nor sufficient (225) for efficient α7 nAChR cell surface expression. Mammalian RIC-3 boosts the effect of NACHO on mammalian α7 activity (222,223). When RIC-3 and NACHO are co-expressed, the acetylcholine current was greatly increased (218). On the other hand, RIC-3 plays an important role in α7 nAChR intracellular retention when it is present in excess (226) and allows multiple proteins to bind to α7 and facilitate intracellular trafficking (227).

In this study, we tested the effect of dNACHO on Dα7-EGFP expression, and we used dNACHO as a tool to increase surface expression of endogenous Drosophila α7 (Dα7) and examine the consequential effect on Kv4/Shal protein and mRNA.

7. Transcriptional Programming in Synaptic Homeostasis

The relationship between neural activity and transcriptional mechanisms was first explored in 1984 when Greenberg and Ziff (228) discovered that *Fos* transcription was rapidly and transiently induced in mammalian cells in response to changes in the external environment (229–232). When the notion that specific transcription events are rapidly activated by synaptic transmission was established, many studies focused on characterizing the immediate early genes (IEGs) of signal-dependent transcription, such as *Fos* (228). IEGs are defined as a class of genes that are rapidly and transiently activated in response to environmental change and do not require newly synthesized proteins (228). Many IEGs encode transcription proteins, such as transcription factors that mediate transcription of late response genes (LRGs), which are known to be cell specific and have specific functions in response to neural activity (233,234).

IEG activation depends on extracellular calcium influx that is mediated by neurotransmitter receptor activation (235). A rise in intracellular calcium positively regulates downstream cascades including the activation of the Ras-mitogen-associated protein kinases (MAPK), calcineurin/calmodulin-dependent protein kinases (CaMKs), and calcineurin-mediated signaling pathways (236–238). Calcium influx take places through different points of entry, such as α7 nAChRs (239),N-methyl-D-aspartate (NMDA), AMPA glutamate receptors and voltage gated calcium channels, as well as intracellular calcium stores (240). IEG activation does not require synthesis of new protein but requires pre-existing constitutively expressed transcription factors, such as cyclic adenosine monophosphate (CREB), serum response factor (SRF) and myocyte enhancer factor 2 (MEF2) (241,242). Although these transcription factors are constitutively expressed, their

activation depend on Ca^{+2} influx in response to neural activity perturbation (243–245). Different gene products are implicated in bidirectional synaptic scaling depending on Ca^{+2} influx (11). For instance, BDNF, TNFα, β3, PICK1 and PSD95 positively regulate synaptic strength in response to prolonged activity blockade by recruiting more surface AMPA receptors to synapses in order to increase Ca^{+2} influx. Arc, Homer1a and EphA4 negatively regulate synaptic strength mainly by down-regulating AMPA receptors through endocytosis and eventually reducing Ca^{+2} influx (246).

7.1 Nuclear Factor of Activated T-cells (NFAT)

The mammalian NFAT family consists of five members (NFAT1-5) and is evolutionary related to the Rel/NFκB family of eukaryotic transcription factors (247,248). Generally, NFATs (NFAT1-4) are transcription factors and regulated by the Ca^{+2}/calmodulin-dependent serine phosphatase, calcineurin. Phosphorylated NFAT resides in the cytoplasm of resting cells, and in response to activation, NFATs are dephosphorylated by calcineurin. Dephosphorylated NFAT, which is the transcriptionally active form, translocate to the nucleus and drives target gene expression, thus providing a bridge between Ca^{+2} signaling and target gene expression(249). T-cells from hereditary severe combined immunodeficiency (SCID) patients, characterized by a severe defect in T-cell activation, show a decrease in multiple cytokines and inability to activate NFAT due to a reduction in Ca^{+2} entry (250,251).

In resting cells, NFAT1-4 are heavily phosphorylated in serine residues that are distributed in four conserved serine-rich sequence motifs, conserved 300 amino acids(252,253). When the cell is excited or depolarized, NFAT is dephosphorylated at these motifs (248). When calcineurin dephosphorylates three out of four conserved

motifs, which is sufficient to dephosphorylated and translocate NFAT to nucleus and drive target gene expression (252,254,255). Calcineurin has a specific docking site on the N-terminus of the NFAT regulatory domain that is required for efficient dephosphorylation (256–258). In addition, calcineurin inhibitors, DSCR1/MCIP1 bind to the calcineurin-binding sequence in the regulatory domain of NFAT and thereby compete with calcineurin for binding to these sites (259–261). Calcineurin activity itself can be controlled by DSCR1/MCIP1 through a negative feedback mechanism, in which calcineurin/NFAT signaling activates DSCR1/MCIP1 expression, which then inhibits calcineurin activity (262).

In resting cells, many constitutively active or inducible kinases work cooperatively to phosphorylate NFAT(249). Interestingly, these kinases have different target sequences (252), for instance, casein kinase 1(CK1) and glycogen synthase kinase 3 (GSK3) are constitutively active kinases with different target motifs. When both phosphorylate NFAT, they trigger NFAT nuclear export (263,264).GSK3-calcineurin-NFAT signaling has been characterized in hippocampal neurons (265,266) and has also been found to be a key player in the growth and plasticity of tectal neuronal dendrites in the tadpole (265,266).

Many studies have shown that NFAT5 is expressed in almost all tissues and have diverse functions other than osmoprotective role (267). NFAT5 is 40% similar identity to rest of *Rel* family members (268,269), and initially renal medulla cells of the urinary system (270–272). It regulates expression of osmolality regulating genes, including the Na^+/Cl^- coupled betaine/g-aminobutyric acid transporter and the synthetic enzyme aldose reductase (271). For this reason, NFAT5was called tonicity enhancer binding protein, TonEBP (273). NFAT5 is highly expressed in the infant and adult brain with various

quantity and distribution (274). NFAT5 is more expressed in fetal brain than adult brain (275,276), and it is highly expressed in hypothalamus and the hippocampus than other brain regions (274). NFAT5 has been found to maintain osmotic equilibrium with plasma in the brain under normal physiological conditions (277). It has various functions in neurons, astrocytes, microglia, and other cell types in the CNS, including the regulation of aquaporin-4 (AQP4), the predominant water channel expressed in astrocytes (278).Thus NFAT5 functions to protect neurons against ischemic damage (279,280), and play an essential role in neuroinflammation (281).

Many studies have shown that NFAT5 is activated and deactivated by different kinases. NFAT5 is phosphorylated by different kinases at various specific phosphorylation sites and control different genes expression during different responses (282). The nuclear translocation of NFAT5 is mediated by different kinases, such as p38α (282), ATM(283), GSK-3β (284), CDK5(285) and CK1 (286). Hypertonicity and hypoxia induce NFAT5 phosphorylation at different sites, including 111 threonines, 216 serines, and 15 tyrosines (287). Phosphorylation at Y143 and T135 led to an increase in nuclear localization of NFAT5 in the human embryonic kidney 293 cells (288,289) and rat renal inner medulla cells (290). On the other hand, other kinases such as, glycogen synthase kinase 3β (GSK3β), casein kinase 1 (CK1), and p38δ negatively regulate the nuclear localization and transcriptional activity of NFAT5 (282). For example, phosphorylation at S155 and S158 of NFAT5 in response to low NaCl reduces the nuclear accumulation of NFAT5 (286).

Multiple studies have shown that NFAT is involved in neural development and plasticity. When NFAT activity was inhibited using CaN phosphatase inhibitor in the visual

system of living *Xenopus Laevis* tadpole, this resulted in an increase in mEPSC frequency and dendritic arbor complexity, and this morphological phenotype was rescued by calineurin/NFAT signaling (265). Other studies have found that NFAT is required for control of morphology and development. For example, sensory and commissural neuronal axons outgrowth in response to neurotrophins (295). In lack of calcineurin phosphatase activity or NFAT2-4, neurons did not responds to neurotrophins (295), suggesting that NFAT/calcineurin signaling plays a role in controlling the neural morphology and development.

Some studies have documented that mammalian NFATs regulates ion channels in neurons. Voltage-gated Kv7 potassium channels play an important role in regulation of neuronal excitability and action potential firing (296). NFAT has been found to be expressed in rat superior cervical ganglion neurons (SCG) (297) and when SCG was activated, this resulted in an increase in NFATc1/c2 activity and an increase in Kv7 channel expression (239), suggesting that NFATc1/c2 is required for Kv7 up-regulation. Other studies have shown that Neuritin plays critical role in regulating neural development, synaptic plasticity, and neuronal survival (298). In cerebellum granule neurons, neuritin elevates intracellular Ca^{+2} and activates Ca^{2+}/CaN-NFATc4 signaling followed by an increase in Kv4.2 expression (299).

Multiple studies have shown that mammalian NFATs regulate ion channels in the cardio-vascular system. For example, in arterial smooth muscle, the vasoactive peptide, angiotensin II, induces an increase in Ca^{2+} through L-type Ca^{2+} channels that subsequently leads to a calcineurin-NFATc3 dependent down-regulation of Kv2.1 channel expression (300). In addition, Ca^{2+}-activated potassium (BK) channels play an

essential role in regulating excitability and the contractile state of arterial smooth muscle (39). During hypertension, expression of the accessory β1 subunit has been found to be decreased relative to the pore forming α subunit (301). In NFATc3$^{-/-}$ mice, Angiotensin II administration led to an increase in systemic blood pressure, suggesting that NFATc3 is required for down-regulation of the β1 (301).

Myocardial infarction (MI) has shown an increase in NFAT activity and reduction in Kv4.2 current (302). When Kv4.2 current were examined after MI in ventricular myocytes from NFATc3 knockout mice, it showed no change, indicating that NFATc3 down-regulates Kv4.2 expression in response to MI (302). Other studies have shown that NFATc3 increases Kv4.2 expression during cardiac hypertrophy (303), and it has also been reported to contribute to the gradient of Kv4 expression across the mouse left ventricular free wall (304).

The *Drosophila* genome encodes only one NFAT homolog, dNFAT, with two splice isoforms originating from two distinct promoters, “a” and “b”. The dNFATa and, dNFATb isoforms have ten exons, and the last eight exons are shared between the two splice forms (305). Three different *Drosophila* d*NFAT* mutant alleles have been generated (*dNFAT*$^{\Delta a}$, *dNFAT*$^{\Delta b}$, and d*NFAT*$^{\Delta ab}$) (306). In the first two mutant alleles, the first exon from each isoform was deleted and, in the third mutant allele, the second and third shared exons were deleted (306).Sequence analysis of putative DNA-binding Rel homology/IPT region showed that dNFAT shows 64% similarity identity to human NFAT5 and 53% identity wit NFAT1(305). Earlier study has shown that dNFAT, similar to NFAT5, lacks AP-1 and calcineurin binding sites, suggesting that dNFAT may not be activated by Ca^{+2}/calmodulin-dependent pathway (305), but another study has identified an AP-1

binding site in dNFAT (306), suggesting that dNFAT may be activated by the similar pathway.

Similar to NFAT5, dNAFT has been identified as an osmo-regulator (305). *Drosophila* uses different organs to maintain homeostasis, such as Malpighian tubules and anal pads, which regulate ionic concentrations in the hemolymph (305). d*NFAT*$^{\Delta ab}$ larvae showed a decrease in their survival rate in high salt concentration (305). Unlike NFAT5, *dNFAT* mutant alleles have been tested if they have immune-related function and the study has shown that dNFAT deletions have no effect on survival rate after bacterial infection (305).

dNFAT regulates presynaptic growth and motor neural excitability (306). dNFAT has been found to regulate pre-synaptic growth in the *Drosophila* NMJ. Although either *dNFAT*$^{\Delta a}$*or dNFAT*$^{\Delta b}$ showed less effect on NMJ size (305), d*NFAT*$^{\Delta ab}$ or RNAi mediated knock down of d*NFAT* exhibited an increase in the number presynaptic boutons (306). When dNFATa or dNFATb was expressed in neurons, the synapses appeared to be smaller compared to genetic background lines and resulted in a decrease in neurotransmitter release (306). When dNFATa was expressed in larva RP2 motorneurons, this resulted in a reduction in excitability, as indicated by slow movement of larva (306).

In this study, we investigated if an NFAT based reporter was activated in response to *Cha*^{ts2}- induced inactivity and Dα7 over-expression. Then, we tested if dNFAT is required in the up-regulation of Kv4/ShaI protein and mRNA in response to activity inhibition.

8. Overview of this dissertation

Homeostatic synaptic plasticity is a compensatory mechanism that neurons deploy as protection from activity perturbations, thereby maintaining overall synaptic strength in an optimal range. Neural circuits experience different types of activity perturbation, including positive feedback from Hebbian types of plasticity. Neurons use homeostatic synaptic plasticity to prevent over-excitation. Homeostatic synaptic plasticity has been found to play a neuro-protective role during times of activity change, such as development, learning and memory and some of neuro-pathological conditions that alter synaptic strength like Alzheimer disease and nicotine addiction.

Most synaptic plasticity studies have focused on glutamatergic receptors. Dr. Tsunoda's lab found that nAChRs mediate synaptic homeostasis in the *Drosophila* CNS. These receptors are among the most widespread and abundant receptors in the mammalian brain, play important physiological roles, and are associated with multiple pathological conditions. α7 nAChRs are highly permeable to Ca^{+2} and play crucial roles in synaptic plasticity.

In a previous *in vitro* study in Dr. Tsunoda's lab, the investigators blocked cholinergic receptor activity using pharmacological tools found that this resulted in an increase in frequency and amplitude of mEPSCs. This homeostatic response was due to a selective increase in the Dα7 nAChRs. The homeostatic response was followed by an increase in expression of the voltage gated potassium channel Kv4/Shal, which tuned the homeostatic response and prevented over-compensation. *In this dissertation, my aim was to test this pathway in vivo, in live flies, using a genetic method to inhibit cholinergic activity. I investigate the mechanisms that underlie the increase in Kv4/Shal expression.*

In addition, I aimed to study the relationship between Dα7 nAChRs and Kv4/Shal potassium channels.

Chapter 3: In This Chapter, I used genetic methods to inhibit cholinergic activity and tested for a change in Dα7-EGFP expression. I found that *in vivo* activity inhibition also up-regulated the nAChR chaperone protein, dNACHO-HA. In addition, I tested the hypothesis that dNACHO-HA up-regulates Dα7-EGFP expression

Chapter 4: In this chapter, I tested if cholinergic activity inhibition *in vivo* triggers an up-regulation of Kv4/Shal expression. I showed that using Cha^{ts2}- induced activity inhibition or block of neurotransmitter release using targeted expression of tetanus resulted in an increase in Kv4/Shal protein and mRNA. This up-regulation is Dα7 nAChRs dependent. I found Kv4/Shal protein up-regulation requires dNACHO-HA. In addition, I characterized the relationship of Dα7 nAChRs and Kv4-Shal. I showed that over-expression Dα7-EGFP and / or NACHO-HA was sufficient to up-regulate Kv4/Shal protein and mRNA.

Chapter 5: In this chapter, I investigated the transcriptional activators that might be involved in Kv4/Shal up-regulation in response to activity inhibition using Cha^{ts2}. I tested if Cha^{ts2}- induced activity inhibition or over-expression Dα7-EGFP and / or NACHO-HA could activate a human NFAT-based reporter. I tested the hypothesis that the Ca^{+2}-dependent transcriptional activators, dNFAT and/or dCREB-2a, might be involved in Kv4/Shal protein and mRNA up-regulation. I showed that *Drosophila* NFAT is required for

Kv4/ShaI up-regulation in response to *Cha*^{ts2}-activity inhibition. In addition, I showed that over-expression of dCREB-2a induces Kv4/ShaI up-regulation.

CHAPTER 2. MATERIALS AND METHODS

1- Fly Stocks.

w^{1118} or genetic background strains were used as control lines in this study. We used previously generated mutant and transgenic lines: *UAS-TnT* (Deitcher et al., 1998; Sweeney et al., 1995); *Cha^{ts2}* and *Cha^{ts3}* alleles (Salvaterra and McCaman, 1985); *UAS-Dα7-EGFP* (Leiss et al., 2009) and *$Dα7^{PΔEY6}$* (Fayyazuddin et al., 2006); *UAS-NACHO-3xHA* (Bischof et al., 2013); *UAS-mLexA-VP16-NFAT, LexAop-CD8-GFP,* and *LexAop-CD2-GFP* transgenes (Masuyama et al., 2012); *$NFAT^{ΔAB}$, $NFAT^{ΔA}$,* and *$NFAT^{ΔB}$* alleles (Keyser et al., 2007); *elav-GAL4* (*$elav\text{-}GAL4^{c155}$*) and *$tub\text{-}GAL80^{ts}$* (Bloomington *Drosophila* Stock Center, Indiana University); *201Y-GAL4* (O'Dell et al., 1995; Yang et al., 1995); *GH146-GAL4* (Stocker et al., 1997); *UAS-RNAi-NACHO* (VDRC, Vienna, Austria), *Dα7-GAL4* (Fayyazuddin et al., 2006), hs-CREB-2a and hs-CREB-2b (J.C.P Yin et al., 1995), and ;;syb-Gal4 (Bloomington *Drosophila* Stock Center, Indiana University).

2. Heat-Treatment/Shock Protocols

Heat treatment (HT) refers to exposure of flies to 30C° and heat shock (HS) refers to subjection of flies to 37C°. Flies carrying a temperature-sensitive mutation (*Cha^{ts}*), heat shock promotor (*hs-Gal4*) and *$Gal80^{ts}$* were raised at 18C°. Other flies such as *w^{1118}* and flies carrying transgenic insertions not sensitive to temperature, such as Dα7-EGFP and NACHO-HA, were grown at room temperature. All crosses that included a temperature-sensitive mutation or transgene were grown at 18C°. Newly-eclosed flies were subjected to HS or HT for different periods. For instance, at 37C°, flies cannot withstand for heat more than two hours, while flies can stay for a long time at 30C° (> 2 days). Then flies,

were returned to 18C° for recovery. We called this HT or HS/ R protocols, as indicated in the text and legend, HT

3. Immunoblotting

3.1 Sample Preparation

All experimental and control flies were collected following the indicated heat-treatment or heat-shock time courses. Each sample contained 5 *Drosophila* heads in 20 ul 1X immunoblotting sample buffer (0.5M Tris pH6.8, 10% SDS, Glycerol, Bromophenol Blue, DTT). Then samples were sonicated (20 cycles) using a sonifier (Branson Ultrasonics, Danbury, CT) and spun at 14,000 RPM / 2 minutes in a table-top microfuge. Samples were stored at -20 °C until used or used immediately.

3.2 Workflow

Same amount (16ul) of samples were loaded in wells of 10% polyacrylamide gels. Proteins were separated based on molecular weight by polyacrylamide gel electrophoresis (SDS-PAGE). Proteins were transferred using the wet transfer method to 0.45 um nitrocellulose membrane (Bio-Rad, Hercules, CA). To reduce the amount of non-specific binding, we blocked the membranes using 5% non-fat dry milk in 1X PBS with 0.05% Tween-20 (Sigma-Aldrich, St. Louis, MO) for approximately 20 min on a tabletop rocker.

The blots were probed with specific primary antibody to detect the target protein. Primary antibody (see Table for concentrations) in block solution with 0.02% sodium azide

(J.T. Baker Chemical Co., Phillipsburg, NJ) was added to blots and incubated over night at room temperature. Then blots were washed in 1X PBS and 0.05% Tween-20 4 times / 5 min each. Blots were incubated with secondary antibodies (Goat α-rabbit or Goat α-mouse) conjugated to horseradish peroxidase, HRP (Jackson ImmunoResearch Inc., West Grove, PA), as listed in Table (1)

Table 1: primary and secondary antibodies concentration against different proteins (Kv4, GFP and HA) and their loading controls (Actin and Syntaxin).

Protein	Primary Antibody Concentration	Incubation	Secondary Antibody Concentration	Incubation
Kv4	1:100	Over night	1:1000 (Goat α-rabbit)	2 hours
GFP	1:10000	Over night	1:10000 (Goat α-rabbit)	1 hour
HA	1:100	Over night	1:1000 (Goat α-mouse)	1 hour
Actin	1:10000	1 hour	1:10000 (Goat α-mouse	1 hour
Syntaxin	1:100	Over Night	1:1000 (Goat α-mouse)	1 hour

Then blots were washed in 1X PBS and 0.05% Tween-20 4 times as mentioned previously. To initiate chemiluminescent reaction, Super Signal West Pico PLUS Chemiluminescent Substrate (ThermoFisher Scientific, Waltham, MA) added to blots at concentration 1:500 for 30 – 60 seconds. The super signal was then removed, chemiluminescent bands were captured using an Epichemi3 Darkroom, and the Lab works Imaging Software (UVP BioImaging, Upland, CA) was used to capture digital exposures.

3.3 Data collection and analysis

Band intensity for target proteins and loading controls were quantified using ImageJ software. Obtained values were transferred to an Excel spreadsheet and each target protein value was normalized to its corresponding loading control (Actin or Syntaxin). Dixon's Q-test was applied on normalized values and identified outlier values were excluded from statistical analysis. Student's t-test was used to detect statistical different between control and experimental groups. Origin 6.0 was used to make representative graphs that were edited in Adobe Photoshop.

4. RNA Extraction

4.1 Sample collection and storage

Total RNA was extracted using 300ul TRIzol reagent. Ten *Drosophila* heads were collected for each sample and homogenized with a clean and autoclaved pestal. The samples were stored at - 80°C until used.

4.2 Workflow (integrity and purity)

RNAase-Free water or DEPC-treated water is prepared by adding 100ul of (DL-Dithiothreitol Cleland's Reagent, DTT) to 100 ml of H_2O. Mixture was shaken vigorously and kept overnight in a hood at room temperature, then autoclaved before use. Frozen samples were completely thawed on ice. To precipitate proteins and genomic DNA, 60ul of Chloroform was added and vigorously vortexed for 60 seconds. Then samples were spun at maximum speed (14.000 RPM) on a tabletop cold centrifuge at 4 ˚C. The supernatant was collected and placed in a new autoclaved eppendorf tube containing 150 ul of 2-propanol and 10 ul of glycogen. To precipitate total RNA, samples were incubated

at -20 °C for one hour. After incubation, samples were spun at 1400 RPM at 4˚C for 15 min. The supernatant was removed, and the RNA pellet was washed with 500 uL of 70% ethanol/DEPC-treated water and spun at maximum speed at 4˚C. To remove TRIzol residue and obtain a high purity of RNA, the RNA pellet was washed three times with 70% ethanol/DEPC-treated water. After washing, the dried pellet was suspended in 16 ul of DEPC-treated water. At this step, RNA samples could be stored at -80 ˚C for future experiments.

To examine RNA integrity, 2 ul of total RNA was examined by agarose gel electrophoresis. The RNA purity and concentrations were evaluated using a NanoDrop spectrophotometer. Acceptable range for RNA purity to be used in reverse transcription was 1.9 – 2.0 (absorbance ratio).

5. Reverse Transcription

Only RNA with a high purity and integrity were used for reverse transcription (RT) reactions. 700 ng total RNA were used for each RT reaction. To remove genomic DNA, 1 ul DNases I (ThermoFisher Scientific, Waltham, MA) was incubated with RNA at 37˚C for 15 minutes. Then the DNAase reaction was deactivated by adding 1uL 50 mM EDTA and incubated at 65 ˚C for 10 minutes. To avoid RNA from forming secondary structures, samples were immediately placed on ice for 5 min. 1uL 0.5 ug/uL Oligo(dT)12-18 primer (ThermoFisher Scientific Waltham, MA) was added to each sample along with 1uL 10 mM dNTP (ThermoFisher Scientific, Waltham, MA). To allow primers to bind mRNA polyA, samples were incubated for 2 min at 42 ˚C. To initiate the reverse transcription reaction, Superscript II RNase H (ThermoFisher Scientific, Waltham, MA) and RNAse OUT

(ThermoFisher Scientific, Waltham, MA) were then added. Reverse transcription reaction was set up for 50 minutes at 42˚C for elongation, and at 70˚C for 15 minutes for enzyme inactivation. Freshly prepared cDNA was preferably used for qPCR and ddPCR experiments.

6. Quantitative Polymerase Chain Reaction (qPCR)

6.1 Primer and Probe design (specificity, sensitivity and efficiency)

We used the Universal Probe Library Assay design center (https://lifescience.roche.com/en_us/brands/universal-probe-library.html) to design our RT-qPCR assays, including the probe and gene specific primers for target genes. Probe finder version 2.35 and the intron-spanning assay were used to find a proper probe and design primers; Primer3 software was used with the following settings: melting temperatures between 59 °C and 61 °C, GC content between 40 and 60% and amplicon length limited to 60-200 base pairs. The maximum self-complementarity of the primers was set at 8 and the maximum 3' complementarity at 3. The PCR primer sets were verified for specificity by Primer-Blast (http://www.ncbi.nlm.nih.gov/tools/primer-blast/) using the *Drosophila* transcriptome. The probe and gene specific primer set were designed for our GOI (*Kv4*) and reference genes (*RpS20* and *eIF1A*) as listed in table (2).

To examine the primer specificity, we ran qualitative PCR using monocolor universal probe RT-qPCR setting (incubation at 95°C for 10 min, followed by 45 cycles of 95 °C for 10 s and 60 °C for 30 s and 72 °C for 1 s). Then, PCR products were analyzed by agarose gel electrophoresis (5%) to confirm that only a single product of the expected size was amplified. To verify target amplicon sequence, we extracted PCR bands

(GeneJET™, ThermoFisher Scientific, Waltham, MA) for sequencing (Proteomics, Metabolomics Facility, Colorado State University, CO)

Table 2: Forward and reverse primers, amplicon size and corresponding probes for *Kv4* and two reference genes (*RpS0A* and *eIF1A*)

Gene	Forward Primer	Reverse Primer	Probe #	Amplicon size(bp)
Kv4	GCTAACGAAAGGAGGAACG	TGAACTTATTGCTGTCATTTTGC	66	145
RpS20	CGACCAGGGAAATTGCTAAA	CGACATGGGGCTTCTCAATA	66	62
eIF1A	TCG TCT GGA GGC AAT GTG	GCC CTG GTT AATCCA CAC C	147	88

To verify primer amplification efficiency, we prepared reverse transcribed cDNA from pooled genotypes of young flies being used in an experiment, then made 10-fold serial dilutions of the cDNA: undiluted, 1:10, 1:100, 1:1000, 1:10000, 1::100000. Each cDNA sample was loaded in triplicate (5ul from cDNA and 15ul from Master Mix as explained in the sample preparation section) into 96-well white qPCR plates and loaded into the LightCycler® 480. Triplicate averages for each dilution were plotted as a function of the Log dilution factor and fitted with a linear regression curve ($R2 \geq 0.95$). The slope of the regression line was used to calculate the primer efficiency (E= [(10^-1/slope)-1] *100). The slope (m) of 100% primer efficiency is -3.32 and acceptable efficiency range was set between 1.80 and 2.10. We measured *Kv4* primer efficiency for *Kv4* (m=-3.336, 99%), RpS20 (m= -3.348, 99%) and eIF1A (m= - 3.475, 94%) as demonstrated in **figure 1**.

6.2 Sample preparation and workflow

Each freshly prepared cDNA was diluted 1:5 with PCR-grade H_2O. Master Mix was

prepared in the following manner: for each reaction, 3.8 uL of PCR-grade H2O, 0.4 uL of 20 uM forward primers, 0.4 uL of 20 uM reverse primer, 0.4 uL of 10 uM Probe from Universal Probe Library (UPL), and 10 uL LightCycler® 480 Probes Master Mix (Roche, Switzerland). Each sample was loaded in triplicate for GOI (*Kv4*) and Ref genes (*RpS20* and *eIF1A*). For each reaction 5 ul of diluted cDNA and 15 ul of master mix were loaded in 96-well white qPCR plates (Roche, Switzerland). Each loaded plate was sealed with a transparent plastic sheet and spun for 2 min in a plate-centrifuge. The plate was then loaded into the LightCycler® 480 Instrument II (Roche, Switzerland). Monocolor hydrolysis universal probe setting was used. The Second Derivative Maximum method was used to identify C_t values as mentioned in LightCycler® 480 manual user.

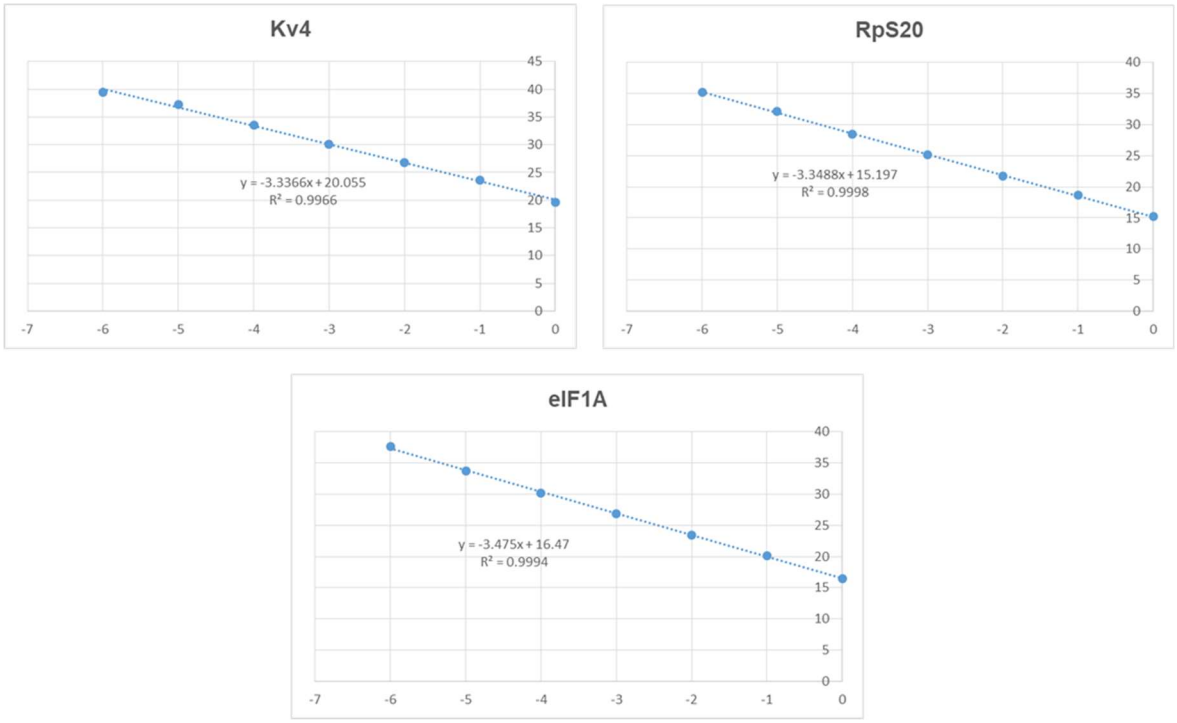

Figure 1. Log of dilution factors plotted against Ct values and slopes were used to estimate primer efficiency.

6.3 Data collection and analysis

To evaluate relative gene expression, Ct values for triplicate were copied and transferred to an Excel spreadsheet. Standard deviation among each sample triplicate for GOI and Ref gene was calculated (criteria of <0.16) and average of each triplicate were reported. The Dixon's Q-test was applied to remove any outliers among averages of GOI and Ref Gene. If any averages were identified as outliers, the sample was excluded from further statistical analysis. Reference gene stability was estimated by examining the standard deviation between averages of triplicates of reference gene in control and experimental groups; we used a criterion of <1.0. To evaluate relative expression, $2^{-\Delta\Delta ct}$ method was used to calculate fold change of cDNA copies relative to a reference gene (307). Student's t-test was applied to determine statistical differences.

7. Digital Droplet Polymerase Chain Reaction (ddPCR)

For ddPCR experiments, we used the same primers as designed for RT-qPCR and followed the same protocol for cDNA preparation. Digital droplet PCR was used to measure the number of target molecules, as predicted using the Poisson distribution. Probability theory of this statistic depends on positive droplets (at least one target copy) and negative droplets (no target copy) (308). If the number of positive droplets and/or negative droplets are too high or low, the Poisson distribution cannot predict the number of target copies per sample. To avoid this, it is important to first determine an appropriate concentration/dilution of the starting material.

7.1 Identifying proper starting material concentration

After preparing a cDNA pool from 700ng total RNA, we tested different cDNA concentrations: no-template, 0.5ng, 1.0ng, 1.5ng, 3.0ng, 5.0ng. We found that 1.5ng was the optimal concentration to obtain an acceptable number of positive and negative droplet populations (Positive population should not be less than 10.000 droplets) that can be analyzing using Poisson distribution.

7.2 Sample preparation and workflow

RNA extraction and cDNA preparation were performed as mentioned in the previous section. 1.5ng cDNA and master mix were prepared ((10ul ddPCR Supermix for probes, 0.4ul forward primer, 0.4ul reverse primer, 0.4ul Probe, 1ul cDNA, 7.4ul H2o). For each sample, two different reactions (*Kv4* and *RpS20*) were prepared. To generate droplets, the 20ul reaction mix and 60ul droplet generation oil were added to wells in the DG8 Cartridge for the QX200 droplet generator, which was then inserted into the automated droplet generator. After that, droplets were transferred to a 96-well plate. The plate was sealed with foil using the PX1 PCR plate sealer, and PCR amplification of template molecules in each separate droplet performed in the C1000 Touch Thermal Cycler with a 96-deep well reaction. The following thermal cycling protocol was used: 95 °C for 10 minutes (one cycle), 94 °C for 30 seconds (40 Cycles) and then 60 °C for 1 minute (40 cycles), 98 °C for 1 minutes (one cycle), and hold at 4 °C. The ramp rate was set at 2 °C/s, the sample volume at 40 mL, and the heated lid at 105 °C. After PCR amplification, the plate was inserted into the QX200 Droplet Reader, and the absolute

template expression in copies per microliter was quantified using QuantaSoft software for *Kv4* and *Rps20* for each sample.

7.3 Data collection and analysis

Any sample that displayed less than 10,000 positive droplets was excluded from analysis. Student's t-test was used to compare the number of positive droplets in control and experimental groups to evaluate reference gene stability. For each sample, the number of *Kv4* copies/ul were normalized to the number of *RpS20* copies/ul from the same sample. Student's t-test applied to evaluate statistical analysis between control and experimental population.

CHAPTER 3. CHOLINERGIC HOMEOSTATIC SYNAPTIC PLASTICITY

3.1 Overview

The capacity of neurons and circuits to maintain activity levels within an appropriate range is accomplished by homeostatic mechanisms crucial for neural network signaling. These compensatory processes constitute homeostatic synaptic plasticity (HSP). HSP is a negative feedback process by which neurons modify (scale) their synaptic strength to adjust for increased or decreased overall input, thereby protecting the neurons from hyper- or hypo-activity that could otherwise lead to neural network instability. Homeostatic regulation of synaptic strength maintains the excitation/inhibition balance in the neural network, which is essential for proper network capacities, including long-term potentiation (LTP) and long-term depression (LTD). Dysregulation of the excitation/inhibition balance often contributed to neurological disorders(309).

Cholinergic receptors in the mammalian brain are exposed to activity changes during development and during pathological conditions. For instance, cholinergic activity is up- regulated in early Alzheimer disease (208,310) with an increase in choline acetyltransferase levels (311) and α7 nAChRs (312,313). Cholinergic receptors at the human neuromuscular junction also experience dynamic changes in activity is some disorders. Myasthenia Gravis (MG) is an autoimmune disease that affects endplates and result in muscle fatigue and weakness due to loss of post-synaptic cholinergic receptors (309). This condition results in an increase in neurotransmitter release in response to network activity alteration (52).

Blocking the nicotinic Acetylcholine Receptor (nAChR) (*in vitro*) which is the major excitatory receptor in the *Drosophila* central nervous system (CNS), has been shown to result in an increase in frequency and amplitude of miniature excitatory post-synaptic currents (mEPSCs), concurrent with a selective increase in levels of the *Drosophila* nAChR α7 subunit (Dα7) (205). This homeostatic change in Dα7 nAChR level was shown to mediate the stabilization synaptic strength (205).

We used a temperature-sensitive choline acetyltransferase mutant allele, Cha^{ts2}, to inhibit cholinergic synaptic activity *in vivo* and studied if this induces a homeostatic response and molecular changes that affect synaptic strength. In this Chapter, we show that Cha^{ts2}-induced inactivity triggers a homeostatic response that is represented by an increase in Dα7-nAchRs. NACHO is a chaperone protein that plays an important role in α7-nAChRs assembly and trafficking (218). We found that *in vivo* activity inhibition using the Cha^{ts2} mutant allele resulted in an increase in *Drosophila* NACHO (dNACHO). We also confirmed that increasing dNACHO causes an increase in Dα7 protein level, suggesting that the mechanism underlying the homeostatic up-regulation of Dα7 might involve dNACHO

3.2 Cha^{ts2}-induced inactivity up-regulates Dα7-nAChRs (Homeostatic response)

An earlier *in vitro* study from our lab showed that prolonged pharmacological blockade of neural activity in *Drosophila* neurons results in a selective increase in the *Drosophila* α7 (Dα7) subunit of nAChRs that mediates an increase in miniature excitatory post-synaptic currents (mEPSCs) (205). Here, we set out to examine whether we could apply an *in vivo* blockade of activity and detect a similar homeostatic response. Since

homozygous *Cha^{ts2}* mutants exhibits significantly reduced levels of ChAT activity even at permissive temperatures (18 °C) (213), we used heterozygous *Cha^{ts2}*/+ mutants, which likely exhibit ChAT activity more similar to wild-type when grown at 18 °C. *Cha^{ts2}/+* heterozygotes raised at 30 °C have been reported to exhibit ~35% less ChAT activity compared to wild type (212).

We used the pan-neural elav/UAS-Gal4 system to express Dα7-EGFP in a *Cha^{ts2}*-(*elav;; Cha^{ts2}/UAS-Dα7-EGFP*) and wild-type background (*elav;;UAS-Dα7-EGFP/+*). In this way, expression of Dα7-EGFP would be constitutively and similarly expressed, so that any change in Dα7-EGFP protein, would indicate an induced change in Dα7-EGFP protein and likely represent the response of endogenous Dα7. Flies were grown at 18 °C, collected at <24 hours after eclosion (AE), and subjected to either no HT, or 3 hours HT at 30°C to test if *Cha^{ts2}*-induced inactivity homeostatically enhanced Dα7-EGFP protein levels. By immunoblot analysis, steady-state levels of Dα7-EGFP were normalized to a loading protein control. We found that levels of Dα7-EGFP were indeed enhanced by ~36% in response to *Cha^{ts2}*-induced activity inhibition, compared to untreated flies; in contrast, similar HT induced no change in Dα7-EGFP levels in the absence of the *Cha^{ts2}* allele (**Figure 2**). This is consistent with Dr.Hahm's finding in our lab that reducing cholinergic activity using the *Cha^{ts2}* allele induces an increase in mEPSCs (314).

It is interesting that in our lab's *in vitro* study, up-regulation was observed immediately after activity blockade, however, in our in *vivo* study, we found that a 3-hour recovery time is necessary to detect the Dα7-EGFP increase in response to *Cha^{ts}*-induced inactivity (**Figure 2**).

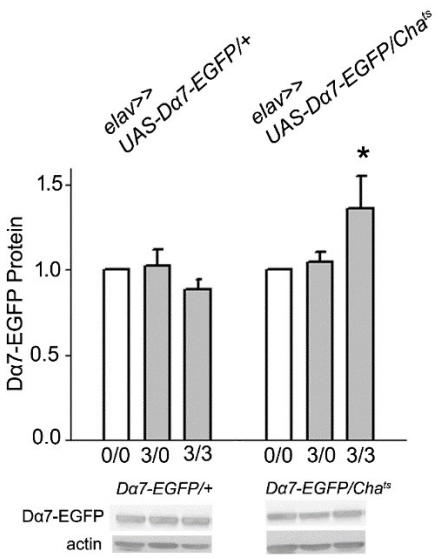

Figure 2. Inhibition of Cholinergic Activity in *Cha^{ts2}*/+ Neurons Induces a Homeostatic Increase in Dα7 Protein. Quantification and representative immunoblots of *elav-Gal4>>UAS-Dα7-EGFP/+* and *elav-Gal4>>UAS-Dα7-EGFP/Cha^{ts2}* flies grown at 18 °C, then subjected to 0 or 3 hours HT and no recovery and 3 hours recovery at 18 °C (0/0, 3/0 and 3/3, respectively). All immunoblots were run with 5 heads per sample per lane. Anti-GFP band intensities were normalized to those of anti-actin, which were used as loading control; for each condition, N=24-46 samples per condition. All data are represented as mean +/- SEM; *$P<0.05$, Students t-test.

This discrepancy probably comes from the method of activity blockade. *In vitro*, cholinergic activity was blocked with curare, an antagonist of cholinergic receptors. With curare, synaptic activity was completely blocked, and this is considered to be a toxic condition for neurons, so the homeostatic response was faster and occurred immediately after washout of the blocker. In our *in vivo* study, cholinergic activity was inhibited but was not completely blocked. There was probably some neurotransmitter still available at cholinergic synapses to bind to Dα7 nAChRs. In addition, in the *in vitro* study, activity was blocked persistently for 24 hours, but in our *in vivo* study, activity inhibition was only for 3 hours. These differences might occur for the late increase in Dα7-EGFP in our *in vivo* study compared to the previous *in vitro* study.

3.3 *Drosophila* NACHO (dNACHO) Up-regulates Dα7 expression

Recent studies have identified NACHO as a transmembrane endoplasmic reticulum resident protein that promotes biogenesis and surface expression of nAChRs (314), and in particular, α7 nAChRs (218). We obtained a *Drosophila* transgenic line that expresses d*NACHO* tagged with a hemagglutinin tag (HA) downstream of the **U**pstream **A**ctivating **S**equences (UAS), the HA epitope tag was used to confirm expression of NACHO-HA. We used the Gal80^{ts}/Gal4 system to express Dα7-EGFP or with dNACHO-HA, and then tested for a change in GFP expression. Gal80^{ts} contains temperature-sensitive mutation. Gal80^{ts} expression under the control of the tubulin promoter is constitutively expressed at 18˚C and negatively regulates Gal4 (Gal80 binds Gal4 C-terminal and forms a complex that blocks DNA binding). At 30˚C, Gal80^{ts} no longer affects Gal4; Gal4 binds to UAS and drives expression the downstream gene. To conditionally express dNACHO-HA and Dα7-EGFP after the completion of development, we generated *elav-Gal4;tub-Gal80^{ts}>>UAS-Dα7-EGFP/+* and *elav-Gal4;tub-Gal80^{ts}>>UAS-Dα7-EGFP/UAS-dNACHO*-HA lines. Both lines were raised at 18˚C at which temperature both genotypes develop normally, without over-expression of Dα7-EGFP and dNACHO, then after eclosion, young male adult flies were subjected to HT at 30°C for 4 days to induce expression of Dα7-EGFP alone or with dNACHO-HA. Dα7-EGFP protein levels were examined by immunoblot analysis. We found that Dα7-EGFP levels were elevated by ~45% when NACHO-HA was expressed (**Figure 3**). These findings suggest that dNACHO promotes Dα7-EGFP biogenesis similar to its mammalian counterpart.

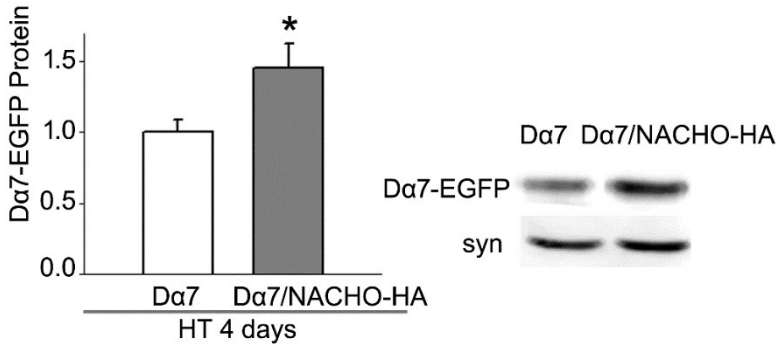

Figure 3. dNACHO positively regulated Dα7-EGFP. Representative immunoblots and quantitative analyses of steady-state levels of Dα7-EGFP. *elav-Gal4;tub-Gal80^{ts}>>UAS-Dα7-EGFP/+* (Dα7 only) and *elav-Gal4;tub-Gal80^{ts}>>UAS-Dα7-EGFP/UAS-NACHO-HA* (Dα7/NACHO). All fly lines were grown at 18 °C, allowing them to develop normally, and then subjected to heat-treatment at 30 °C (HT) for 4 days. Immunoblots lanes were run with 5 male heads per lane. Anti-GFP band intensities were normalized to those of anti-syntaxin (syn), which was used as a loading control. Data are represented as mean +/- SEM; *$P<0.05$, Students T-test.

3.4 Dα7-EGFP up-regulation has no effect on dNACHO protein level

To understand more about the relationship between dNACHO and Dα7, we next set out to test if Dα7-EGFP over-expression enhances expression of dNACHO. We used the Gal80/Gal4 system to express dNACHO-HA alone and to express Dα7-EGFP with dNACHO-HA and analyze for a change in dNACH-HA levels. To conditionally express dNACHO and Dα7-EGFP, we generated *elav-Gal4;tub-Gal80^{ts}>>UAS-* dNACHO-HA */+* and *elav-Gal4;tub-Gal80^{ts}>>UAS-Dα7-EGFP/UAS-dNACHO*-HA lines. Both lines were grown at 18˚C, at which temperature both genotypes develop, without over-expression of Dα7-EGFP or dNACHO-HA. Since heterozygous *elav>>UAS-dNACHO-HA* flies do not live more than two days at 30˚C, newly-eclosed flies were subjected to HT at 30 °C for 2 days to induce expression of dNACHO-HA alone and with Dα7-EGFP. dNACHO-HA protein levels were examined by immunoblotting analysis and we found that expression of Dα7-EGFP had no effect on dNACHO-HA levels (**Figure 4**), suggesting that Dα7-EGFP over-expression is not sufficient to induce an increase in dNACHO-HA expression.

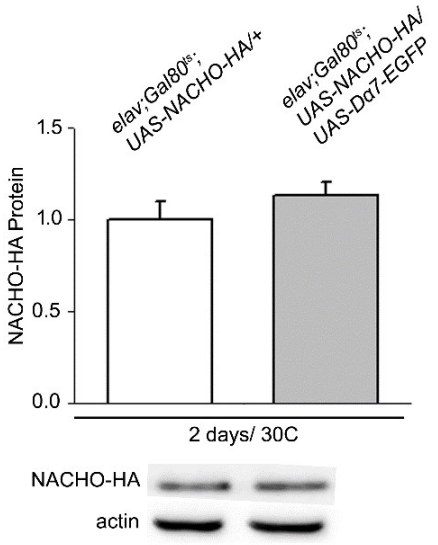

Figure 4. Dα7-EGFP over-expression does not affect dNACHO-HA protein level.
Representative immunoblots and quantitative analyses of steady-state levels of dNACHO-HA. *elav-Gal4;tub-Gal80^{ts}>>UAS- dNACHO-HA/+* (dNACHO-HA only) and *elav-Gal4;tub-Gal80^{ts}>>UAS-Dα7-EGFP/UAS-dNACHO-HA* (Dα7/dNACHO). All fly lines were raised at 18 °C, allowing them to develop normally, and then young adult flies subjected to heat-treatment at 30 °C (HT) for 2 days. Immunoblots lanes were run with 5 male heads per lane. Anti-HA band intensities were normalized to those of anti-actin, which was used as a loading control. Data are represented as mean +/- SEM; *$P<0.05$, Students T-test.

3.5 *Cha^{ts2}*-induced inactivity up-regulates dNACHO-HA protein level

Since *Cha^{ts2}* -induced inactivity resulted in an increase in Dα7-EGFP; we next set out to test if *Cha^{ts2}*-induced inactivity up-regulates α7 nAChRs chaperon protein, dNACHO. We used the UAS/Gal4 system to drive dNACHO-HA expression in a *Cha^{ts2}* mutant (*elav;; Cha^{ts2}/UAS-NACHO- HA*) and wild type background *(elav;; UAS-NACHO-HA/+).* Both genotypes were raised at 18°C, then after eclosion, flies were subjected to 3hrs at 30°C followed by 3hrs recovery at 18˚C. By immunoblot analysis, steady-state levels of dNACHO-HA were normalized to a loading protein control. We found that *Cha^{ts2}*-activity inhibition up-regulated dNACHO-HA compared to NACHO-HA in wild type background by over 40 X (**Figure 5**). Our results suggest that *Cha^{ts2}*-induced inactivity

up-regulation of dNACHO might be part of the mechanism underlying the homeostatic response, or alternatively, it may be a consequence of the increase in Dα7 nAChRs.

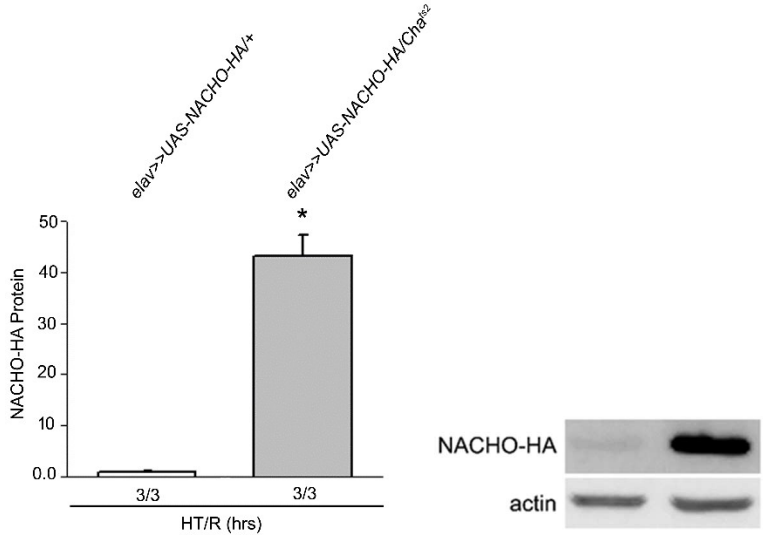

Figure 5. *Cha^{ts2}*-Induced Inactivity Induces dNACHO-HA Up-Regulation. Quantification and representative immunoblots of *elav-Gal4>>UAS-dNACHO*-HA */+* and *elav-Gal4>>UAS-NACHO*-HA */Cha^{ts2}* flies grown at 18 °C, then subjected to 3 hours HT at 30˚C and 3 hours recovery at 18 °C. All immunoblots were run with 5 heads per sample per lane. Anti-HA band intensities were normalized to those of anti-actin, which were used as loading control; for each condition, N=20-21 samples per condition. All data are represented as mean +/- SEM; *$P<0.05$, Students t-test.

3.6 Conclusion

Cha^{ts2}-induced inactivity *in vivo* induces a homeostatic response mediated by an increase in Dα7 nAChRs. Over-expression of the Dα7 nAChR chaperone protein, dNACHO, up-regulates the Dα7-EGFP subunit. Conversely, however, over-expression of Dα7-EGFP was not sufficient to up-regulate dNACHO-HA protein levels. In addition, we found that *Cha^{ts2}*-induced inhibition positively regulates dNACHO-HA, suggesting that dNACHO might contribute to mechanisms underlying the homeostatic response.

CHAPTER 4. REGULATION OF HSP BY KV4/SHAL CHANNELS

4.1 Overview

Our lab's previous *in vitro* study showed that prolonged inhibition of nicotinic acetylcholine receptors led to a homeostatic response that is mediated by a selective increase in the Dα7 subunit (205). Improper regulation of HSP, however, might cause additional under or over-compensation. Dr.Tsunoda's lab discovered a regulatory mechanism that prevents over-compensation and maintains the activity in an optimal range (205). Prolonged activity blockade of nAChRs in *Drosophila* neurons resulted in a homeostatic response that is tuned by an increase in the expression of the potassium channel Kv4/Shal (205). Kv4/Shal channels encode the transient A-type potassium current and they operate at subthreshold potentials, and plays a crucial role in initiating action potential firing, and regulating the frequency of action potential firing (315). In mammals, the Kv4.2 channel was down-regulated in response to glutamate receptors stimulation and led to an increase mEPSC amplitude, this down-regulation of Kv4.2 was shown to contribute to synaptic LTP (316–318).

We used the Cha^{ts2} mutant allele and a transgene that expresses tetanus toxin light chain to inhibit/reduce cholinergic activity *in vivo,* and then examined if a similar pathway was observed *in vitro*. In the previous chapter, we reported that the Cha^{ts2} mutant allele induces a homeostatic response mediated by an increase in Dα7 nAChRs. In this chapter, we characterize the regulatory mechanism that counterbalances the homeostatic response. We found that Kv4/Shal protein and mRNA were up-regulated in response to Cha^{ts2}-induce inactivity and TnT-activity blockade. We report that an increase in Kv4/Shal

protein and mRNA depends on Dα7 nAChRs. We also studied the relationship between Dα7 nAChRs and Kv4/ShaI. We found that over-expression Dα7-EGFP and/or dNACHO-HA is sufficient to induce an increase in Kv4/ShaI protein and mRNA. We then used *UAS-NACHO-RNAi* to knockdown dNACHO in a Cha^{ts2} mutant background and found that the Kv4/ShaI increase in response to Cha^{ts2}-induced inactivity was blocked with a knock down of dNACHO. We found that in *vivo* activity inhibition triggers a similar regulatory mechanism as described *in vitro*.

4.2 Cholinergic activity blockade increases Kv4/ShaI protein and mRNA levels

We first tested if *in vivo* activity inhibition using the Cha^{ts2} allele induces an up-regulation of Kv4/ShaI channels. Newly-eclosed Cha^{ts2}/+ and wild-type flies were collected and subjected to HT at 30°C. We tested different durations of HT, followed by a 3-hour recovery period at 18°C. We found that Cha^{ts2}/+ flies displayed a ~27% increase in Kv4 protein with a 3- or 6-hour HT (**Figure 6A**); we refer to the 3 or 6 hours of heat-treatment, followed by 3 hours recovery, as 3/3 or 6/3-protocols, respectively. Similarly treated wild-type flies showed no change in relative Kv4/ShaI protein levels (**Figure 6B**). Since *in vitro* studies had shown that the up-regulation of Kv4/ShaI was not apparent immediately following cholinergic blockade (3/0-protocol), but required recovery of synaptic transmission, we subjected Cha^{ts2}/+ flies to HT for 3 hours with different durations of recovery. Indeed, we found that no increase in Kv4/ShaI protein was observed immediately following activity inhibition and required a 3-hour recovery period (**Figure 6C**). For further confirmation that HT of Cha^{ts2} was a reliable method of inducing HSP, we tested another Cha^{ts} allele, Cha^{ts3} (213). Heterozygous Cha^{ts3}/+ flies subjected

to the 3/3 heat-treatment protocol also exhibited ~29% increase in Kv4/Shal protein (**Figure 6D**).

Although inactivity-induced up-regulation of Kv4/Shal protein was previously shown to be blocked by transcriptional inhibitors (205), it has been unclear whether this was due to a transcriptional block of *Kv4/Shal* itself since mRNA levels of *Kv4/Shal* could not be examined in that preparation. Our *in vivo* Cha^{ts2} model, however, allowed for sufficient mRNA to be isolated for reverse transcription-quantitative polymerase chain reactions (RT-qPCR). We examined if mRNA levels of *Kv4/Shal* are indeed elevated following activity blockade.

To this end, we validated universal probes with corresponding PCR primers for *Kv4/Shal, RpS20* and *eIF1A*, for efficient amplification, and optimized RNA preparation, RT reactions, and cDNA dilution factors for reliable RT-qPCR. For every experimental genotype and genetic background tested, stability each reference genes, *ribosomal protein S20* (*RpS20*) and *eukaryotic initiation factor 1A* (*eIF1A*), were validated before use. We tested the $Cha^{ts2}/+$ line immediately after inhibiting activity with a 3-hour HT at 30°C and prior to an up-regulation of Kv4/Shal protein that is detectable after a subsequent 3 hours of recovery (**Figure 6A**). We quantified *Kv4/Shal* mRNA levels relative to reference gene expression without HT (0/0), and after 3 hours HT. In wild type, *Kv4/Shal* mRNA levels showed no change with HT (**Figure 6E**). In contrast, when HT was applied to the $Cha^{ts2}/+$ line, *Kv4/Shal* mRNA levels were significantly elevated by 23% compared to untreated controls (**Figure 6F**). Interestingly, the rise in *Kv4/Shal* mRNA was rather short-lived when examined in Cha^{ts2} flies, returning to baseline levels

after 3 hours of recovery at 18 °C (3/3-protocol; **Figure 6F**), suggesting a transient and dynamic regulation of *Kv4/Shal* mRNA.

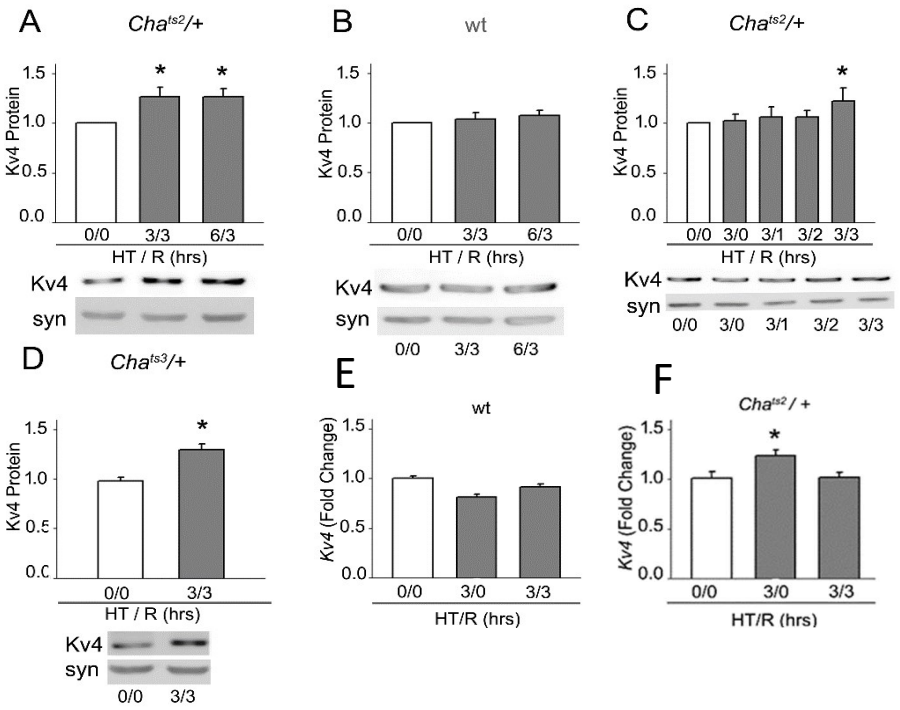

Figure 6. Blocking Neural Activity *In Vivo* Results in an Up-Regulation of Kv4/Shal Protein. (**A-C**) Quantification of relative Kv4/Shal protein levels and representative immunoblots from *Cha*^{ts2}/+ (**A, C**), wild-type (wt; **B**), and *Cha*^{ts3}/+ (**D**) after HT protocols, indicated as hours of HT at 30°C/hours of recovery at 18°C (e.g. 3/3, 6/3; 0/0 indicates flies kept at 18°C with no HT). Note that 3-6 hours HT of *Cha*^{ts2}/+ induces an increase in Kv4/Shal protein. (**E** and **F**) RT-qPCR analyses of *Kv4/Shal* mRNA levels normalized to reference gene expression, expressed as "Fold Change". Comparison of wt and *Cha*^{ts2}/+ male flies subjected to heat-treatment and recovery (HT/R; hours at 30°C/hours of recovery at 18°C) protocols, as indicated.

4.3 Cholinergic activity blockade using tetanus toxin induces Kv4/Shal Protein and mRNA up-regulation

We also inhibited cholinergic activity by another approach, using a transgenic line that expresses tetanus toxin light chain (TnT), which cleaves n-synaptobrevin and has been shown to completely block evoked neurotransmitter release and reduce spontaneous release by 50- 75% (319,320). We used a *heat-shock-GAL4* (*hs-Gal4*) line to induce expression of *UAS-TnT* (*hs-GAL4>>UAS-TnT*) in all neurons for 2 hours. After

heat-shock at 37°C, we allowed the flies to recover at 18°C. Fly heads were analyzed by immunoblot analysis for steady-state levels of Kv4/Shal normalized to a loading control protein. We found that levels of Kv4/Shal were increased by 29% after heat-shock and a two-hour recovery period (this protocol is indicated as “2/2”; **Figure 7A,** *right*). Kv4/Shal protein levels remained elevated for up to 24 hours following inactivity; in contrast, age-matched wild-type flies exposed to the same heat-shock protocols showed no significant change in relative Kv4/Shal protein levels (**Figure 7A,** *left*). Then inducing inactivity in these flies with a 2-hour heat shock at 37 °C, also up-regulates Kv4/Shal mRNA levels. We quantified *Kv4/Shal* mRNA levels relative to reference gene expression without heat-shock (0/0), and after 2 hours of heat-shock. Since 37°C activates endogenous heat-shock pathways and has been reported to have immediate effects on transcriptional activity (321), we quantified mRNA levels at later times: after 24 and 48 hours at 18°C (2/24 and 2/48 heat-shock protocols, respectively). In wild-type, *Kv4/Shal* mRNA levels showed no change with either the 2/24 or 2/48 heat-shock protocol (**Figure 7B,** *left*). In contrast, when heat-shock protocols were applied to the *hs-GAL4>>UAS-TnT* line, *Kv4Shal* mRNA levels were significantly elevated by ~46% at 24 hours following heat-shock, compared to untreated controls (**Figure 7B,** *right*). Relative *Kv4/Shal* mRNA levels then returned to basal levels after 48 hours (**Figure 7B,** *right*). In addition, we used a *Chat-Gal4* line, which drives expression of Gal4 in *choline acetyltransferase* (*Chat*) expressing neurons, to induce expression of *UAS-TnT.*

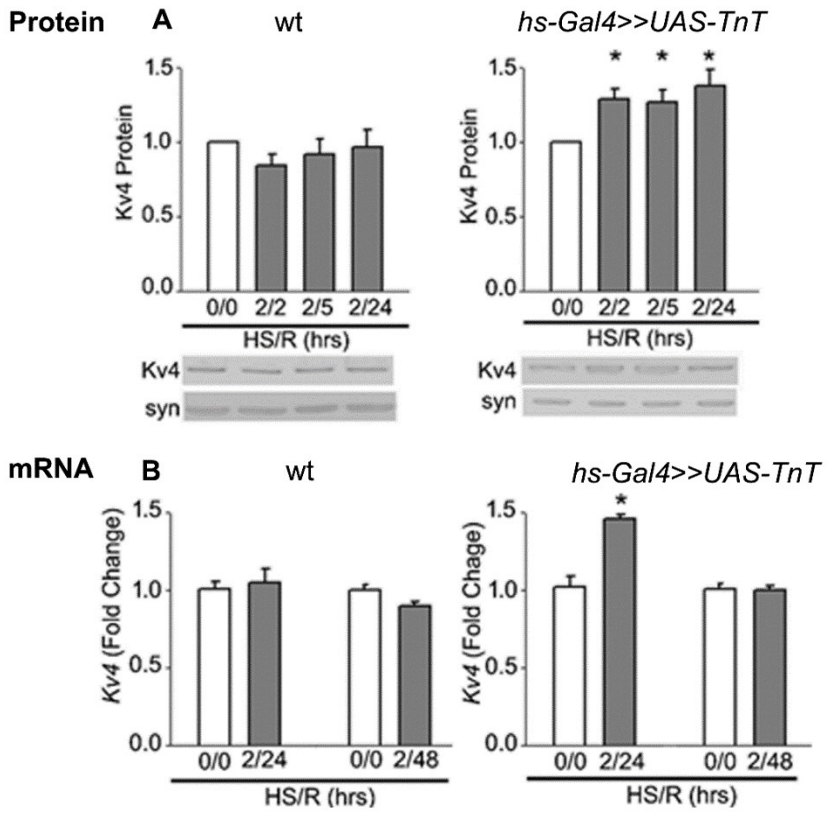

Figure 7. Blocking Neural/Cholinergic Activity Using Pan-neural Driver, *elav-Gal4*, to Drive Tetanus Toxin Expression Up-Regulates Kv4/Shal Protein/mRNA. (**A**) Quantification and representative immunoblots of wild-type (wt) and *hs-Gal4>>UAS-TnT* samples after various treatment protocols, indicated as hours of heat-shock at 37 °C/hours of recovery at 18°C (eg. 2/2, 2/5; note that 0/0 indicates flies kept at 18°C with no heat-shock). (**B**) RT-qPCR analyses of *Kv4/Shal* mRNA levels normalized to reference gene expression, expressed as "Fold Change". Comparison of wild-type (wt) and *hs-Gal4>>UAS-TnT* male flies subjected to heat-shock and recovery (HS/R; hours at 37 °C/hours of recovery at 18°C) protocols, as indicated. Note that 0/0 indicates no heat-shock treatment, and aged-matched 0/0 flies were used for 2/24 and 2/48 comparisons.

To induce expression transiently, we included expression of the temperature-sensitive Gal80^{ts} protein (Gal80^{ts}) to negatively regulate the function of Gal4. At 18 °C, Gal80^{ts} inhibits Gal4; at 30 °C, Gal80^{ts} is no longer functional and Gal4 promotes transcription of the *UAS-TnT* transgene in cholinergic neurons. We raised *Chat-Gal4;tub-Gal80^{ts}>>UAS-TnT* and wild-type lines at 18°C to allow them to develop normally, without expression of *UAS-TnT*, then after eclosion, young adult flies were subjected to HT at 30°C for 3 or 6

hours. After HT, we allowed flies to recover at 18°C for 3 hours. Flies' heads were analyzed by immunoblot analysis for steady-state levels of Kv4/Shal normalized to a loading control protein. We found that levels of Kv4/Shal protein were increased when heat treatment protocols were applied to the *hs-GAL4>>UAS-TnT* line by 42% after a 6/3 protocol (**Figure 8A,** *right*). In wild-type, Kv4/Shal protein levels showed no change under the same experimental conditions (**Figure 8A,** *left*).

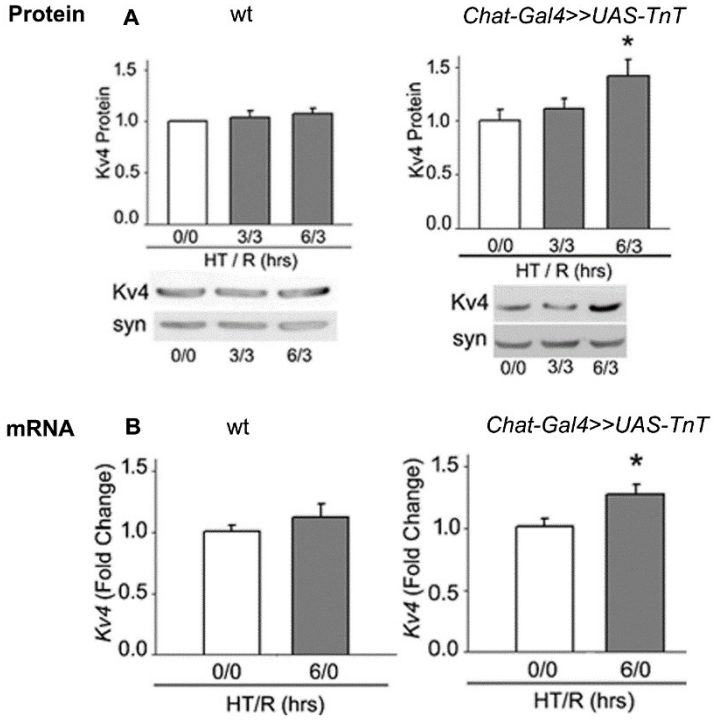

Figure 8. Blocking Neural/Cholinergic Activity Using *Chat* Driver, *Chat-Gal4*, to Drive Tetanus Toxin Expression Up-Regulates Kv4/Shal Protein/mRNA. (**A**) Quantification and representative immunoblots of wild-type (wt) and *Chat-Gal4>>UAS-TnT* samples after various treatment protocols, indicated as hours of heat-shock at 30°C/hours of recovery at 18°C (eg. 3/3, 3/6; note that 0/0 indicates flies kept at 18°C with no heat-shock). (**B**) RT-qPCR analyses of *Kv4/Shal* mRNA levels normalized to reference gene expression, expressed as "Fold Change". Comparison of wild-type (wt) and *Chat-Gal4>>UAS-TnT* male flies subjected to heat-shock and recovery (HT/R; hours at 30°C/hours of recovery at 18°C) protocols, as indicated.

Since *Kv4/Shal* mRNA levels were increased immediately and prior to the increase in Kv4/Shal protein following inhibition of cholinergic activity, we tested for a change in *Kv4/Shal* mRNA level in *Chat-Gal4;tub-Gal80ts>>UAS-TnT* immediately after inhibiting

activity with a 6-hour HT at 30°C. We quantified *Kv4/Shal* mRNA levels relative to reference gene expression without HT (0/0), and after 6 hrs HT. In wild-type, *Kv4/Shal* mRNA levels showed no change with HT (**Figure 8B,** *left*). In contrast, when HT was applied to *Chat-Gal4;tub-Gal80ts>>UAS-TnT* line, *Kv4/Shal* mRNA levels were significantly elevated by 27% compared to untreated controls (**Figure 8B,** *right*). These findings suggest, that blocking neural activity using tetanus toxin is sufficient to up-regulate Kv4/Shal protein and mRNA.

Altogether, our results show that activity inhibition or blockade using Cha^{ts2} mutant allele, or a transgene expressing tetanus toxin, induces an increase in Kv4/Shal protein and mRNA.

4.4 Kv4/Shal protein and mRNA Up-Regulation depends on Dα7-nAChRs

In previous *in vitro* studies, inactivity induced Kv4/Shal protein and current up-regulation required Dα7-nAchRs (205). We set out to test if the up-regulation of Kv4/Shal protein and mRNA induced by *in vivo* activity blockade also requires the Dα7 nAChR. Heat treatment and recovery protocols (0/0 and 3/3) were applied to Cha^{ts2}/+ flies in a $D\alpha7^{P\Delta EY6}$ null mutant background ($D\alpha7^{P\Delta EY6};;Cha^{ts2}$/+). We found that in the absence of Dα7 nAChRs, Cha^{ts2}-induced up-regulation of Kv4/Shal protein was indeed inhibited (**Figure 9A**, *left*). Then we examined relative *Kv4/Shal* mRNA levels in $D\alpha7^{P\Delta EY6};;Cha^{ts2}$/+ flies. We found that the 3/0 HT protocol that induced an increase in *Kv4/Shal* mRNA in Cha^{ts2}/+ mutants resulted in no significant increase in *Kv4/Shal* mRNA in the $D\alpha7^{P\Delta EY6}$ null background (**Figure 9B**, *right*). As an additional control, we tested $D\alpha7^{P\Delta EY6}$ null

mutants alone and found no change in Kv4/Shal protein and mRNA levels with HT (**Figure 9A** *right* and **9B** *left*, respectively).

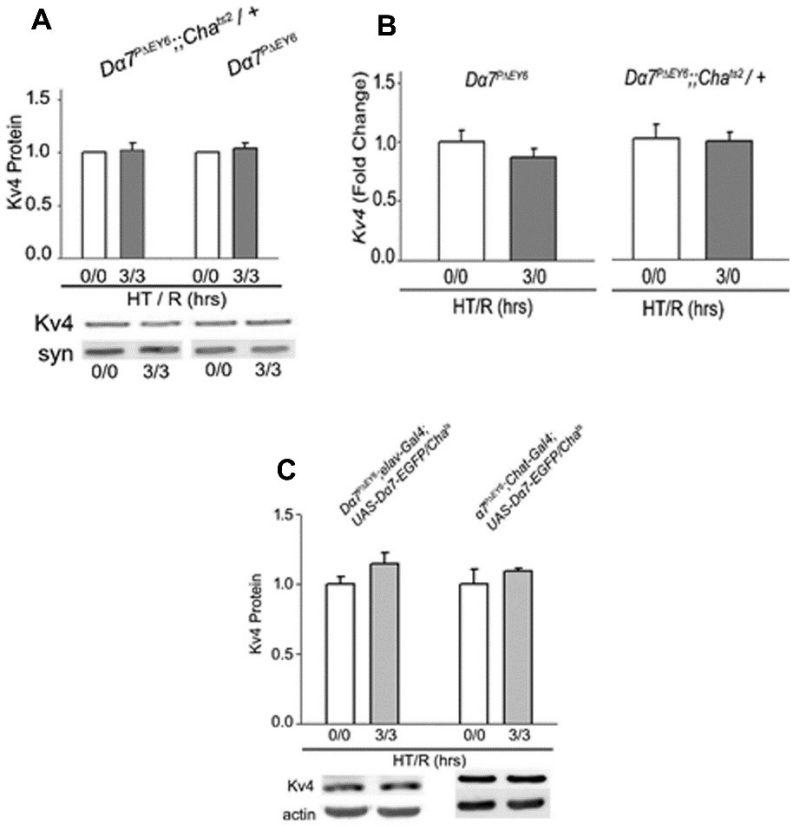

Figure 9. Kv4/Shal protein and mRNA up-Regulation in response to *Cha^{ts2}*-Induced inactivity requires Dα7 nAChRs. (**A**) Quantification and representative immunoblots of *Dα7^{PΔEY6};; Cha^{ts2}*/+, and *Dα7^{PΔEY6}* samples after indicated HT protocols shows no significant change in Kv4/Shal in the absence of Dα7. All immunoblots were run with 5 male heads per lane; for each condition, number of samples N=15-46. Anti-Kv4/Shal band intensities were normalized to those of anti-syntaxin (syn), which was used as a loading control. (**B**) Comparisons of *Dα7^{PΔEY6}* null mutants and *Dα7^{PΔEY6};; Cha^{ts2}*/+ flies subjected to HT/R, as indicated. Data are represented as mean fold-change +/- SEM (means are from N=10-17 independent RNA extraction and RT-qPCR); note that fold-changes are calculated in comparison to the corresponding 0/0 condition shown. (**C**) Quantification and representative immunoblots of rescue experiment for Kv4/Shal protein levels in *Dα7^{PΔEY6};elav-Gal4;UAS-D7-EGFP/Cha^{ts2}* (left) and *Dα7^{PΔEY6};Chat-Gal4;UAS-D7-EGFP/Cha^{ts2}* (right). HT/R protocols shows no significant change in Kv4/Shal protein level. Data are represented as mean +/- SEM; *$P<0.05$, Students t-test.

We attempted to rescue the inactivity-induced regulation of Kv4/Shal protein in the mutant Dα7 background by expressing transgenic Dα7-EGFP. We used elav-Gal4 and/or Chat-Gal4 to drive expression UAS-Dα7-EGFP in *Cha^{ts2}* mutant flies (*Dα7^{PΔEY6};elav-*

Gal4;Cha^{ts2}/UAS-Dα7-EGFP and *Dα7^{PΔEY6};Chat-Gal4;Cha^{ts2}/UAS- Dα7-EGFP* , respectively). We applied 0/0 and 3/3 protocols to these genotypes and found no change in Kv4/Shal levels (**Figure 9C**). The inability to rescue the increase in Kv4/Shal protein might be due to insufficient Dα7-EGFP expression because the location of elav-Gal4 system . Together, our results suggest that *in vivo* inhibition of cholinergic activity induces a homeostatic up-regulation of Dα7 nAChRs that is required for subsequent increase in Kv4/Shal protein/mRNA.

4.5 Over-expression of Dα7-EGFP and/or dNACHO-HA results in Shal/Kv4 protein and mRNA Up-Regulation

We aimed to overexpress Dα7-EGFP alone and test if it is sufficient to induce an increase in Kv4/Shal channel protein and mRNA. We used the pan-neural elav/Gal4 system to constitutively express UAS-Dα7-EGFP. Newly-eclosed *elav;; UAS-EGFP* and genetic background flies were raised at room temperature for 2 ,4 ,6 , and 10 days. Kv4/Shal steady-state protein levels were tested by immunoblot analysis. We found that constitutively expressed Dα7-EGFP had no effect on Kv4/Shal protein levels at 2 days and 10 days. However, 4 days and 6 days showed a decrease in Kv4/Shal protein level (**Figure 10**). Since constitutive expression of Dα7-EGFP might be complicated by development and long-term expression, we next used the Gal80^{ts}/Gal4 system to conditionally induce expression of Dα7-EGFP after development. We raised *elav-Gal4;tub-Gal80^{ts}>>UAS-Dα7-EGFP/+* and background control lines at 18°C to allow them

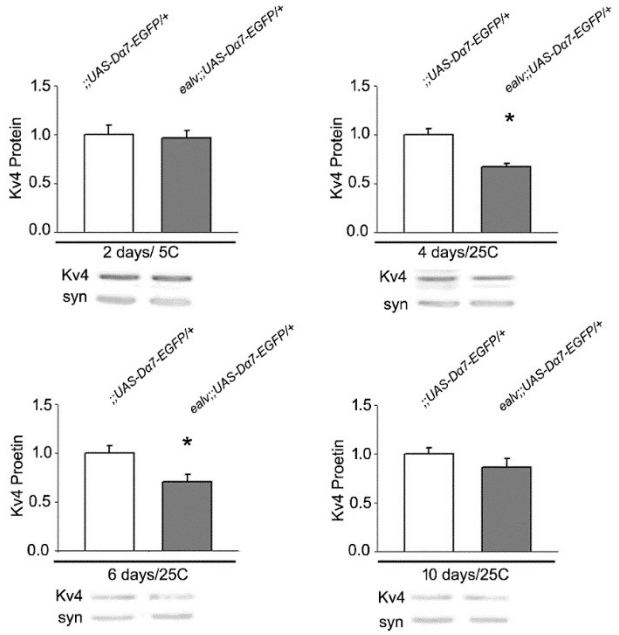

FIGURE 10. Constitutive expression of Dα7-EGFP has no effect on Kv4/Shal protein. Quantification and representative immunoblots of *elav;;UAS-Dα7-EGFP and ;;UAS-Dα7-EGFP* samples after different times of age show no increase in Kv4/Shal in response to constitutive Dα7-EGFP expression. All immunoblots were run with 5 male heads per lane; for each condition. Anti-Kv4/Shal band intensities were normalized to those of anti-syntaxin (syn), which was used as a loading control. Data are represented as mean +/- SEM; **P<0.05*, Students t-test.

to develop normally, without over-expression of Dα7-EGFP, then after eclosion, young adult flies were subjected to HT at 30°C for 2days, 4 days, and 6 days to induce expression of Dα7-EGFP. We then, tested whether this post-eclosion over-expression of Dα7-EGFP induced an increase in the level of Kv4/Shal protein. After 4 days, we found that induced expression of Dα7-EGFP resulted in an increase in Kv4/Shal protein levels, which were elevated by ~14% (**Figure 11A***)*. At 2 and 6 days, however, Kv4/Shal protein levels were decreased (data not shown).

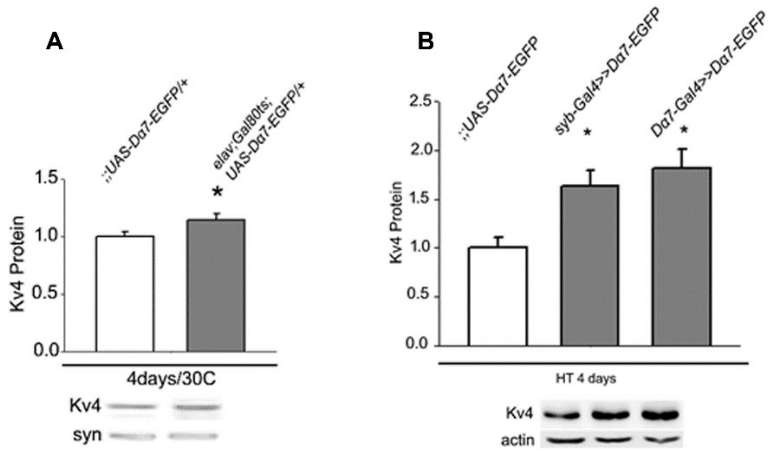

Figure 11. **Effect of Dα7-EGFP Over-Expression expression on Kv4/Shal protein. (A)** Quantification and representative immunoblots of *elav;Gal80^{ts};UAS-Dα7-EGFP and ;;UAS-Dα7-EGFP* samples. 4 days of HT shows increase in Kv4/Shal in response to transient Dα7-EGFP expression. Anti-Kv4/Shal band intensities were normalized to those of anti-syntaxin (syn), which was used as a loading control (**B**) Representative immunoblots and quantitative analyses for K_v4 expression in *UAS-Dα7-EGFP/+*, *W; tub-Gal80^{ts}>>UAS-Dα7-EGFP/ syb-Gal4* and *Dα7-Gal4;tub-Gal80^{ts}>>UAS-Dα7-EGFP/+.* Newly eclosed flies (<24 hours) were subjected to heat-treatment (HT) for 4 days at 30 °C. Samples were collected for immunoblot analyses and probed for K_v4/Shal. Anti-K_v4 signals were normalized to anti-actin signals as a loading control. 5 heads/sample/lane; N= 12 samples for each condition. Means normalized to the *UAS-Dα7-EGFP* background control samples on the same immunoblots are shown +/- SEM; **P<0.05*, Students t-test.

To further examine similarly up-regulation of Kv4/Shal was observed when we used a *Dα7-Gal4* driver or *syb-Gal4* (*Dα7-Gal4;tub-Gal80^{ts}>>UAS-Dα7-EGFP/+ and W;tub-Gal80^{ts}>>UAS-Dα7-EGFP/syb-Gal4* respectively) (**Figure 11B**). To further test the Dα7-Kv4/Shal relationship, we set out to increase the expression of endogenous Dα7 and test for effects on Kv4/Shal protein levels. Recent studies have identified NACHO as a transmembrane endoplasmic reticulum resident protein that promotes biogenesis and surface expression of nAChRs (220), and in particular, α7 nAChRs (218). Thus, we aimed to over-express the *Drosophila* ortholog, NACHO, in neurons, as a way of increasing the expression/trafficking of endogenous Dα7 nAChRs (reported in chapter3 **Figure 3**), and

then test if this results in a consequent increase in Kv4/Shal expression. We used an *UAS-dNACHO-HA* transgenic line in combination with *elav-Gal4* and *tub-Gal80^{ts}* transgenes to conditionally over-express *UAS-dNACHO-HA* in the nervous system of adult flies. The HA epitope tag was used to confirm expression of NACHO-HA. We raised *elav-Gal4;tub-Gal80^{ts}>>UAS-dNACHO-HA* and background control lines at 18 °C, then after eclosion, flies were subjected to HT at 30°C. *elav-Gal4;tub-Gal80^{ts}>>UAS-dNACHO-HA* flies, which were homozygous for the *UAS-NACHO-HA* insertion, were only viable for 12-15 hours at 30°C. As such, we assayed Kv4/Shal protein at 12 hours and found that Kv4/Shal protein levels were indeed elevated in heat-treated *elav-Gal4;tub-Gal80^{ts}>>UAS-dNACHO-HA* flies by ~33%, while no change in Kv4/Shal protein level was observed in similarly treated background control lines (**Figure 12B**, *left*).

Interestingly, Kv4/Shal protein levels were increased by ~33% with dNACHO-HA over-expression but were increased by only ~14% with Dα7-EGFP over-expression. One possibility is that endogenous dNACHO is limiting when Dα7-EGFP is over-expressed, preventing maximal Dα7/Dα7-EGFP surface expression and thereby more limited up-regulation of Kv4/Shal. To address this, we conditionally over-expressed both *UAS-dNACHO-HA* and *UAS-Dα7-EGFP*, using the *elav-Gal4;tub-Gal80^{ts}* driver line. To allow for more balanced expression of dNACHO-HA and Dα7-EGFP, experimental and background control lines used were heterozygous for each insertion. Both lines were raised at 18°C during development, then after eclosion, flies were subjected to HT at 30°C. With co-expression of *UAS-dNACHO-HA/UAS-Dα7-EGFP*, flies lived longer than those over-expressing two copies of *UAS-dNACHO-HA* alone, allowing us to apply heat-treatment for days. We then examined how co-over-expression of dNACHO-HA and

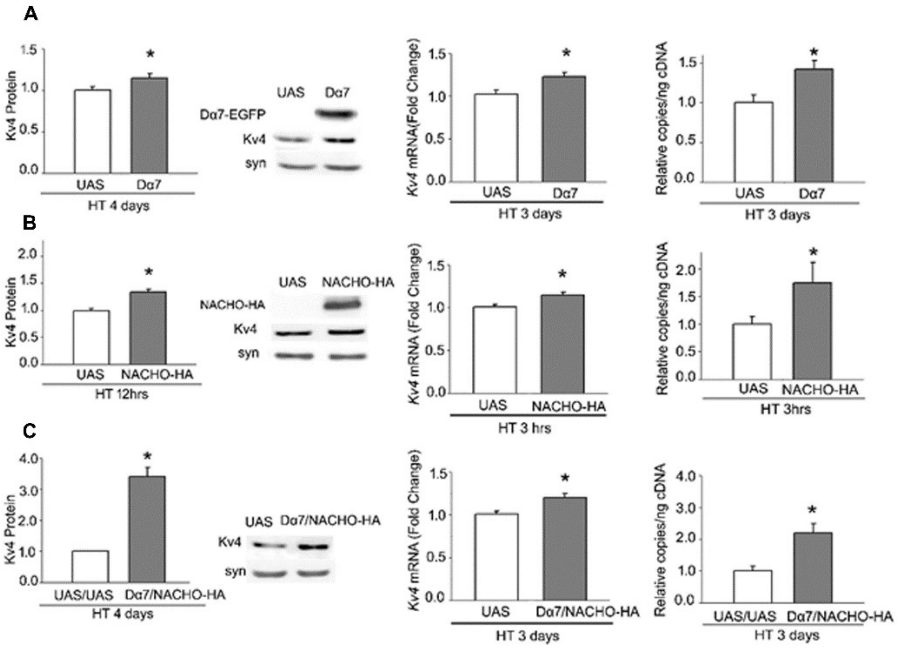

Figure 12. Over-expression Dα7 alone is sufficient to up-Regulate Kv4/Shal Protein/mRNA. (A-C) Representative immunoblots and quantitative analyses of steady-state protein levels (*Left*) and digital droplet PCR (ddPCR) analyses (*Right*) of samples from: (**A**) *UAS-Dα7-EGFP/+* (UAS) and *elav-Gal4;tub-Gal80^{ts}>> UAS-Dα7-EGFP/+* (Dα7), (**B**) *UAS-NACHO-3xHA* (UAS) and *elav-Gal4;tub-Gal80^{ts}>>UAS-NACHO-3xHA* (NACHO), (**C**) *UAS-Dα7-EGFP/UAS-NACHO-3xHA* (UAS/UAS) and *elav-Gal4;tub-Gal80^{ts}>>UAS-Dα7-EGFP/UAS-NACHO-3xHA* (Dα7/NACHO). All fly lines were grown at 18°C, allowing them to develop normally, then subjected to heat-treatment at 30°C (HT) for the indicated times. All immunoblots (*Left*) were run with 5 male heads per lane. Anti-Kv4/Shal, Anti-GFP and Anti-HA band intensities were normalized to those of anti-syntaxin (syn), which was used as a loading control. Experimental means were then normalized to similarly treated genetic background control (UAS) means on the same immonblots; for each condition, N=17-23, data are represented as mean +/- SEM; **P<0.05*, Students T-test. For RT-qPCR analyses of *Kv4/Shal* mRNA levels normalized to reference gene expression, expressed as "Fold Change" (**A-C** Middle).For ddPCR (**A-C** Right), data are represented as mean copy number per ng cDNA +/- SEM (means are from N=10-21 independent RNA extractions and RTs), normalized to mean copy number/ng cDNA from similarly treated genetic background control (UAS) values.

Dα7-EGFP affected Kv4/Shal protein levels. We found that Kv4/Shal protein levels more than tripled (**Figure 12C**, *left*).

We next tested if induced expression of Dα7-EGFP and/or dNACHO-HA results in an elevation in *Kv4/Shal* mRNA. We used the *elav-Gal4* driver in combination with Gal80^{ts}, as performed when examining Kv4/Shal protein expression. For each genotype,

we assayed for *Kv4/Shal* mRNA levels at times prior to detected elevations in Kv4/Shal protein. Indeed, *Kv4/Shal* mRNA levels were enhanced by Dα7-EGFP or NACHO-HA over-expression (**Figure 12A-C**, *middle*). We noticed that when we over-expressed Dα7-EGFP or dNACHO-HA alone, an increase in protein levels are similar to increase in mRNA levels , but when we co-expressed Dα7-EGFP and NACHO-HA, the increase in Kv4/Shal protein was much greater than the increases in mRNA seen. Since Digital Droplet polymerase Chain Reaction (ddPCR) is more sensitive than RT-qPCR (308), we reexamined Kv4/Shal mRNA levels using ddPCR. We found that *Kv4/Shal* mRNA levels were increased by Dα7-EGFP or NACHO-HA over-expression by 42 % and 74%, respectively (**Figure 12A-C**, *right*), and more than 100% with over-expression of Dα7-EGFP and NACHO-HA (**Figure 12A-C,** *left*). Together, our results suggest that an increase in Dα7-EGFP alone is sufficient to trigger an up-regulation of *Kv4/Shal* mRNA and protein expression.

4.6 RNAi knockdown of *dNACHO* block the Cha^{ts2}-induced increase in Kv4/Shal protein

Since dNACHO positively regulates Dα7-EGFP (**Figure 3**) and Kv4/Shal (**Figure 12B**), we set out to test if dNACHO is required for Kv4/Shal up-regulation in response to Cha^{ts2}-induced inactivity. We used *UAS-NACHO-RNAi* to knockdown dNACHO in the Cha^{ts2} mutant background and then investigated for change in Kv4/Shal protein level after activity inhibition. At 18˚C *w;Chat-Gal4/UAS-Dcr2;*Cha^{ts2}*/UAS-NACHO-RNAi* flies were subjected to heat treatment at 30C° for 3 hours and then returned to 18˚C for recovery for 3 hours (3/3). Flies' heads were analyzed by immunoblot analysis for steady state

levels of Kv4/Shal normalized to a loading control protein. We found that dNACHO knockdown prevented any *Cha*^{ts2}-induced increase in Kv4/Shal (**Figure 13**), suggesting that dNACHO is required for the inactivity-induced up-regulation of Kv4/Shal.

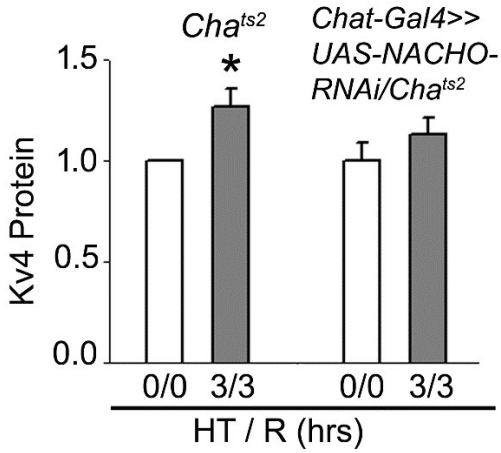

Figure 13. *dNACHO* knockdown inhibits Kv4/Shal protein up-regulation in response to *Cha*^{ts2}-Induced inactivity. Representative immunoblots and quantitative analyses of steady-state Kv4/Shal protein levels from heads of *Chat-Gal4/UAS-Dcr2>>UAS-NACHO-RNAi/Cha*^{ts2} (*Right*, *Chat-Gal4>>UAS-NACHO-RNAi/Cha*^{ts2}) flies grown at 18 °C, then either not heat-treated (0/0) or subjected to heat-treatment at 30°C for 3 hours followed by recovery at 18°C for another 3 hours (3/3). Flies' heads were analyzed for steady-state levels of Kv4/Shal protein by immunoblot analysis, N = 15. Note that no significant increase in Kv4/Shal is observed when expression of dNACHO is inhibited, in contrast to samples from similarly treated *Cha*^{ts2}/+ flies (*Left*; data here is the same as shown in **Figure 5A**). **P<0.05*, Students t-test.

4.7 Conclusion

We conclude that activity inhibition/blockade using the *Cha*^{ts2} mutant allele and transgenic expression tetanus toxin in *in vivo* induces an increase in Kv4/Shal protein and mRNA, similar to our lab's previous *in vitro* observations. The increase in Kv4/Shal protein, not mRNA, requires a recovery time after *Cha*^{ts2}-induced inactivity as well as the Dα7 nAChR. We studied the relationship of Dα7 nAChRs and Kv4/Shal. We found that Dα7-EGFP subunit over-expression is sufficient to increase in Kv4/Shal protein and mRNA expression, suggesting that an increase in Dα7 nAChRs under any condition may induce Kv4/Shal expression. Our finding that dNACHO knockdown blocks the increase

Kv4/Shal protein in response to *Cha*^{ts2}-induced inactivity is consistent with the idea that a dNACHO-dependent increase in Dα7 induces Kv4/Shal up-regulation.

CHAPTER 5. Ca^{+2}-DEPENDENT TRANSCRIPTIONAL ACTIVATORS, INCLUDING DNFAT AND DCREB-2, ARE INVOLVED IN KV4/SHAL UP-REGULATION IN RESPONSE TO *Cha^{ts2}*-ACTIVITY INHIBITION

5.1 Overview

We tested candidate Ca^{+2}-dependent transcriptional activators, including *Drosophila* **N**uclear **F**actor of **A**ctivated **T**-cell (dNFAT) and *Drosophila* cAMP-**R**esponsive **E**lement **B**inding protein-2 (dCREB-2), that might be involved in the inactivity-induced Kv4/Shal up-regulation. First, we tested if *Cha^{ts2}*-induced inactivity and Dα7-EGFP over-expression activates a human NFAT based reporter system, the Ca^{2+}-dependent nuclear import of LexA (*CaLexA*) system. We found that both, inactivity or Dα7-EGFP expression activates the *CaLexA* system. In addition, we found that dNFAT is required for Kv4/Shal protein and mRNA up-regulation in response to activity inhibition using *Cha^{ts2}*. When we over-expressed dCREB-2a, the activated form of CREB-2, we observed an increase in Kv4/Shal protein and mRNA.

5.2 *Cha^{ts2}*-Induced Inactivity, or Over-Expression of Dα7, Activates the dNFAT-Based CaLexA Reporter

With mounting evidence that *Kv4/Shal* is dynamically and transcriptionally regulated downstream of changing neural activity and Dα7 nAChR levels, we set out to identify transcriptional regulators involved. Previously, the Tsunoda lab demonstrated that the inactivity-induced increase in Kv4/Shal protein was dependent on intracellular Ca^{2+},

likely enhanced by the increased number of Ca^{2+}-permeable Dα7 nAChRs (308). We considered Ca^{2+}-dependent transcriptional regulators, including Nuclear Factor of Activated T-cells (NFATs), which are activated by the Ca^{2+}-dependent protein phosphatase 2b, calcineurin (CaN). CaN has been shown to trigger translocation of mammalian NFATs into the nucleus, where they lead to increases or decreases in transcription (322–324). To test if *dNFAT* might be a Ca^{2+}-dependent transcriptional regulator involved in the inactivity-induced up-regulation of *Kv4/ShaI*, we first examined if inactivity induced with the Cha^{ts2} allele would activate an *in vivo* NFAT-based reporter system, the Ca^{2+}-dependent nuclear import of LexA (CaLexA) system (325). In the CaLexA system, a transgene containing the regulatory domain of human NFATc1 is fused to the mutant bacterial DNA-binding protein mLexA and the VP16 activation domain, *UAS-mLexA-VP16-NFAT*. When the mLexA-VP16-NFAT protein is expressed, it is cytoplasmic, and if the NFAT regulatory domain is activated, the fusion proteins translocate to the nucleus, where it promotes transcription from a *LexAop* sequence upstream of a reporter gene. This modified human NFAT has been shown to successfully translocate to the nucleus and drive expression of *LexAop-CD2/8-GFP* in the fly CNS and has been used as a Ca^{2+} reporter (325).

We used *elav-Gal4* to drive neuronal expression of *UAS-mLexA-VP16-NFAT*, in a Cha^{ts2}/+ mutant background, which also contained reporter insertions, *LexAop-CD8-GFP* and *LexAop-CD2-GFP*. These flies were subjected to 0/0 and 3/0 HT (30 °C) protocols. We then tested for CD8/CD2-GFP expression by immunoblot analysis, as an indicator for CaLexA activation. Indeed, we found that CD8/CD2-GFP expression was increased by ~49% with the 3/0 HT protocol, compared with age-matched flies not subjected to HT

(0/0) (**Figure 14A**); and levels of CD8/CD2-GFP continue to rise with additional recovery time after HT (**Figure 14C**). In contrast, *elav-Gal4>>UAS-mLexA-VP16-NFAT/LexAop-CD8-GFP;LexAop-CD2-GFP/+* lines, without the Cha^{ts2} allele, showed no increase in CD2/8-GFP with the same HT. These results suggest that inactivity induced by Cha^{ts2} does indeed activate an NFAT-based reporter system *in vivo*. We additionally tested whether over-expression of Dα7-EGFP alone was sufficient to activate the CaLexA reporter. We raised *elav-GAL4;tub-GAL80^{ts}>>UAS-Dα7-EGFP/UAS-mLexA-VP16-NFAT,LexAop-CD8-GFP;LexAop-CD2-GFP/+* flies at 18°C to allow for normal development, then after eclosion, young adult flies were subjected to HT at 30°C to induce expression of Dα7-EGFP. Since HT on the order of days was required to observe sufficient over-expression of Dα7-EGFP using the *elav-GAL4;tub-GAL80^{ts}* inducible driver to induce Kv4/ShaI expression (**Figure 11A,** *left*), we expected that activation of the CaLexA reporter would require at least 24 hours HT to induce sufficient over-expression of Dα7-EGFP. We found that CD8/CD2-GFP reporter expression more than doubled after 24 hours of heat-induced Dα7-EGFP expression compared to HT of the background control line, *elav-GAL4;tub-GAL80ts>>UAS-mLexA-VP16-NFAT,LexAop-CD8-GFP/+;LexAop-CD2-GFP/+* (**Figure 14B**). Our results demonstrate that inactivity, which homeostatically up-regulates Dα7, or even direct over-expression of Dα7, is sufficient to activate an NFAT-based reporter system, and possibly endogenous dNFAT itself.

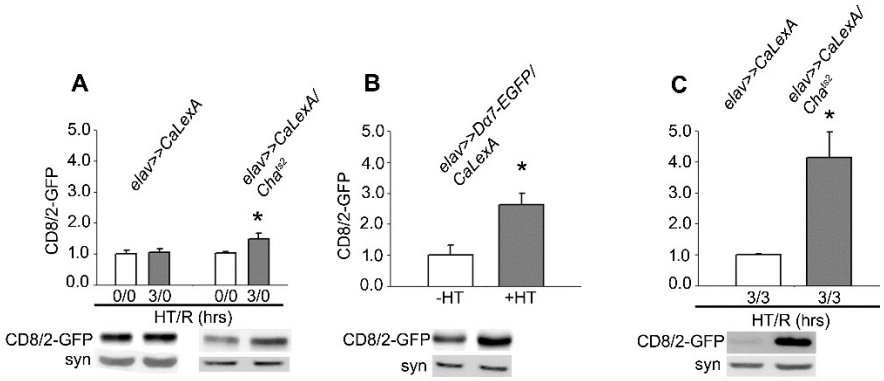

Figure 14. *In vivo* Activity Inhibition, or Dα7 Over-Expression, Activates the NFAT-Based CaLexA Reporter. (**A**)Representative immunoblots and quantitative analyses for CD8/CD2-GFP expression in *elav-Gal4>>LexAop-CD8-GFP/+;UAS-mLexA-VP16-NFAT*,*LexAop-CD2-GFP/+* (*elav>>CaLexA*) and *elav-Gal4>>LexAop-CD8-GFP/+;UAS-mLexA-VP16-NFAT*,*LexAop-CD2-GFP/Cha^{ts2}* (*elav>>CaLexA/Cha^{ts2}*) flies subjected to 0/0 and 3/0 heat-treatment protocols (HT/R; hours at 30 °C/hours of recovery at 18 °C), as indicated. Anti-GFP signals were normalized to anti-syntaxin (syn) signals, as a loading control, then normalized to control (0/0) samples on the same immunoblots; N=11-12 samples for *elav>>CaLexA*, N=18 for *elav>>CaLexA/Cha^{ts2}*. Note that the CD8/2-GFP levels responding to activation of the CaLexA reporter are elevated with HT of *Cha^{ts2}*. (**B**) Representative immunoblots and quantitative analyses for CD8/CD2-GFP expression in heads from *elav-Gal4;tub-GAL80ts>>UAS-mLexA-VP16-NFAT*,*LexAop-CD2-GFP/UAS-Dα7-EGFP; LexAop-CD8-GFP/+* flies were grown at 18°C, then either not heat-treated (-HT) or heat-treated at 30°C for 24 hours (+HT). Quantification of GFP, normalized to anti-syntaxin, was performed as described above; N=12-14 samples. Note that the CD8/2-GFP levels responding to activation of the CaLexA reporter are elevated with HT to induce over-expression of Dα7-EGFP. (**C**)Representative immunoblots and quantitative analyses for CD8/CD2-GFP expression in *elav-Gal4>>LexAop-CD8-GFP/+;UAS-mLexA-VP16-NFAT*,*LexAop-CD2-GFP/+* (*elav>>CaLexA*) and *elav-Gal4>>LexAop-CD8-GFP/+;UAS-mLexA-VP16-NFAT*,*LexAop-CD2-GFP/Cha^{ts2}* (*elav>>CaLexA/Cha^{ts2}*) flies subjected to the 3/3 heat-treatment protocol (3 hours at 30 °C, followed by 3 hours of recovery at 18°C). Anti-GFP signals were normalized to anti-syntaxin (syn) signals, as a loading control, then normalized to *elav>>CaLexA* samples on the same immunoblots; N=13 samples for *elav>>CaLexA*, N=16 for *elav>>CaLexA/Cha^{ts2}*. Note that the CD8/2-GFP levels responding to activation of the CaLexA reporter are significantly elevated with HT of *Cha^{ts2}*.

5.3 dNFAT is required for inactivity-induced up-regulation of Kv4/Shal

We next investigated whether NFAT might be involved in the regulation of *Kv4/Shal* expression. In *Drosophila*, there is only a single *NFAT* gene, dNFAT, that express two isoforms (-a and –b) under the control of two different promoters (305). First, we tested flies, which were null mutants for either or both d*NFAT-a* and/or d*NFAT-b and*

compared them to wild-type controls. We found no significant difference in the steady-state Kv4/Shal protein or mRNA levels (**Figure 15**), suggesting that dNFAT does not regulate basal levels of *Kv4/Shal* expression.

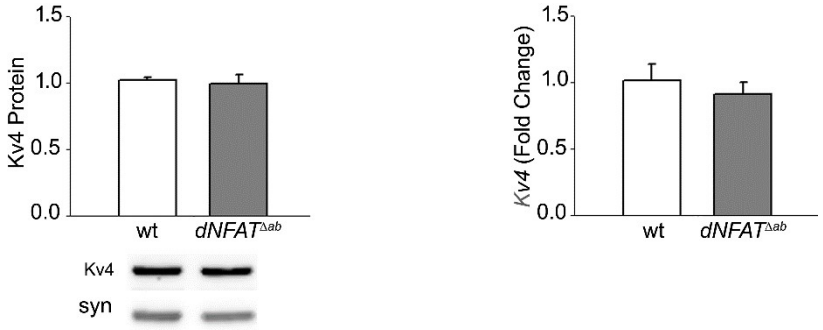

Figure 15. dNFAT does not affect basal levels of Kv4/Shal protein and mRNA levels. Representative Immunoblots and quantitative analyses for Kv4/shal protein and mRNA expression. Wild type (W^{1118}) and dNFAT mutant allele ($NFAT\Delta^{ab}$) flies were grown at room temperature for 4 days. Immunoblotting analysis of steady-state levels of Kv4/Shal normalized to loading control protein are shown on left. RT-qPCR analyses for *Kv4/Shal* mRNA, expressed as fold change shown on right.

Next, we tested test if dNFAT is required for the inactivity-induced up-regulation of Kv4/Shal. We crossed *dNFAT* mutant alleles into the Cha^{ts2}/+ mutant background and assayed whether inhibition of activity could still induce an up-regulation of Kv4/Shal protein in these flies. We subjected mutant combinations of Cha^{ts2} with $dNFAT^{\Delta a}$, $dNFAT^{\Delta b}$, or $dNFAT^{\Delta ab}$, as well as background control lines, to the 0/0 and 3/3 HT protocols that up-regulate Kv4/Shal expression in Cha^{ts2}/+ mutants. We found that Cha^{ts2}-induced inactivity was unable to elicit an increase in Kv4/Shal protein in the absence of *dNFAT-a* and/or *dNFAT-b* (**Figure 16 A-C**, *left*)*; NFAT* mutant alleles alone also showed no difference in Kv4/Shal levels with heat-treatment.

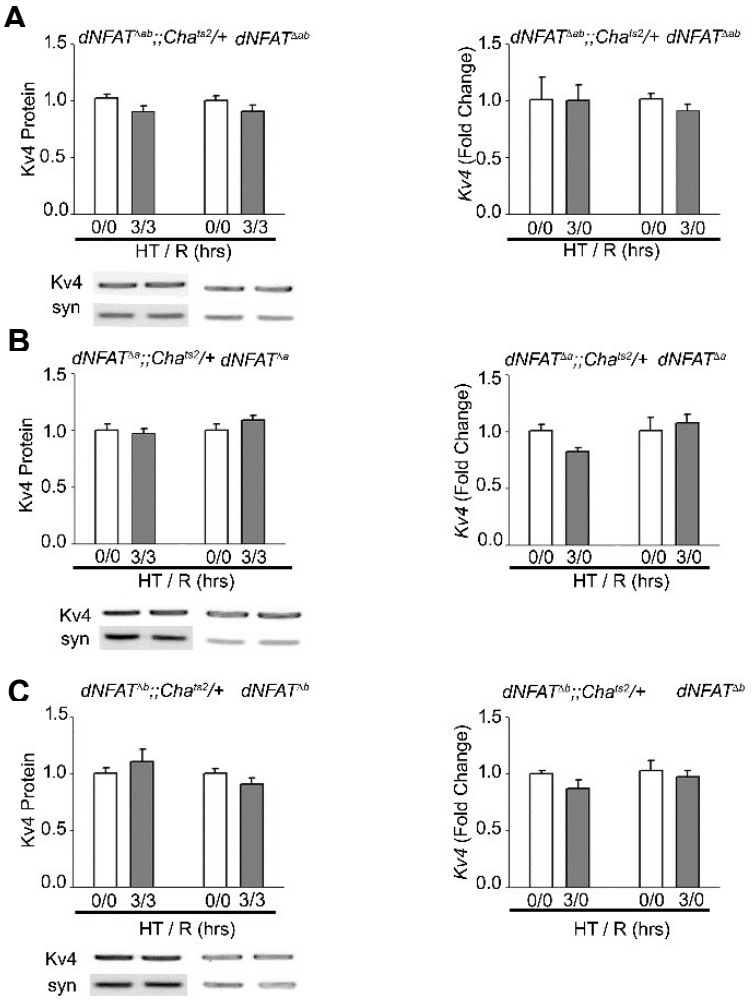

Figure 16. dNFAT is Required for the *Cha^{ts2}*-induced Increase in Kv4/Shal Protein and mRNA. (A-C) Representative immunoblots and quantitative analysis of relative Kv4/Shal protein levels (Left) and RT-qPCR analyses for *Kv4/Shal* mRNA, expressed as fold change (Right) comparing (**A**) *NFAT$^{\Delta ab}$* mutants and *NFAT$^{\Delta ab}$;;Cha^{ts2}/+* , (**B**) *NFAT$^{\Delta a}$* and *NFAT$^{\Delta a}$;;Cha^{ts2}/+,* (**C**) *NFAT$^{\Delta b}$* and *NFAT$^{\Delta b}$;;Cha^{ts2}/+* lines, subjected to heat-treatment/recovery (HT/R; hours at 30°C/hours of recovery at 18°C) protocols, as indicated. All immunoblots were run with 5 heads per lane. Anti-Kv4/Shal band intensities were normalized to those of anti-syntaxin (syn), which was used as a loading control; for each condition, N=15-25, data are represented as mean +/- SEM. For RT-qPCR, data are represented as mean fold-change +/- SEM (means are from N=9-14 independent RNA extraction and RT-qPCR); note that fold-changes are calculated in comparison to the corresponding 0/0 condition shown. *$P<0.05$, Students t-test.

We then tested these same genotypes for inactivity-induced up-regulation of *Kv4/Shal* mRNA. We subjected flies to the 0/0 and 3/0 HT protocols in which an up-regulation in *Kv4/Shal* mRNA is detected following inactivity. Similar to Kv4/Shal protein

analyses, we found that loss of *dNFAT-a and/ or dNFAT-b* blocked the up-regulation of *Kv4/Shal* mRNA (**Figure 16 A-C**, *right*); heat-treatment of *dNFAT* alleles alone also had no effect on *Kv4/Shal* mRNA levels. Altogether, our results suggest that while dNFAT does not affect basal levels of Kv4/Shal mRNA or protein, dNFAT is required for the transient up-regulation of Kv4/Shal mRNA and protein induced by cholinergic activity blockade.

For further study of the effect of dNFAT on Kv4/Shal, we used the *Gal4/Gal80^{ts}* system to conditionally over-express dNFAT, downstream of an UAS insertion (EP1353), in resting cells and test for a change in Kv4/Shal protein level. Both experimental flies (*NFAT^{EP1353};elav-Gal4;Gal80^{ts}*) and control flies (*w;elav-Gal4;Gal80^{ts} and NFAT^{EP1353}*;;) were raised in 18˚C without dNFAT over-expression. Newly-eclosed flies were subjected to HT for 4 days to over-express dNFAT. Flies' heads were analyzed for steady-state levels of Kv4/Shal protein by immunoblot analysis. We found that dNFAT over-expression has no effect on Kv4/Shal protein levels in resting cells (**Figure 17**). These findings suggesting that over-expressed dNFAT in resting cells needs to be activated in order to enter the nucleus and drive gene expression.

5.4 dCREB2-a over-expression up-regulates Kv4/Shal protein and mRNA

cAMP **R**esponse **E**lement –**B**inding **P**rotein-2 (CREB-2) has been found in all cell types. In mammalian nervous system, CREB is implicated in different systemic and cellular processes including responses to stress, circadian rhythm, and learning and memory (326–328). CREB is localized in the nucleus and when it is phosphorylated at

Ser 133, it is activated and transcribes target genes by binding to **c**AMP **R**esponse **E**lement (CRE) sites (329). CREB can be phosphorylated by different kinases, such as

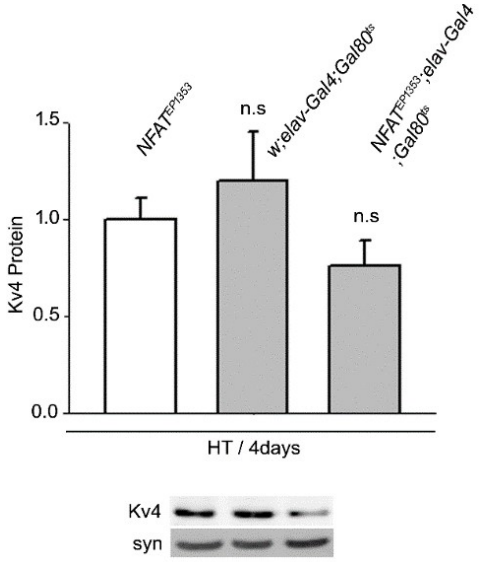

Figure 17. dNFAT Over-Expression Does Not Affect Kv4/Shal protein levels. Quantification and representative immunoblots of *NFAT^{EP1353}, W;elav-Gal4;Gal80^{ts}, NFAT^{EP1353},* and *elav-Gal4;Gal80^{ts}* samples after indicated HT protocols show no significant change in Kv4/Shal protein with dNFAT over -expression. All immunoblots were run with 5 male heads per lane; for each condition. Anti-Kv4/Shal band intensities were normalized to those of anti-syntaxin (syn), which was used as a loading control. Means normalized to the *NFAT^{EP1353}* background control samples on the same immunoblots are shown +/- SEM; *$P<0.05$, Students t-test.

protein kinase A (PKA), calmodulin-dependent protein kinase (CaMK), and mitogen-activated protein kinases (327). Multiple studies have reported that neurotransmitters are able to activate gene expression in a Ca^{+2} -dependent manner (232,330). In mammals CREB2-a is Ca^{+2}- dependent transcription activator (331,332). In neurons, intracellular Ca^{+2} largely comes through voltage or ion-gated channels. For instance, when the neurons are depolarized, the Ca^{+2} enters through L-type Ca^{+2} channels (326) or through α7 nAChRS (326). Intracellular Ca^{+2} binds to protein calmodulin (CaM) that activates CaMKI, CaMKII, and CaMKIV that are capable to phosphorylate and activate CREB2-a and initiate transcription (240,331,332).

In *Drosophila*, the orthlog of mammalian CREB is dCREB-2. dCREB-2 has multiple isoforms, including dCREB-2a that functions as a transcriptional activator and dCREB-2b that works as a transcriptional inhibitor by dimerizing with dCREB-2a and inhibiting its transcriptional activity (333). Over-expression of dCREB-2a, under the control of the heat-shock promoter enhances long-term memory (LTM) formation, while dCREB-2b over-expression blocks LTM (334). dCREB-2a positively regulates *slo*-encode BK-type Ca^{+2} activated K^{+} channels in response to drug tolerance (334). In addition, drug addiction affects dCREB2 expression, increasing dCREB-2a expression and reducing CREB-2b expression (334).

One possibility is that dCREB-2a is required for Kv4/Shal up-regulation in response to Cha^{ts2}-induced activity inhibition. We first over-expressed dCREB-2a using a heat-shock promoter in resting cells and assayed for in Kv4/Shal protein and mRNA. Flies carrying a *hs-CREB-2a* insertion were raised at 18˚C, at which temperature the heat-shock promoter is turned off. Newly-eclosed flies were subjected to heat-shock to turn on the promoter at 37˚C for 2hrs. Then, flies were returned to 18˚C for recovery for 2, 5, and 24 hrs since recovery was found to be required for Kv4/Shal protein up-regulation. Flies' heads were analyzed by immunoblot analysis for steady-state levels of Kv4/Shal, normalized to a loading control protein. We found that levels of Kv4/Shal protein were increased by 16%, 19%, and 42% after 2hrs, 5hrs and 24hrs of recovery, respectively, (this protocol is indicated as 2/2, 2/5; 2/24 **Figure 18A**, *left*) compared to non-heat shocked flies of the same genotype. Kv4/Shal protein levels remained elevated for up to 24 hours following inactivity. In contrast, age-matched wild-type flies exposed to the same heat-shock protocols showed no significant change in relative Kv4/Shal protein levels

(**Figure 18A**, *right*). Then we tested if inducing *dCREB-2a* over-expression in the *hs-CREB-2a* line with a 2-hour heat shock at 37°C, up-regulates *Kv4/Shal* mRNA levels. We quantified *Kv4/Shal* mRNA levels relative to reference gene expression without heat-shock (0/0), and after 2 hours of heat-shock. As discussed in chapter 4 subsection3, we could not measure the difference change in mRNA expression at early times (2-15hrs). We quantified mRNA levels at later times: after 24 at 18 °C (2/24 heat-shock protocols). We found that when heat-shock protocols were applied to the *hs-dCREB-2a* line, *Kv4/Shal* mRNA levels were significantly elevated by ~69% at 24 hours following heat-shock, compared to untreated controls (**Figure 18B**, *left*). In contrast, in wild-type, *Kv4/Shal* mRNA levels showed no change with 2/24 heat-shock protocol (**Figure 18B**, *right*). These findings suggest that dCREB2-a positively regulated Kv4/Shal protein and mRNA. We next set out to test if dCREB-2a is implicated in Kv4/Shal protein and mRNA up-regulation in response to Cha^{ts2}-induced inactivity.

Using the heat-shock promoter, we over-expressed negatively acting CREB variant (CREB-2b) in Cha^{ts2}-background and wild-type background and, then studied the effect of dCREB-2b on levels of Kv4/Shal protein and mRNA. We applied the 3/3 heat-shock protocol to *hs-CREB-2b;;*Cha^{ts2}/+ and *hs-CREB-2b;;* lines. Flies' heads were analyzed by immunoblot analysis for steady-state levels of Kv4/Shal normalized to a loading control protein. We found that there was no increase in Kv4/Shal protein in response to Cha^{ts2}-induced inactivity when *dCREB-2b* was over expressed (**Figure 18**). However, when we applied the same heat-shock protocol to the genetic background, *hsCREB-2b/+,* Kv4/Shal protein levels were down-regulated (**Figure 18C**).

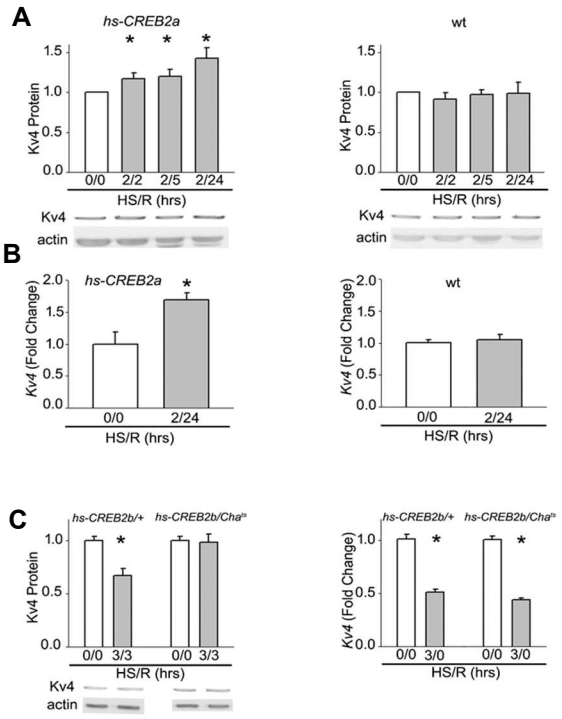

Figure 18. *dCREB-2a* is involved in Kv4/Shal Protein and mRNA up-regulation. (A-C) Representative immunoblots and quantitative analysis of relative Kv4/Shal protein levels and RT-qPCR analyses for *Kv4/Shal* mRNA, expressed as fold change. (**A**) *hs-CREB-2a* and *wt* Kv4/Shal protein. (**B**) *hs-CREB-2a* and *wt* Kv4/Shal mRNA, (**C**) *CREB-2b;;Cha^{ts2}/+* and *hs-CREB2-b;;* lines, subjected to heat-treatment/recovery (HT/R; hours at 37 °C/hours of recovery at 18 °C) protocols, as indicated. All immunoblots were run with 5 heads per lane. Anti-Kv4/Shal band intensities were normalized to those of anti-actin, which was used as a loading control; for each condition, data are represented as mean +/- SEM. For RT-qPCR, data are represented as mean fold-change +/- SEM. *$P<0.05$, Students t-test.

These findings showed that dCREB2-b negatively affected Kv4/Shal protein levels in resting cells making the lack of Kv4/Shal up-regulation in the *Cha^{ts2}* mutant background uninterpretable / inconclusive. Interestingly, expression of *d-CREB-2b,* in *Cha^{ts2}* resulted in a down-regulate *Kv4/Shal* mRNA.

5.5 Conclusion

We found that *Cha^{ts2}*-induced inhibition or Dα7-nAChRs over-expression activated the human NFAT-based reporter, CaLex A system. Then we tested the of involvement dNFAT in Kv4/Shal protein and mRNA up-regulation in response to induced inactivity.

We reported that the increase in Kv4/Shal protein and mRNA was blocked in the absence of either isoform of dNFAT. When we over-expressed the activated transcription factor, dCREB-2a, using a heat-shock promoter, we found an increase in Kv4/Shal protein and mRNA. These observations suggest that dNFAT is required for Kv4/Shal up-regulation and that dCREB2 might be also play a role Kv4/Shal up-regulation in response of cholinergic inactivity.

CHAPTER 6. DISCUSSION

6.1 Overview

Homeostatic synaptic plasticity is a crucial mechanism that protects neurons from activity perturbation (under/ over-activity) and maintains activity in an optimal range. HSP has been suggested to play a neuroprotective role during times of activity change, including during learning and memory formation, development, and some neuropathological conditions, such as Alzheimer's disease and nicotine addiction (335–338). Most HSP studies have focused on glutamatergic synapses, but a previous study in Dr. Tsunoda's lab has suggested that cholinergic receptors also mediate HSP in primary neurons from *Drosophila*. In this study, we used genetic and pharmacological tools to test for cholinergic HSP and its regulation by Kv4/Shal *in vivo.* We used tetanus toxin and Cha^{ts2} mutants to inhibit cholinergic activity. We found that Cha^{ts2}-induced inhibition resulted in a homeostatic response mediated by an increase in Dα7-nAChRs and an increase in Kv4/Shal protein and mRNA levels. We found that Kv4/Shal protein and mRNA up-regulation in response to Cha^{ts2}-induced inhibition depends on Dα7. In addition, we found that TnT-activity blockade resulted in an increase in Kv4/Shal protein and mRNA levels. We studied the relationship between Kv4/Shal and Dα7. We found that over-expression of Dα7-EGFP and/or dNACHO-HA is sufficient to induce an increase in Kv4/Shal protein and mRNA. We tested dNFAT, as a Ca^{+2}- dependent transcriptional activator, which might be involved in Kv4/Shal up-regulation in response to Cha^{ts2}-induced inactivity. We found that Cha^{ts2}-induced inhibition and/or Dα7-EGFP over-

expression activate a human NFAT-based reported, and that dNFAT is required for Kv4/Shal up-regulation in response to activity inhibition. Then we investigated the effect of dCREB-2 on Kv4/Shal levels. When we over-expressed the activated form,dCREB-2a, we found an increase in Kv4/Shal protein and mRNA. Since HSP is involved in multiple neuropathological conditions, understanding the underlying mechanisms and identifying the molecular players is important for potential treatment strategies of such conditions.

6.2 Cholinergic activity inhibition induces a homeostatic response and Kv4/Shal protein and mRNA up-regulation

Previous HSP studies have used pharmalogical agents to block neural activity. Disadvantages of using pharmacological approaches, such as tetanus toxin, to block neural activity are well known. For example, there is an uncertainty that the toxin is acting exclusively on specific enzymes/receptors**.** In addition**,** adding tetanus toxin will inhibit release of all neurotransmitters (339). It is also difficult to establish an efficient distribution and concentration of the toxin or know its effective period. For our study, we decided to choose a genetic approach to specifically block cholinergic activity and overcome some of these difficulties. Genetic tools have often served as an elegant method in *Drosophila melanogaster* to study many processes related to assembly and function of the nervous system (340)**.** We used the Cha^{ts2} allele that encodes a mutant protein that was found to function at the permissive temperature of 18˚C, but displayed reduced ChAT activity at the non-permissive temperature of 30˚C (212). The HT-induced change in ACh level is reversible and returns back to basal levels at 18˚C (214).

Greenspan (1980) (212) and Salvaterra and McCaman (1985) (214) have found that homozygous *Cha*^{ts} mutant flies raised at 18˚C, then shifted to 30˚C for 24hrs showed behavioral abnormalities including paralysis, starting as an inability to stand up, and later as a complete discontinuation of all movement. (212). This paralysis is likely related to the decrease in ACh levels and ChAT activity when *Cha*^{ts} mutant flies were shifted to 30˚C (214). The maximum time we exposed *Cha*^{ts2} mutant flies to HT was 48hrs and because the flies were heterozygous, we did not observe any paralysis, suggesting that heterozygous *Cha*^{ts2} mutants do not exhibit complete inhibition of ACh synthesis or complete diminishment ChAT activity during this time.

6.2.1 *Cha*^{ts2}- induced activity inhibition induces homeostatic response

We found an increase in Dα7-EGFP in response to *Cha*^{ts2}- induced inhibition *in vivo*. Dr. Hahm, in the Tsunoda lab, measured synaptic strength after transient inhibition of acetylcholine synthesis. With HT, he found progressively decreased activity, as expected, with a consequential enhancement in inter-event times (314). In addition, he found an increase in amplitude of mEPSCs (314), most likely mediated by the increase in Dα7 nAChRs, and similar to the observations reported by Dr. Tsunoda's lab previously (205). It is interesting that curare- induced activity blockade induced a homeostatic response in a Dα7 null mutant background, suggesting that another nAChR may also play a role in mediating the homeostatic response (205). It would be interesting for further studies to test for a change in all *Drosophila* nAChRs subunits in response to cholinergic activity inhibition. One possible experiment would be to use null mutants of different *Drosophila* nAChR subunits and test for HSP in response to cholinergic activity inhibition.

Additionally, in Dr.Tsunoda's lab, Dr. Justice immunostained the whole *Drosophila* brain to examine the effect of *Cha*^{ts2}-induced inactivity on endogenous Dα7. Dr. Justice found that cholinergic inhibition up-regulates the endogenous Dα7 subunit (314), consistent with the increase in Dα7-EGFP observed in *vivo*.

Dr. Justice, in Dr. Tsunoda's Lab, used the UAS/Gal4 system to express Dα7-EGFP in well-known and characterized neurons, the projection neurons and Kenyon cells, and examined the subcellular localization of Dα7-EGFP in resting cells. She found that Dα7-EGFP is localized in presynaptic and post-synaptic compartments (314) similar to its mammalian counterpart (201). To confirm that Dα7-EGFP was not mislocalized as consequences of overexpression, Dα7-EGFP was also expressed in Dα7 null mutant background. The study showed that Dα7-EGFP was similarly localized in pre- and post-synaptic compartments (314). In Dr. Tsunoda's lab, Dr. Hahm found that cholinergic activity inhibition using the *Cha*^{ts2} allele induces a decrease in mEPSC frequency in early times of HT, suggesting that a decrease in acetylcholine synthesis limits the available vesicles of ACh for release (314). He also found an increase in amplitude of mEPSCs, suggesting a postsynaptic homeostatic response most likely mediated by postsynaptic Dα7 nAChRs. At later times of HT, Dr. Hahm also found that an increase in the frequency of mEPSCs, suggesting that this later homeostatic response may be mediated by presynaptic Dα7 nAChRs (314). Further studies would be interesting to investigate Dα7 subunit localization in response to cholinergic activity inhibition. Additionally, multiple studies suggest that nAChRs mediate trans-synaptic or retrograde signaling at the mice NMJ and play a crucial role in presynaptic homeostasis (341). Further studies would be interesting to investigate if semaphorin–plexin signaling is implicated in presynaptic

homeostasis in response to *Cha*^{ts2}- induced activity inhibition to understand how postsynaptic neuron could communicate presynaptic neuron and initiate presynaptic homeostatic response.

6.2.2 *Cha*^{ts2}- induced activity inhibition induces a regulatory mechanism

The Kv4/Shal channel modulates the homeostatic response to prevent over-excitation. Dr.Tsunoda's lab discovered this regulatory mechanism that tunes the homeostatic response and prevents over-compensation (205). The Kv4/Shal channel mediates a transient A-type potassium current and because it is activated at subthreshold potentials, it plays a crucial role in initiating and regulating the frequency of action potential (315). Transient A-type current of potassium channel has been suggested to be pharmacological target to improve epileptogenic activity by suppressing EPSPs (340) and it is considered as essential player for modulating Ca^{+2} influx through synaptic NMDA receptors (342). In mammals, the Kv4.2 channel was down-regulated in response to glutamate receptor stimulation and led to an increase in mEPSC amplitude. Down-regulation of K4.2 has also been shown to contribute to the induction of LTP (316–318). We found that cholinergic activity inhibition in *vivo* resulted in an increase in Kv4/Shal protein after recovery of synaptic transmission similar to observations made after activity blockade in *vitro* (205).

Dr. Hahm, in Dr. Tsunoda's lab, measured changes in transient A-type potassium currents and delayed rectifier currents in response to *Cha*^{ts2}-induced inhibition. He found that the transient A-type current, mediated by Kv4/Shal, was up-regulated (314), similar to our lab's previous study observations (205). These findings are consistent with an

increase in Kv4/ShaI mRNA immediately after activity inhibition followed by Kv4/ShaI protein up-regulation (3/3).

Kv4/ShaI up-regulation requires the Dα7 subunit. Our lab's previous *in vitro* study documented that an increase in Kv4/ShaI protein in response to cholinergic activity blockade depends on the Dα7 subunit (205). We found that up-regulation of Kv4/ShaI protein and mRNA due to Cha^{ts2}- induced inhibition in *vivo* depends on Dα7 subunit too. *Drosophila* Dα5-7 subunits share high sequence identity (~60%) with mammalian α7, suggesting that Dα5-7 are orthologs of mammalian α7 (195–197). It would be interesting to test the possible involvement of Dα5 and Dα6 in Kv4/ShaI up-regulation in response to activity inhibition in *vivo*.

6.2.3 Cha^{ts2}- induced activity inhibition induces Dα7 chaperone protein up-regulation

Cha^{ts2}-induced activity inhibition resulted in an increase in dNACHO-HA. Mammalian and *Drosophila* NACHO are able to mediate α7 nAChRs expression and induce ACh currents in non- permissive cells (218). We showed that dNACHO-HA over-expression up-regulates Dα7-nAChRs. An interesting question is whether the increase in dNACHO-HA a mechanism is required for the homeostatic response, or a consequence of the Dα7 increase. It could be answered by testing for a change in dNACHO-HA in response to Cha^{ts2}-induced inhibition in a mutant *Dα7* background. If the increase in NACHO-HA is a part of the homeostatic response, it will be up-regulated and will not depend on the presence of Dα7, but if the increase is dependent on Dα7 up-regulation, we would see no change in dNACHO-HA levels.

6.3 Over-expression of Dα7 nAChRs alone is sufficient to up-regulate Kv4/Shal protein and mRNA

We studied the relationship between Kv4/Shal and Dα7 nAChRs. In *Drosophila* neurons, nAChRs mediate fast excitatory synaptic transmission (343)**.** We found that conditional expression of Dα7-EGFP or dNACHO-HA resulted in Kv4/Shal protein and mRNA up-regulation, suggesting that conditions that cause an increase Dα7 nAChRs would be followed by an up-regulation of Kv4/Shal as regulatory mechanism.

NACHO is a transmembrane chaperone protein that resides in the endoplasmic reticulum and plays an essential role in the folding, assembly, and trafficking of α7 nAChRs (218). When we over-expressed dNACHO-HA, immunoblot analysis showed that dNACHO-HA positively regulates Dα7-EGFP protein expression. These findings are consistent with other studies showing that dNACHO can recruit human nAChRs and induce ACh current in cell lines that normally do not form functional nAChRs (218). Our results showed that dNACHO-HA over-expression increases Dα7-EGFP protein levels, but that Dα7-EGFP over-expression did not affect dNACHO-HA protein level. This may be because Dα7-EGFP expression did not to require more dNACHO-HA, or there are other molecular mechanisms to prevent Dα7-EGFP from exceeding an allowed level (226,344). We did not test how dNACHO could play a role in the assembly and trafficking or recruitment of functional receptors to cell surface. Further studies should investigate how dNACHO affects Dα7 nAChRs, whether it be through cell surface expression, gene expression, or other pathways such as posttranslational changes.

Drosophila RIC-3 (dRIC-3) has 11 alternative splice forms, but only isoforms containing exon two, which encode a proline-rich N-terminal region, are unability to induce nAChRs maturation (345). When dRIC-3 is co-expressed with human α7 nAChRs and with a mixture of *Drosophila* and rat α7 nAChRs, many of dRIC-3 variants greatly enhanced α7 nAChRs maturation compared to human RIC-3 (345). It would be interesting to express dRIC-3 in *Drosophila* cholinergic neurons and test for a change in Dα7-EGFP protein levels and an effect on Kv4/Shal protein levels. In addition, one could investigate how dRIC-3 affects the ability of dNACHO to up-regulate Dα7-EGFP.

Lansdell et al 2012 (346) have found that Dα5 and Dα7 subunits are able to form homomeric nAChRs in *Xenopus* oocytes when they are co-expressed with the molecular chaperone RIC-3. In addition, they found that when RIC-3 is co-expressed with Dα5 and Dα6, this resulted in detectable cell-surface binding of α-bungarotoxin in both *Drosophila* and mammalian cell lines (346). Further studies could test for an effect of dRIC-3 on Dα5-Dα7 expression. Other studies have shown that when RIC-3 is co-expressed with a mixture of subunits, including Dα7 with Dα5 and Dα6, the specific binding of α-bungarotoxin was blocked in cell lines, suggesting that nAChR assembly and maturation can be blocked in some cellular environments (346).

6.4 dNFAT and dCREB2 are implicated in Kv4/Shal up-regulation

We used a human NFAT-based reporter to investigate if NFAT can be activated in response to Cha^{ts2}-activity inhibition or Dα7 over-expression. We found that both Cha^{ts2}-activity inhibition and Dα7 over-expression activated this NFAT based reporter. We tried to test if dNACHO-HA over-expression could activate NFAT based reporter but because

of multiple insertions are on the same chromosomes, we could not perform this experiment. The regulatory domain that was used to design the NFAT based reporter belongs to NFAT1 and this domain has calcineurine binding site, which plays a role in NFAT activity (249). Some studies have shown that dNFAT is similar to NFAT5 that lacks AP-1 and calcineurin binding sites (347), and is activated by a different pathway (282). Other studies have documented that dNFAT has part of AP-1 and calcineurin binding sites (348), suggesting that dNFAT may activated by Ca^{+2} / calcineurin pathway. It would be beneficial to design another NFAT-based reporter using the NFAT5 or dNFAT regulatory domain to test if *Cha*^{ts2}-activity inhibition or Dα7 over-expression might activate this dNFAT based reporter.

NFAT5 is activated and inhibited by different kinases. Many kinases, such as P38α, ERK1/2, c-ABI, and ATM induces NFAT5, activate NFAT5, however, GSK3β, CK1 and p38δ negatively regulate nuclear localization and transcription activity of NFAT5 (282). Activity inhibition of P38α and/or ERK1/2 using specific inhibitors resulted in blocking NFAT5 activity in response to hypertonic environment (349,350). In contrast, GSK3β negatively affects nuclear localization and transcription activity of NFAT5 in response to isotonic conditions (284). Further studies are needed to test if these enzymes are involved in dNFAT activation. This could be done by transfecting siRNA or mutating the functional domain of *Drosophila* P38α and examining effects on dNFAT activation. When we over-expressed dNFAT, we found no effect on Kv4/Shal protein and mRNA levels, however, we did not test if dNFAT protein and mRNA levels were indeed changed in response to dNFAT over-expression.

We tested if dNFAT is implicated in Kv4/Shal protein and mRNA up-regulation in response to *Cha*^{ts2}-activity inhibition. We found that an increase in Kv4/Shal protein and mRNA was blockade in the absence of dNFAT. We concluded that dNFAT is involved in Kv4/Shal regulation downstream of activity inhibition using the *Cha*^{ts2} mutant. Further studies are needed to examine if NFAT directly regulates Kv4/Shal expression. One could generate a reporter fused to sequence from the 5' upstream region of *Kv4/Shal* and test if dNFAT could drive expression of this reporter in response to *Cha*^{ts2}- induced activity inhibition *in vitro,* and eventually *in vivo*. In addition, studies should identify putative sites that may be recognized by dNFAT, and test whether or not dNFAT would bind to these sites *in vitro* and eventually, *in vivo* by mutational analyses. It is possible that dNFAT might not directly regulate Kv4/Shal expression. It could control expression of another transcription factor or transcription-required proteins, such as polymerase subunits that regulates Kv4/Shal expression.

Drosophila CREB2 (dCREB-2) plays important role in the expression of ion channels expression, such as the Ca^{+2}-dependent BK potassium channel, which plays a role in learning and memory formation (351). We showed that dCREB-2a over-expression positively regulate Kv4/Shal protein and mRNA levels. Although dNFAT is similar to NFAT5 and multiple studies have shown that NFAT5 does not interact with other transcription factors (352), further studies should examine whether dNFAT and dCREB-2a work independently in different ways or work cooperatively to regulate Kv4/Shal. Multiple transcription factors form complexes and synergistically activate transcription. For example, NFAT1-4 can interact with the AP-1 transcription factor, which often has binding sites close to regulatory sequences of NFAT1-4 (352). Although NFAT1-4 and

AP-1 have different binding sites on the regulatory sequence of NFAT target genes, NFAT1-4 and AP-1 coupling is often required for NFAT transcriptional activation (322,324,353). First, we need to identify the binding sites for dNFAT and dCREB-2a in the regulatory regions of *Kv4/Shal*. Preliminary studies in Dr. Tsunoda's lab have identified binding sites for dNFAT in regulatory sequence of *Kv4/Shal*. We could test if these transcription factors are working cooperatively. One could use CRISPR technique to induce mutations within binding sites of dNFAT and/or dCREB-2 and test for changes in Kv4/Shal in response to Cha^{ts2}- induced activity inhibition.

6.5 Conclusion

In this study, we used a genetic method of inhibiting activity *in vivo* that induces HSP and modulation by Kv4/Shal channels. We used the Cha^{ts2} mutant allele (**Figure 19**) and a transgene that expresses tetanus toxin light chain to inhibit/reduce cholinergic activity *in vivo*. Cha^{ts2}-induced inhibition induced a homeostatic response mediated by an increase in Dα7 nAChRs followed by an increase in Kv4/Shal protein and mRNA that was dependent on Dα7 nAChR subunit, demonstrating *in vivo* a pathway (**Figure 19**) has been observed in our lab's previous *in vitro* study.

Then we studied the relationship between Dα7 and Kv4/Shal. We tested if over-expression Dα7 alone, without activity manipulation, would be sufficient to up-regulate Kv4/Shal expression. We identified Dα7-Kv4/Shal coupled regulatory system. NACHO has been shown to play a role in α7 nAChRs biogenesis. We found that over-expression of Dα7-EGFP and/or dNACHO-HA was sufficient to up-regulate Kv4/Shal protein and mRNA. Additionally, we found that dNACHO-HA positively regulates Dα7-EGFP

expression and that *Cha*^{ts2}-induce activity inhibition up-regulates dNACHO-HA. Knocking down dNACHO blocked the up-regulation of Kv4/ShaI protein levels in response to cholinergic activity inhibition, suggesting that dNACHO is required for Kv4/ShaI up-regulation in response to *Cha*^{ts2}-induced activity inhibition.

In our lab's previous in *vitro* study, Kv4/ShaI protein increase in response to activity blockade was suggested to be transcriptionally regulated and dependent on Ca^{+2} influx. We tested if the Ca^{+2}-dependent transcriptional activator, dNAFT, might be involved in *Kv4/ShaI* mRNA up-regulation due to *Cha*^{ts2}- induced activity inhibition (**Figure 19**). First, we tested if activity inhibition the using *Cha*^{ts2} mutant allele or Dα7-EGFP over-expression could activate an NFAT-based reporter. We found that both activated this reporter. Then we examined if dNFAT is required for Kv4/ShaI up-regulation in response to *Cha*^{ts2}-induced activity inhibition. Although, dNFAT had not effect on basal levels of Kv4/ShaI, we found that dNFAT was required to up-regulate Kv4/ShaI protein and mRNA in response to activity inhibition. In addition, we tested the possibility that dCREB-2 might affect Kv4/ShaI expression. We over-expressed the transcription activator form of CREB-2 (hs-CREB-2a) and found an increase in Kv4/ShaI protein and mRNA levels. Altogether, our results show that cholinergic signaling inhibition in *vivo* using *Cha*^{ts2} mutant allele induces HSP mediated by Dα7 nAChRs and that this Dα7 upregulation itself is sufficient to trigger transcriptional activation, mediated by NFAT, of the *Kv4/ShaI* gene, revealing a novel receptor-ion channel coupled system for homeostatic tuning in cholinergic neurons.

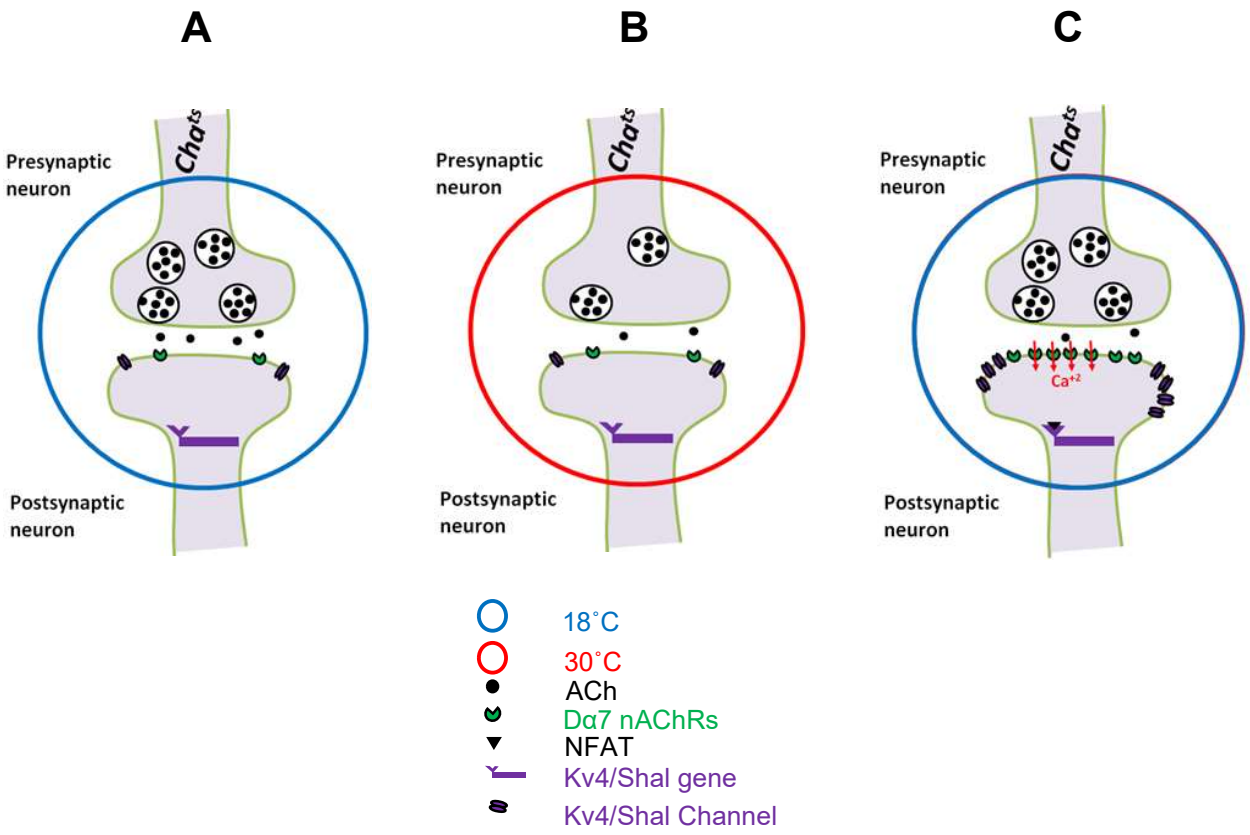

Figure 19. **Working model of homeostatic synaptic plasticity and regulatory mechanism in response to *Cha^{ts2}*- induced activity inhibition.** (**A**) Representive synapse at the permissive temperature of18˚C, at which the temperature-sensitive protein encoded by *Cha^{ts2}* functions normally and synthesizes sufficient acetylcholine (ACh). (**B**) At the restrictive temperature of 30˚C Cha^{ts2} activity is transiently inhibited as indicated by a reduction in ACh neurotransmitter vesicles. (**C**) Where the temperature is returned to the permissive temperature, there is an increase in ACh neurotransmitter vesicle release and a concurrent increase in pre- and post-synaptic Dα7 nAChRs. Note that these receptors are highly permeable to Ca^{+2}. As a second messenger, Ca^{+2} activates calcineurin which dephosphorylates cytoplasmic dNFAT. Activated dNFAT translocates into the nucleus and promotes Kv4/Shal expression.

REFERENCES

1. Marder E, Prinz AA. Modeling stability in neuron and network function: The role of activity in homeostasis. BioEssays. 2002;24(12):1145–54.
2. Marder E, Goaillard JM. Variability, compensation and homeostasis in neuron and network function. Nat Rev Neurosci. 2006;7(7):563–74.
3. Turrigiano GG. Self tuning neuron. 2010;135(3):422–35.
4. Turrigiano GG, Nelson SB. Homeostatic plasticity in the developing nervous system. Nat Rev Neurosci. 2004;5(2):97–107.
5. Davis GW. Homeostatic signaling and the stabilization of neural function. Neuron [Internet]. 2013;80(3):718–28. Available from: http://dx.doi.org/10.1016/j.neuron.2013.09.044
6. Hahm ET, Nagaraja RY, Waro G, Tsunoda S. Cholinergic Homeostatic Synaptic Plasticity Drives the Progression of Aβ-Induced Changes in Neural Activity. Cell Rep [Internet]. 2018;24(2):342–54. Available from: https://doi.org/10.1016/j.celrep.2018.06.029
7. Turrigiano G. Stabilizing Neuronal Function Homeostatic Synaptic Plasticity: Local and Global Mechanisms for Homeostatic Synaptic Plasticity: Local and Global Mechanisms for Stabilizing Neuronal Function. Cold Spring Harb Perspect Biol [Internet]. 2011;1–17. Available from: http://cshperspectives.cshlp.org/cgi/doi/10.1101/cshperspect.a005736
8. Thiagarajan TC, Lindskog M, Malgaroli A, Tsien RW. LTP and adaptation to inactivity: Overlapping mechanisms and implications for metaplasticity. Neuropharmacology. 2007;52(1):156–75.
9. Davis GW. Homeostatic control of neural activity: From phenomenology to molecular design. Annu Rev Neurosci. 2006;29:307–23.
10. Pozo K, Goda Y. Europe PMC Funders Group Unraveling mechanisms of homeostatic synaptic plasticity. 2011;66(3):337–51.
11. Turrigiano G. Too many cooks? Intrinsic and synaptic homeostatic mechanisms in cortical circuit refinement. Annu Rev Neurosci. 2011;34:89–103.
12. Stickgold RJ, Alsop D, Gaab N, Schlaug G, Born J, Cirelli C, et al. Sleep and Synaptic Homeostasis : 2011;(June):1576–82.
13. Malenka RC, Bear MF. LTP and LTD: An embarrassment of riches. Neuron. 2004;44(1):5–21.
14. Collingridge GL, Isaac JTR, Yu TW. Receptor trafficking and synaptic plasticity. Nat Rev Neurosci. 2004;5(12):952–62.
15. Neves G, Cooke SF, Bliss TVP. Synaptic plasticity, memory and the hippocampus: A neural network approach to causality. Nat Rev Neurosci. 2008;9(1):65–75.
16. Feldman DE. Synaptic mechanisms for plasticity in neocortex. Annu Rev Neurosci. 2009;32:33–55.
17. Seeburg DP, Sheng M. Activity-induced polo-like kinase 2 is required for homeostatic plasticity of hippocampal neurons during epileptiform activity. J Neurosci. 2008;28(26):6583–91.
18. Roth-Alpermann C, Morris RGM, Korte M, Bonhoeffer T. Homeostatic shutdown of long-term potentiation in the adult hippocampus. Proc Natl Acad Sci U S A. 2006;103(29):11039–44.
19. Miller KD. π = Visual cortex. Science (80-). 2010;330(6007):1059–60.
20. Greenhill SD, Ranson A, Fox K. Hebbian and Homeostatic Plasticity Mechanisms in Regular Spiking and Intrinsic Bursting Cells of Cortical Layer 5. Neuron [Internet].

2015;88(3):539–52. Available from: http://dx.doi.org/10.1016/j.neuron.2015.09.025
21. Turrigiano GG. The dialectic of hebb and homeostasis. Philos Trans R Soc B Biol Sci. 2017;372(1715):4–6.
22. Kaneko M, Hanover JL, England PM, Stryker MP. TrkB kinase is required for recovery, but not loss, of cortical responses following monocular deprivation. Nat Neurosci. 2008;11(4):497–504.
23. Magee JC, Johnston D. Plasticity of dendritic function. Curr Opin Neurobiol. 2005;15(3 SPEC. ISS.):334–42.
24. Campanac E, Debanne D. Plasticity of neuronal excitability: Hebbian rules beyond the synapse. Arch Ital Biol. 2007;145(3–4):277–87.
25. Davis GW, Martin M. Homeostatic Control of Presynaptic Neurotransmitter Release. 2015;
26. Grasselli G, Hansel C. Cerebellar Long-Term Potentiation : Cellular Mechanisms and Role in Learning [Internet]. 1st ed. Vol. 117, Cerebellar Conditioning and Learning. Elsevier Inc.; 39–51 p. Available from: http://dx.doi.org/10.1016/B978-0-12-420247-4.00003-8
27. Huganir RL, Nicoll RA. Perspective AMPARs and Synaptic Plasticity : The Last 25 Years. Neuron [Internet]. 2013;80(3):704–17. Available from: http://dx.doi.org/10.1016/j.neuron.2013.10.025
28. Bourne JN, Harris KM. NIH Public Access. 2008;47–67.
29. Yu X, Zuo Y. Spine plasticity in the motor cortex. Curr Opin Neurobiol [Internet]. 2011;21(1):169–74. Available from: http://dx.doi.org/10.1016/j.conb.2010.07.010
30. Rabinowitch I, Segev I. The Interplay Between Homeostatic Synaptic Plasticity and Functional Dendritic Compartments. 2020;276–83.
31. Rabinowitch I, Segev I. Two opposing plasticity mechanisms pulling a single synapse. 2008;(July):377–83.
32. Treiman DM. GABAergic Mechanisms in Epilepsy.
33. Echegoyen J, Neu A, Graber KD, Soltesz I. Homeostatic Plasticity Studied Using In Vivo Hippocampal Activity-Blockade : Synaptic Scaling , Intrinsic Plasticity and Age-Dependence. 2007;02167(8).
34. Buckby LE, Jensen TP, Smith PJE, Empson RM. Network stability through homeostatic scaling of excitatory and inhibitory synapses following inactivity in CA3 of rat organotypic hippocampal slice cultures. 2006;31:805–16.
35. Karmarkar UR, Buonomano D V. Different forms of homeostatic plasticity are engaged with distinct temporal profiles.
36. Soden ME, Chen L. Fragile X Protein FMRP Is Required for Homeostatic Plasticity and Regulation of Synaptic Strength by Retinoic Acid. 2010;30(50):16910–21.
37. Qiu Z, Sylwestrak EL, Lieberman DN, Zhang Y, Liu X, Ghosh A. The Rett Syndrome Protein MeCP2 Regulates Synaptic Scaling. 2012;32(3):989–94.
38. Blackman MP, Djukic B, Nelson SB, Turrigiano GG. Neurobiology of Disease A Critical and Cell-Autonomous Role for MeCP2 in Synaptic Scaling Up. 2012;32(39):13529–36.
39. Houweling AR, Bazhenov M, Timofeev I, Steriade M. Homeostatic Synaptic Plasticity Can Explain Post-traumatic Epileptogenesis in Chronically Isolated Neocortex. 2005;15(6):834–45.
40. Dickman DK, Davis GW. NIH Public Access. 2011;326(5956):1127–30.
41. Kim S, Violette CJ, Ziff EB. Neurobiology of Aging Reduction of increased calcineurin activity rescues impaired homeostatic synaptic plasticity in presenilin 1 M146V mutant. Neurobiol Aging [Internet]. 2015;36(12):3239–46. Available from: http://dx.doi.org/10.1016/j.neurobiolaging.2015.09.007
42. Pratt KG, Zimmerman EC, Cook DG, Sullivan JM. Presenilin 1 regulates homeostatic synaptic scaling through Akt signaling. Nat Publ Gr. 2011;14(9):1112–4.

43. Flores M, Rogers SW, Pabreza LA, Wolfe BB. A Subtype of Nicotinic Cholinergic Composed of and 32 Subunits Chronic Nicotine Treatment Receptor in Rat Brain Is and Is Up-regulated by However ,.
44. Nashmi R, Xiao C, Deshpande P, Mckinney S, Grady SR, Whiteaker P, et al. Chronic Nicotine Cell Specifically Upregulates Functional ⌴ 4 * Nicotinic Receptors : Basis for Both Tolerance in Midbrain and Enhanced Long-Term Potentiation in Perforant Path. 2007;27(31):8202–18.
45. Quick MW, Lester RAJ. Desensitization of Neuronal Nicotinic Receptors. 2002;(June).
46. Neurochemistry JOF. Hebbian and homeostatic synaptic plasticity. 2016;973–96.
47. Manuscript A. NIH Public Access. 2009;60(2):308–20.
48. Gao M, Whitt JL, Huang S, Lee A, Mihalas S, Kirkwood A, et al. Experience-dependent homeostasis of ' noise ' at inhibitory synapses preserves information coding in adult visual cortex. 2017;11–3.
49. Timofeev I, Sejnowski TJ, Bazhenov M, Chauvette S, Grand LB. Age dependency of trauma-induced neocortical epileptogenesis. 2013;7(September):1–14.
50. Krishnan GP, Chauvette S, Timofeev I, Sejnowski T, Bazhenov M. Neurobiology of Disease Modeling of Age-Dependent Epileptogenesis by Differential Homeostatic Synaptic Scaling. 2015;35(39):13448–62.
51. Plomp JJ, Kempen GTH Van, Baets MB De, Graus YMF, Kuks JBM, Molenaar PC. Acetylcholine Release in Myasthenia Gravis : Regulation at Single End-Plate Level. 1995;627–36.
52. Miledi R. Gower Street, London WC1E. 1980;50:621–38.
53. Rocher AB, Gubellini P, Merienne N, Boussicault L, Petit F, Gipchtein P, et al. Neurobiology of Disease Synaptic scaling up in medium spiny neurons of aged BACHD mice : A slow-progression model of Huntington ' s disease. Neurobiol Dis [Internet]. 2016;86:131–9. Available from: http://dx.doi.org/10.1016/j.nbd.2015.10.016
54. Gittis AH, Lac S. Intrinsic and synaptic plasticity in the vestibular system.
55. Casey M. Network Stability from Activity-Dependent Regulation of Neuronal Conductances. 1999;1096:1079–96.
56. Marder E, Prinz AA. Modeling stability in neuron and network function : the role of activity in homeostasis. 2002;1145–54.
57. Activity-dependent regulation of conductances in model neuro. 1993;
58. Baccaglini BYPI, Spitzer NC. By paola i. baccaglini. 1977;93–117.
59. Nature LTO. Distinct aspects of neuronal differentiation encoded by frequency of spontaneous Ca 2 + transients. 1995;375(June):784–7.
60. Dallman JE, Davis AK, Moody WJ. Spontaneous activity regulates calcium-dependent K ¤ current expression in developing ascidian muscle. 1998;
61. Sexuality D, Francisco S. Activity-dependent scaling of quantal amplitude in neocortical neurons. 1998;391(February).
62. Desai NS, Rutherford LC, Turrigiano GG. Plasticity in the intrinsic excitability of cortical pyramidal neurons. 2015;(July 1999).
63. Desai NS, Rutherford LC, Turrigiano GG. BDNF Regulates the Intrinsic Excitability of Cortical Neurons. :284–92.
64. Manuscript A. NIH Public Access. 2011;68(5):921–35.
65. Fan Y, Fricker D, Brager DH, Chen X, Lu H, Chitwood RA, et al. Activity-dependent decrease of excitability in rat hippocampal neurons through increases in I h. 2005;8(11).
66. Frick A, Magee J, Johnston D. LTP is accompanied by an enhanced local excitability of pyramidal neuron dendrites. 2020;7(2):126–35.
67. Maclean JN, Zhang Y, Goeritz ML, Casey R, Oliva R, Guckenheimer J, et al. Activity-Independent Coregulation of I A and I h in Rhythmically Active Neurons. 2020;3601–17.
68. Maclean JN, Zhang Y, Johnson BR, Harris-warrick RM. Activity-Independent

Homeostasis in Rhythmically Active Neurons. 2003;37:109–20.
69. Tierney AJ. Physiological Role of the Transient Potassium Current in the Pyloric Circuit of the Lobster Stomatogastric Ganglion. 2020;67(3).
70. Tien N, Kerschensteiner D. Homeostatic plasticity in neural development. 2018;1–7.
71. Signaling TH, Bergquist S, Dickman DK, Davis GW. Article A Hierarchy of Cell Intrinsic. Neuron [Internet]. 2010;66(2):220–34. Available from: http://dx.doi.org/10.1016/j.neuron.2010.03.023
72. Pratt KG, Aizenman CD. Homeostatic Regulation of Intrinsic Excitability and Synaptic Transmission in a Developing Visual Circuit. 2007;27(31):8268–77.
73. Baines RA, Uhler JP, Thompson A, Sweeney ST, Bate M. Altered Electrical Properties in Drosophila Neurons Developing without Synaptic Transmission. 2001;21(5):1523–31.
74. Hamodi AS, Pratt KG. Region-specific regulation of voltage-gated intrinsic currents in the developing optic tectum of the Xenopus tadpole. 2020;(2011):1644–55.
75. Khaliq ZM, Raman IM. Relative Contributions of Axonal and Somatic Na Channels to Action Potential Initiation in Cerebellar Purkinje Neurons. 2006;26(7):1935–44.
76. Palmer LM, Stuart GJ. Site of Action Potential Initiation in Layer 5 Pyramidal Neurons. 2006;26(6):1854–63.
77. Kuba H, Oichi Y, Ohmori H. Presynaptic activity regulates Na 1 channel distribution at the axon initial segment. Nature [Internet]. 2010;465(7301):1075–8. Available from: http://dx.doi.org/10.1038/nature09087
78. Cohen S, Greenberg ME. Communication Between the Synapse and the Nucleus in Neuronal Development , Plasticity , and Disease. 2008;
79. Martin KC, Zukin RS. RNA Trafficking and Local Protein Synthesis in Dendrites : An Overview. 2006;26(27):7131–4.
80. Bramham CR, Wells DG. Dendritic mRNA : transport , translation and function. 2007;8.
81. Tzingounis A V, Nicoll RA, Arg A. Arc / Arg3 . 1 : Linking Gene Expression to Synaptic Plasticity and Memory Minireview. 2006;1:403–7.
82. Guzowski JF, Timlin JA, Roysam B, Bruce L, Worley PF, Barnes CA. Mapping behaviorally relevant neural circuits with immediate-early gene expression. 2005;599–606.
83. Chowdhury S, Shepherd JD, Okuno H, Lyford G, Petralia RS, Plath N, et al. Receptor Trafficking. 2007;52(3):445–59.
84. Sutton MA, Wall NR, Aakalu GN, Schuman EM. Regulation of Dendritic Synaptic Events. 2004;304(June):1979–84.
85. Sutton MA, Taylor AM, Ito HT, Pham A, Schuman EM. Article Postsynaptic Decoding of Neural Activity : eEF2 as a Biochemical Sensor Coupling Miniature Synaptic Transmission to Local Protein Synthesis. 2007;648–61.
86. Lu Y, Christian K, Lu B. NIH Public Access. 2009;89(3):312–23.
87. Balkowiec A, Katz DM. Cellular Mechanisms Regulating Activity-Dependent Release of Native Brain-Derived Neurotrophic Factor from Hippocampal Neurons. 2002;22(23):10399–407.
88. Dean C, Liu H, Dunning FM, Chang PY, Jackson MB, Chapman ER. Synaptotagmin-IV modulates synaptic function and long-term potentiation by regulating BDNF release. 2009;12(6).
89. Minichiello L. TrkB signalling pathways in LTP and learning. 2009;10(December):850–60.
90. Carvalho AL, Caldeira M V, Santos SD, Duarte CB. Role of the brain-derived neurotrophic factor at glutamatergic synapses. 2008;(July 2007):310–24.
91. Tyler WJ, Perrett SP, Pozzo-miller LD. NIH Public Access. 2010;8(6):524–31.
92. Stellwagen D, Beattie EC, Seo JY, Malenka RC. Differential Regulation of AMPA Receptor and GABA Receptor Trafficking by Tumor Necrosis Factor- ⎵. 2005;25(12):3219–28.

93. Knutson B, Westdorp A, Kaiser E, Hommer D, Beattie EC, Stellwagen D, et al. Control of Synaptic Strength by Glial TNF ⎵. 2002;295(March):2282–6.
94. Stellwagen D, Malenka RC. Synaptic scaling mediated by glial TNF- a. 2006;440(April):1–6.
95. Words KEY. Retinoic Acid Signaling in the Nervous System of Adult Vertebrates. 2004;10(5):409–21.
96. Maghsoodi B, Poon MM, Nam CI, Aoto J, Ting P, Chen L. Retinoic acid regulates RARα-mediated control of translation in dendritic RNA granules during homeostatic synaptic plasticity. Proc Natl Acad Sci U S A. 2008;105(41):16015–20.
97. Chiang MY, Misner D, Kempermann G, Schikorski T, Giguère V, Sucov HM, et al. An essential role for retinoid receptors RARβ and RXRγ in long-term potentiation and depression. Neuron. 1998;21(6):1353–61.
98. Hynes RO. Integrins: Bidirectional, allosteric signaling machines. Cell. 2002;110(6):673–87.
99. Cingolani LA, Goda Y. Differential involvement of β3 integrin in pre- and postsynaptic forms of adaptation to chronic activity deprivation. Neuron Glia Biol. 2008;4(3):179–87.
100. Hoda Badr, Cindy L. Carmack, Deborah A. Kashy, Massimo Cristofanilli and TAR. 基因的改变NIH Public Access. Bone. 2011;23(1):1–7.
101. Takeichi M, Abe K. Synaptic contact dynamics controlled by cadherin and catenins. Trends Cell Biol. 2005;15(4):216–21.
102. Mysore SP, Tai CY, Schuman EM. N-Cadherin, Spine Dynamics, and Synaptic Function. Front Neurosci. 2008;2(2):168–75.
103. Murase S, Mosser E, Schuman EM, Hhmi C. Depolarization Drives ☒ -Catenin into Neuronal Spines Promoting Changes in Synaptic Structure and Function. 2002;35:91–105.
104. Bamji SX, Rico B, Kimes N, Reichardt LF. BDNF mobilizes synaptic vesicles and enhances synapse formation by disrupting cadherin– β -catenin interactions. 2006;174(2):289–99.
105. Okuda T, Yu LMY, Cingolani LA, Kemler R, Goda Y. ☒ -Catenin regulates excitatory postsynaptic strength at hippocampal synapses. 2007;104(33).
106. Saglietti L, Dequidt C, Kamieniarz K, Rousset M, Valnegri P, Thoumine O, et al. Article Extracellular Interactions between GluR2 and N-Cadherin in Spine Regulation. 2007;461–77.
107. Moulder KL, Jiang X, Taylor AA, Olney JW, Mennerick S. Physiological Activity Depresses Synaptic Function through an Effect on Vesicle Priming. 2006;26(24):6618–26.
108. Murthy VN, Schikorski T, Stevens CF, Zhu Y, Jolla L. in Neurotransmitter Release and Synapse Size. 2001;32:673–82.
109. Bacci A, Coco S, Pravettoni E, Schenk U, Armano S, Frassoni C, et al. Chronic Blockade of Glutamate Receptors Enhances Presynaptic Release and Downregulates the Interaction between Synaptophysin- Synaptobrevin – Vesicle-Associated Membrane Protein 2. 2001;21(17):6588–96.
110. Thiagarajan TC, Lindskog M, Tsien RW. Adaptation to Synaptic Inactivity in Hippocampal Neurons. 2005;47:725–37.
111. Burrone J, Byrne MO, Murthy VN. Multiple forms of synaptic plasticity triggered by selective suppression of activity in individual neurons. 2002;420(November).
112. Han EB, Stevens CF. Development regulates a switch between post- and presynaptic strengthening in response to activity deprivation. 2009;106(26):10817–22.
113. Branco T, Staras K, Darcy KJ, Goda Y. Article Local Dendritic Activity Sets Release

Probability at Hippocampal Synapses. 2008;475–85.
114. Moulder KL, Meeks JP, Shute AA, Hamilton CK, Erausquin G De, Mennerick S, et al. Plastic Elimination of Functional Glutamate Release Sites by Depolarization. 2004;42:423–35.
115. Wilson NR, Kang J, Hueske E V, Leung T, Varoqui H, Murnick JG, et al. Presynaptic Regulation of Quantal Size by the Vesicular Glutamate Transporter VGLUT1. 2005;25(26):6221–34.
116. Gois D, Scha MK, Defamie N, Chen C, Ricci A, Weihe E, et al. Homeostatic Scaling of Vesicular Glutamate and GABA Transporter Expression in Rat Neocortical Circuits. 2005;25(31):7121–33.
117. Brien RJO, Kamboj S, Ehlers MD, Rosen KR, Fischbach GD, Huganir RL, et al. Activity-Dependent Modulation of Synaptic AMPA Receptor Accumulation. 1998;21(1989):1067–78.
118. Glutamate C. CLONED GLUTAMATE. 1994;31–108.
119. Elias GM, Nicoll RA. Synaptic trafficking of glutamate receptors by MAGUK scaffolding proteins. 2007;17(7).
120. Bredt DS, Nicoll RA. AMPA Receptor Trafficking at Excitatory Synapses. 2003;40:361–79.
121. Collingridge GL, Isaac JTR, Wang YT. RECEPTOR TRAFFICKING AND SYNAPTIC PLASTICITY. 2004;5(December):952–62.
122. Manuscript A. NIH Public Access. 2009;58(4):472–97.
123. Ju W, Morishita W, Tsui J, Gaietta G, Deerinck TJ, Adams SR, et al. Activity-dependent regulation of dendritic synthesis and trafficking of AMPA receptors. 2004;7(3):244–53.
124. Sutton MA, Ito HT, Cressy P, Kempf C, Woo JC, Schuman EM. Miniature Neurotransmission Stabilizes Synaptic Function via Tonic Suppression of Local Dendritic Protein Synthesis. 2006;785–99.
125. Man H, Sekine-aizawa Y, Huganir RL. Regulation of ␣ -amino-3-hydroxy-5-methyl-4-isoxazolepropionic acid receptor trafficking through PKA phosphorylation of the Glu receptor 1 subunit. 2007;104(9).
126. Oh MC, Derkach VA, Guire ES, Soderling TR. Extrasynaptic Membrane Trafficking Regulated by GluR1 Serine 845 Phosphorylation Primes AMPA Receptors for. 2006;281(2):752–8.
127. Kilman V, Rossum MCW Van, Turrigiano GG. Activity Deprivation Reduces Miniature IPSC Amplitude by Decreasing the Number of Postsynaptic GABA A Receptors Clustered at Neocortical Synapses. 2002;22(4):1328–37.
128. Lee H, Takamiya K, Han J, Man H, Kim C, Rumbaugh G, et al. Phosphorylation of the AMPA Receptor GluR1 Subunit Is Required for Synaptic Plasticity and Retention of Spatial Memory. 2003;112:631–43.
129. Sanderson JL, Gorski JA. HHS Public Access. 2017;89(5):1000–15.
130. Lee H, Kameyama K, Huganir RL, Bear MF, Hughes H. NMDA Induces Long-Term Synaptic Depression and Dephosphorylation of the GluR1 Subunit of AMPA Receptors in Hippocampus. 1998;21:1151–62.
131. Diering GH, Gustina AS, Huganir RL. Article PKA-GluA1 Coupling via AKAP5 Controls AMPA Receptor Phosphorylation and Cell-Surface Targeting during Bidirectional Homeostatic Plasticity. Neuron [Internet]. 2014;84(4):790–805. Available from: http://dx.doi.org/10.1016/j.neuron.2014.09.024
132. Chowdhury D, Hell JW. Homeostatic synaptic scaling: molecular regulators of synaptic AMPA-type glutamate receptors. F1000Research [Internet]. 2018;7(0):234. Available from: https://f1000research.com/articles/7-234/v1
133. Groth RD, Lindskog M, Thiagarajan TC, Li L, Tsien RW. β Ca 2 + / CaM-dependent kinase type II triggers upregulation of GluA1 to coordinate adaptation to synaptic inactivity

in hippocampal neurons. 2011;
134. Béïque J, Na Y, Kuhl D, Worley PF, Huganir RL. homeostatic plasticity. 2010;
135. Soares C, Lee KFH, Nassrallah W, Be J. Differential Subcellular Targeting of Glutamate Receptor Subtypes during Homeostatic Synaptic Plasticity. 2013;33(33):13547–59.
136. Ehrlich I, Malinow R. Postsynaptic Density 95 controls AMPA Receptor Incorporation during Long-Term Potentiation and Experience-Driven Synaptic Plasticity. 2004;24(4):916–27.
137. Carlisle HJ, Fink AE, Grant SGN, Dell TJO. Opposing effects of PSD-93 and PSD-95 on long-term potentiation and spike timing-dependent plasticity. 2008;24:5885–900.
138. Sun Q, Turrigiano GG. PSD-95 and PSD-93 Play Critical But Distinct Roles in Synaptic Scaling Up and Down. 2011;31(18):6800–8.
139. Stein V, House DRC, Bredt DS, Nicoll RA. Postsynaptic Density-95 Mimics and Occludes Hippocampal Long-Term Potentiation and Enhances Long-Term Depression. 2003;23(13):5503–6.
140. Chen L, Chetkovich DM, Petralia RS, Sweeney NT, Kawasaki Y, Wenthold RJ, et al. Stargazin regulates synaptic targeting of AMPA receptors by two distinct mechanisms. 2000;408(December).
141. Bats C, Groc L, Choquet D. Article The Interaction between Stargazin and PSD-95 Regulates AMPA Receptor Surface Trafficking. 2007;719–34.
142. Steinberg JP, Takamiya K, Shen Y, Xia J, Rubio ME, Yu S, et al. Targeted In Vivo Mutations of the AMPA Receptor Subunit GluR2 and Its Interacting Protein PICK1 Eliminate Cerebellar Long-Term Depression. 2006;845–60.
143. Pfennig S, Foss F, Bissen D, Harde E, Treeck JC, Segarra M, et al. GRIP1 Binds to ApoER2 and EphrinB2 to Induce Activity-Dependent AMPA Receptor Insertion at the GRIP1 Binds to ApoER2 and EphrinB2 to Induce Activity-Dependent AMPA Receptor Insertion at the Synapse. CellReports [Internet]. 2017;21(1):84–96. Available from: https://doi.org/10.1016/j.celrep.2017.09.019
144. Thiagarajan TC, Piedras-renteria ES, Tsien RW. ⎵ - and ☒ CaMKII : Inverse Regulation by Neuronal Activity and Opposing Effects on Synaptic Strength. 2002;36:1103–14.
145. Arendt KL, Zhang Z, Ganesan S, Hintze M, Shin MM, Tang Y. Calcineurin mediates homeostatic synaptic plasticity by regulating retinoic acid synthesis. 2015;
146. Daniels RW, Collins CA, Gelfand M V., Dant J, Brooks ES, Krantz DE, et al. Increased expression of the Drosophila vesicular glutamate transporter leads to excess glutamate release and a compensatory decrease in quantal content. J Neurosci. 2004;24(46):10466–74.
147. Leslie KR, Nelson SB, Turrigiano GG. Postsynaptic depolarization scales quantal amplitude in cortical pyramidal neurons. J Neurosci. 2001;21(19):1–6.
148. Davis GW, Goodman CS. Terminals of a Single Neuron. Nature. 1998;392(November 1997):655–7.
149. Mee CJ, Pym ECG, Moffat KG, Baines RA. Regulation of neuronal excitability through pumilio-dependent control of a sodium channel gene. J Neurosci. 2004;24(40):8695–703.
150. Baines RA. Neuronal homeostasis through translational control. Mol Neurobiol. 2005;32(2):113–21.
151. Paradis S, Sweeney ST, Davis GW. Homeostatic control of presynaptic release is triggered by postsynaptic membrane depolarization. Neuron. 2001;30(3):737–49.
152. Davis GW, Diantonio A, Petersen SA, Goodman CS. and Reveals a Retrograde Signal that Regulates Presynaptic Transmitter Release in Drosophila. Cell. 1998;20:305–15.
153. Schuster CM, Ultsch A, Schloss P, Cox JA, Schmrrr B, Betzt H. Molecular Cloning of an Invertebrate Glutamate Receptor Subunit Expressed in Drosophila Muscle Author (s): Christoph M . Schuster , Andreas Ultsch , Patrick Schloss , Jane A . Cox , Bertram

Schmitt and Heinrich Betz Source : Science , Oct . 4 , 1991 , N. 1991;254(5028):8–11.
154. Petersen SA, Fetter RD, Noordermeer JN, Goodman CS, DiAntonio A. Genetic analysis of glutamate receptors in drosophila reveals a retrograde signal regulating presynaptic transmitter release. Neuron. 1997;19(6):1237–48.
155. Davis GW, DiAntonio A, Petersen SA, Goodman CS. Postsynaptic PKA controls quantal size and reveals a retrograde signal that regulates presynaptic transmitter release in Drosophila. Neuron. 1998;20(2):305–15.
156. Frank CA, Pielage J, Davis GW. A Presynaptic Homeostatic Signaling System Composed of the Eph Receptor, Ephexin, Cdc42, and CaV2.1 Calcium Channels. Neuron [Internet]. 2009;61(4):556–69. Available from: http://dx.doi.org/10.1016/j.neuron.2008.12.028
157. Wang X, Engisch KL, Li Y, Pinter MJ, Cope TC, Rich MM. Decreased synaptic activity shifts the calcium dependence of release at the mammalian neuromuscular junction in vivo. J Neurosci. 2004;24(47):10687–92.
158. Zhao CJ, Dreosti E, Lagnado L. Homeostatic synaptic plasticity through changes in presynaptic calcium influx. J Neurosci. 2011;31(20):7492–6.
159. Lazarevic V, Schöne C, Heine M, Gundelfinger ED, Fejtova A. Extensive remodeling of the presynaptic cytomatrix upon homeostatic adaptation to network activity silencing. J Neurosci. 2011;31(28):10189–200.
160. Burrone J, O'Byrne M, Murthy VN. Multiple forms of synaptic plasticity triggered by selective suppression of activity in individual neurons. Nature. 2002;420(6914):414–8.
161. Qu JF, Tan M, Hou YL, Ge MY, Wang AN, Wang K, et al. E Ffects of the S Tability of R Eclaimed S Oil. 2018;34(5):843–54.
162. Aberle H, Haghighi AP, Fetter RD, McCabe BD, Magalhães TR, Goodman CS. Wishful thinking encodes a BMP type II receptor that regulates synaptic growth in Drosophila. Neuron. 2002;33(4):545–58.
163. McCabe BD, Marqués G, Haghighi AP, Fetter RD, Crotty ML, Haerry TE, et al. The BMP homolog Gbb provides a retrograde signal that regulates synaptic growth at the Drosophila neuromuscular junction. Neuron. 2003;39(2):241–54.
164. Eglen RM. Muscarinic Receptor Subtype Pharmacology and Physiology. Prog Med Chem. 2005;43(C):105–36.
165. ALBUQUERQUE EX, PEREIRA EFR, CASTRO NG, ALKONDON M, REINHARDT S, SCHRÖDER H, et al. Nicotinic Receptor Function in the Mammalian Central Nervous System. Ann N Y Acad Sci. 1995;757(1):48–72.
166. Dani JA, Bertrand D. Nicotinic acetylcholine receptors and nicotinic cholinergic mechanisms of the central nervous system. Annu Rev Pharmacol Toxicol. 2007;47:699–729.
167. Gotti C, Clementi F. Neuronal nicotinic receptors: From structure to pathology. Prog Neurobiol. 2004;74(6):363–96.
168. Lein ES, Hawrylycz MJ, Ao N, Ayres M, Bensinger A, Bernard A, et al. Genome-wide atlas of gene expression in the adult mouse brain. Nature. 2007;445(7124):168–76.
169. Cooper E, Couturier S, Ballivet M. [Letters to nature]. Nature. 1973;246(5429):170.
170. Unwin N. Acetylcholine receptor channel imaged in the open state. Nature. 1995;373(6509):37–43.
171. and Myasthenia. Muscle Nerve. 2000;(April):453–77.
172. Miyazawa A, Fujiyoshi Y, Unwin N. Structure and gating mechanism of the acetylcholine receptor pore. Nature. 2003;423(6943):949–55.
173. Aga Lewelt. 乳鼠心肌提取 HHS Public Access. Physiol Behav. 2015;176(3):139–48.
174. Colombo SF, Mazzo F, Pistillo F, Gotti C. Biogenesis, trafficking and up-regulation of nicotinic ACh receptors. Biochem Pharmacol [Internet]. 2013;86(8):1063–73. Available from: http://dx.doi.org/10.1016/j.bcp.2013.06.023
175. Millar NS, Harkness PC. Assembly and trafficking of nicotinic acetylcholine receptors

(Review). Mol Membr Biol. 2008;25(4):279–92.
176. King JR, Nordman JC, Bridges SP, Lin MK, Kabbani N. Identification and characterization of a G protein-binding cluster in α7 nicotinic acetylcholine receptors. J Biol Chem. 2015;290(33):20060–70.
177. King JR, Kabbani N. Alpha 7 nicotinic receptor coupling to heterotrimeric G proteins modulates RhoA activation, cytoskeletal motility, and structural growth. J Neurochem. 2016;532–45.
178. To MNARFS, Function, Edson X. Albuquerque, Edna F. R. Pereira, Manickavasagom Alkondon and SWR. NIH Public Access. Physiol Rev. 2009;89(1):73–120.
179. Ping Y, Tsunoda S. Homeostatic plasticity in Drosophila central neurons and implications in human diseases. Fly (Austin). 2012;6(3).
180. Ballivet M, Alliod C, Bertrand S, Bertrand D. Nicotinic acetylcholine receptors in the nematode Caenorhabditis elegans. J Mol Biol. 1996;258(2):261–9.
181. Seguela P, Wadiche J, Dineley-Miller K, Dani JA, Patrick JW. Molecular cloning, functional properties, and distribution of rat brain α7: A nicotinic cation channel highly permeable to calcium. J Neurosci. 1993;13(2):596–604.
182. Fenster CR, Whitworth TL, Sheffield EB, Quick MW, Lester RAJ. Upregulation of surface α4β2 nicotinic receptors is initiated by receptor desensitization after chronic exposure to nicotine. J Neurosci. 1999;19(12):4804–14.
183. Haghighi AP, Cooper E. A molecular link between inward rectification and calcium permeability of neuronal nicotinic acetylcholine α3β4 and α4β2 receptors. J Neurosci. 2000;20(2):529–41.
184. Vernino S, Amador M, Luetje CW, Patrick J, Dani JA. Calcium modulation and high calcium permeability of neuronal nicotinic acetylcholine receptors. Neuron. 1992;8(1):127–34.
185. Bertrand D, Galzi JL, Devillers-Thiery A, Bertrand S, Changeux JP. Mutations at two distinct sites within the channel domain M2 alter calcium permeability of neuronal α7 nicotinic receptor. Proc Natl Acad Sci U S A. 1993;90(15):6971–5.
186. Castro NG, Albuquerque EX. alpha-Bungarotoxin-sensitive hippocampal nicotinic receptor channel has a high calcium permeability. Biophys J. 1995;68(2):516–24.
187. Xu J, Zhu Y, Heinemann SF. Identification of sequence motifs that target neuronal nicotinic receptors to dendrites and axons. J Neurosci. 2006;26(38):9780–93.
188. Zarei MM, Radcliffe KA, Chen D, Patrick JW, Dani JA. Distributions of nicotinic acetylcholine receptor α7 and β2 subunits on cultured hippocampal neurons. Neuroscience. 1999;88(3):755–64.
189. Wada E, Wada K, Boulter J, Deneris E, Heinemann S, Patrick J, et al. Distribution of alpha2, alpha3, alpha4, and beta2 neuronal nicotinic receptor subunit mRNAs in the central nervous system: A hybridization histochemical study in the rat. J Comp Neurol. 1989;284(2):314–35.
190. Mielke JG, Mealing GAR. Cellular distribution of the nicotinic acetylcholine receptor α7 subunit in rat hippocampus. Neurosci Res. 2009;65(3):296–306.
191. Khiroug L, Giniatullin R, Klein RC, Fayuk D, Yakel JL. Functional mapping and Ca2+ regulation of nicotinic acetylcholine receptor channels in rat hippocampal CA1 neurons. J Neurosci. 2003;23(27):9024–31.
192. Lena C, Changeux JP, Mulle C. Evidence for “preterminal” nicotinic receptors on GABAergic axons in the rat interpeduncular nucleus. J Neurosci. 1993;13(6):2680–8.
193. Couturier S, Bertrand D, Matter JM, Hernandez MC, Bertrand S, Millar N, et al. A neuronal nicotinic acetylcholine receptor subunit (α7) is developmentally regulated and forms a homo-oligomeric channel blocked by α-BTX. Neuron. 1990;5(6):847–56.
194. Chen DN, Patrick JW. The α-bungarotoxin-binding nicotinic acetylcholine receptor from rat brain contains only the α7 subunit. J Biol Chem. 1997;272(38):24024–9.

195. Man HY. GluA2-lacking, calcium-permeable AMPA receptors - inducers of plasticity? Curr Opin Neurobiol [Internet]. 2011;21(2):291–8. Available from: http://dx.doi.org/10.1016/j.conb.2011.01.001
196. Thiagarajan TC, Lindskog M, Tsien RW. Adaptation to synaptic inactivity in hippocampal neurons. Neuron. 2005;47(5):725–37.
197. Lindskog M, Li L, Groth RD, Poburko D, Thiagarajan TC, Han X, et al. Postsynaptic GluA1 enables acute retrograde enhancement of presynaptic function to coordinate adaptation to synaptic inactivity. Proc Natl Acad Sci U S A. 2010;107(50):21806–11.
198. Role LW, Berg DK. Nicotinic receptors in the development and modulation of CNS synapses. Neuron. 1996;16(6):1077–85.
199. Xbar P, R PSN, Ctgcggccgcgg CCG, Gcaaat A, All A, Grayt R, et al. Letters to nature. 1996;383(October):713–6.
200. Mcgehee DS, Heath MJS, Gelber S, Devay P, Lorna W, Mcgehee DS, et al. Receptors Nic [ine E anceent of : ast xcitat ory Sysnaptic Transmission nN Pres na tic Receptors. 2018;269(5231):1692–6.
201. Racca C, Stephenson FA, Streit P, Roberts JDB, Somogyi P. NMDA receptor content of synapses in stratum radiatum of the hippocampal CA1 area. J Neurosci. 2000;20(7):2512–22.
202. McKay BE, Placzek AN, Dani JA. Regulation of synaptic transmission and plasticity by neuronal nicotinic acetylcholine receptors. Biochem Pharmacol. 2007;74(8):1120–33.
203. Johnston D, Christie BR, Frick A, Gray R, Hoffman DA, Schexnayder LK, et al. Active dendrites, potassium channels and synaptic plasticity. Philos Trans R Soc B Biol Sci. 2003;358(1432):667–74.
204. Stuart G, Spruston N, Sakmann B, Häusser M. Action potential initiation and backpropagation in neurons of the mammalian CNS. Trends Neurosci. 1997;20(3):125–31.
205. Ping Y, Tsunoda S. Inactivity-induced increase in nAChRs upregulates Shal K + channels to stabilize synaptic potentials. Nat Neurosci. 2012;15(1):90–7.
206. Brian E. Saelens and Susan L. Handy. 基因的改变NIH Public Access. Bone. 2008;23(1):1–7.
207. Flores CM, Rogers SW, Pabreza LA, Wolfe BB, Kellar KJ. A subtype of nicotinic cholinergic receptor in rat brain is composed of α4 and β2 subunits and is up-regulated by chronic nicotine treatment. Mol Pharmacol. 1992;41(1):31–7.
208. Nordberg A. Nicotinic receptor abnormalities of Alzheimer's disease: Therapeutic implications. Biol Psychiatry. 2001;49(3):200–10.
209. Frölich L. The cholinergic pathology in Alzheimer's disease - Discrepancies between clinical experience and pathophysiological findings. J Neural Transm. 2002;109(7–8):1003–14.
210. Purpose A. REGULATION OF CHOLINE A. 1989;31.
211. Wu D, Hersh LB. Choline Acetyltransferase: Celebrating Its Fiftieth Year. J Neurochem. 1994;62(5):1653–63.
212. Greenspan RJ. Mutations of choline acetyltransferase and associated neural defects. J Comp Physiol ??? A. 1980;137(1):83–92.
213. Kitamoto T, Xie X, Wu CF, Salvaterra PM. Isolation and characterization of mutants for the vesicular acetylcholine transporter gene in Drosophila melanogaster. J Neurobiol. 2000;42(2):161–71.
214. Salvaterra PM, McCaman RE. Choline acetyltransferase and acetylcholine levels in Drosophila melanogaster: a study using two temperature-sensitive mutants. J Neurosci. 1985;5(4):903–10.
215. Wang W, Kitamoto T, Salvaterra PM. Drosophila choline acetyltransferase temperature-

sensitive mutants. Neurochem Res. 1999;24(8):1081–7.
216. Crespi A, Colombo SF, Gotti C. Proteins and chemical chaperones involved in neuronal nicotinic receptor expression and function: an update. Br J Pharmacol. 2018;175(11):1869–79.
217. Jackson LP, Lewis M, Kent HM, Edeling MA, Evans PR, Duden R, et al. Molecular Basis for Recognition of Dilysine Trafficking Motifs by COPI. Dev Cell [Internet]. 2012;23(6):1255–62. Available from: http://dx.doi.org/10.1016/j.devcel.2012.10.017
218. Gu S, Matta JA, Lord B, Harrington AW, Sutton SW, Davini WB, et al. Brain α7 Nicotinic Acetylcholine Receptor Assembly Requires NACHO. Neuron [Internet]. 2016;89(5):948–55. Available from: http://dx.doi.org/10.1016/j.neuron.2016.01.018
219. Orr-Urtreger A, Göldner FM, Saeki M, Lorenzo I, Goldberg L, De Biasi M, et al. Mice deficient in the neuronal nicotinic acetylcholine receptor lack α- bungarotoxin binding sites and hippocampal fast nicotinic currents. J Neurosci. 1997;17(23):9165–71.
220. Matta JA, Gu S, Davini WB, Lord B, Siuda ER, Harrington AW, et al. NACHO Mediates Nicotinic Acetylcholine Receptor Function throughout the Brain. Cell Rep [Internet]. 2017;19(4):688–96. Available from: http://dx.doi.org/10.1016/j.celrep.2017.04.008
221. Nguyen M, Alfonso A, Johnson CD, Rand JB. Caenorhabditis elegans mutants resistant to inhibitors of acetylcholinesterase. Genetics. 1995;140(2):527–35.
222. Millar NS. RIC-3: A nicotinic acetylcholine receptor chaperone. Br J Pharmacol. 2008;153(SUPPL. 1):177–83.
223. Halevi S, Yassin L, Eshel M, Sala F, Sala S, Criado M, et al. Conservation within the RIC-3 gene family: Effectors of mammalian nicotinic acetylcholine receptor expression. J Biol Chem. 2003;278(36):34411–7.
224. Koperniak TM, Garg BK, Boltax J, Loring RH. Cell-specific effects on surface α7 nicotinic receptor expression revealed by over-expression and knockdown of rat RIC3 protein. J Neurochem. 2013;124(3):300–9.
225. Kuryatov A, Mukherjee J, Lindstrom J. Chemical Chaperones Exceed the Chaperone Effects of RIC-3 in Promoting Assembly of Functional α7 AChRs. PLoS One. 2013;8(4):1–11.
226. Dau A, Komal P, Truong M, Morris G, Evans G, Nashmi R. RIC-3 differentially modulates α4β2 and α7 nicotinic receptor assembly, expression, and nicotine-induced receptor upregulation. BMC Neurosci. 2013;14:1–18.
227. Mulcahy MJ, Blattman SB, Barrantes FJ, Lukas RJ, Hawrot E. Resistance to inhibitors of cholinesterase 3 (Ric-3) expression promotes selective protein associations with the human α7-nicotinic acetylcholine receptor interactome. PLoS One. 2015;10(8):1–25.
228. Yap EL, Greenberg ME. Activity-Regulated Transcription: Bridging the Gap between Neural Activity and Behavior. Neuron [Internet]. 2018;100(2):330–48. Available from: https://doi.org/10.1016/j.neuron.2018.10.013
229. Kruijer W, Cooper JA, Hunter T, Verma IM. Platelet-derived growth factor induces rapid but transient expression of the c-fos gene and protein. Nature. 1984;312(5996):711–6.
230. Lau LF, Nathans D. Expression of a set of growth-related immediate early genes in BALB/c 3T3 cells: Coordinate regulation with c-fos or c-myc. Proc Natl Acad Sci U S A. 1987;84(5):1182–6.
231. Greenberg ME, Greene LA, Ziff EB. Nerve growth factor and epidermal growth factor induce rapid transient changes in proto-oncogene transcription in PC12 cells. J Biol Chem. 1985;260(26):14101–10.
232. Stimulation of Neuronal Acetylcholine Receptors Induces Rapid Gene Transcription Author (s): Michael E . Greenberg , Edward B . Ziff and Lloyd A . Greene Published by : American Association for the Advancement of Science Stable URL : http://www.jstor.or. 2016;234(4772):80–3.
233. Sheng M, Greenberg ME. The regulation and function of c-fos and other immediate early

genes in the nervous system. Neuron. 1990;4(4):477–85.
234. Mardinly AR, Spiegel I, Patrizi A, Centofante E, Bazinet JE, Tzeng CP, et al. Sensory experience regulates cortical inhibition by inducing IGF1 in VIP neurons. Nature. 2016;531(7594):371–5.
235. Yap E, Greenberg ME. Review Activity-Regulated Transcription : Bridging the Gap between Neural Activity and Behavior. Neuron [Internet]. 2018;100(2):330–48. Available from: https://doi.org/10.1016/j.neuron.2018.10.013
236. Hardingham GE, Chawla S, Johnson CM, Bading H. Distinct functions of nuclear and cytoplasmic calcium in the control of gene expression. Nature. 1997;385(6613):260–5.
237. Bito H, Deisseroth K, Tsien RW. CREB phosphorylation and dephosphorylation: A Ca2+- and stimulus duration-dependent switch for hippocampal gene expression. Cell. 1996;87(7):1203–14.
238. Xing J, Ginty DD, Greenberg ME. Coupling of the RAS-MAPK Pathway to Gene Activation by RSK2 , a Growth Factor- Regulated CREB Kinase Published by : American Association for the Advancement of Science Stable URL : https://www.jstor.org/stable/2891532 American Association for the Advancem. 1996;273(5277):959–63.
239. Ruben Martin and Stephen L. Buchwald. 基因的改变NIH Public Access. Bone [Internet]. 2008;23(1):1–7. Available from: https://www.ncbi.nlm.nih.gov/pmc/articles/PMC3624763/pdf/nihms412728.pdf
240. West AE, Chen WG, Dalva MB, Dolmetsch RE, Kornhauser JM, Shaywitz AJ, et al. Calcium regulation of neuronal gene expression. Proc Natl Acad Sci U S A. 2001;98(20):11024–31.
241. Norman C, Runswick M, Pollock R, Treisman R. Isolation and properties of cDNA clones encoding SRF, a transcription factor that binds to the c-fos serum response element. Cell. 1988;55(6):989–1003.
242. Sheng M, Dougan ST, McFadden G, Greenberg ME. Calcium and growth factor pathways of c-fos transcriptional activation require distinct upstream regulatory sequences. Mol Cell Biol. 1988;8(7):2787–96.
243. Aizawa H, Hu S, Bobb K, Balakrishnan K, Ince G, Gurevich I, et al. Esearch rticles. 2004;303(January):197–203.
244. Deisseroth K, Bito H, Tsien RW. Signaling from synapse to nucleus: Postsynaptic CREB phosphorylation during multiple forms of hippocampal synaptic plasticity. Neuron. 1996;16(1):89–101.
245. Chawla S, Hardingham GE, Quinn DR, Bading H. CBP: A signal-regulated transcriptional coactivator controlled by nuclear calcium and CaM kinase IV. Science (80-). 1998;281(5382):1505–9.
246. Schaukowitch K, Reese AL, Kim S, Kilaru G, Joo J, Kavalali ET, et al. An Intrinsic Transcriptional Program Underlying Synaptic Scaling during Activity Suppression Article An Intrinsic Transcriptional Program Underlying Synaptic Scaling during Activity Suppression. CellReports [Internet]. 2017;18(6):1512–26. Available from: http://dx.doi.org/10.1016/j.celrep.2017.01.033
247. Chytil M, Verdine GL. The Rel family of eukaryotic transcription factors. Curr Opin Struct Biol. 1996;6(1):91–100.
248. Graef IA, Gastier JM, Francke U, Crabtree GR. Evolutionary relationships among rel domains indicate functional diversification by recombination. Proc Natl Acad Sci U S A. 2001;98(10):5740–5.
249. Hogan PG, Hogan PG, Chen L, Chen L. Transcriptional regulation by calcium, calcineurin. NFAT Genes Dev. 2003;17(18):2205–32.
250. Feske S, Draeger R, Peter H-H, Eichmann K, Rao A. The Duration of Nuclear Residence

of NFAT Determines the Pattern of Cytokine Expression in Human SCID T Cells. J Immunol. 2000;165(1):297–305.
251. Feske S, Giltnane J, Dolmetsch R, Staudt LM, Rao A. Gene regulation mediated by calcium signals in T lymphocytes. Nat Immunol. 2001;2(4):316–24.
252. Okamura H, Aramburu J, García-Rodríguez C, Viola JPB, Raghavan A, Tahiliani M, et al. Concerted dephosphorylation of the transcription factor NFAT1 induces a conformational switch that regulates transcriptional activity. Mol Cell. 2000;6(3):539–50.
253. Beals CR, Clipstone NA, Ho SN, Crabtree GR. Nuclear localization of NF-ATc by a calcineurin-dependent, cyclosporin- sensitive intramolecular interaction. Genes Dev. 1997;11(7):824–34.
254. Shaw KTY, Ho AM, Raghavan A, Kim J, Jain J, Park J, et al. Immunosuppressive drugs prevent a rapid dephosphorylation of transcription factor NFAT1 in stimulated immune cells. Proc Natl Acad Sci U S A. 1995;92(24):11205–9.
255. Porter CM, Havens MA, Clipstone NA. Identification of amino acid residues and protein kinases involved in the regulation of NFATc subcellular localization. J Biol Chem. 2000;275(5):3543–51.
256. Liu J, Arai K, Arai N. Inhibition of NFATx Activation by an Oligopeptide: Disrupting the Interaction of NFATx with Calcineurin. J Immunol. 2001;167(5):2677–87.
257. Aramburu J, García-Cózar F, Raghavan A, Okamura H, Rao A, Hogan PG. Selective inhibition of NFAT activation by a peptide spanning the calcineurin targeting site of NFAT. Mol Cell. 1998;1(5):627–37.
258. Chow C-W, Rincón M, Davis RJ. Requirement for Transcription Factor NFAT in Interleukin-2 Expression. Mol Cell Biol. 1999;19(3):2300–7.
259. Kingsbury TJ, Cunningham KW. A conserved family of calcineurin regulators. Genes Dev. 2000;14(13):1595–604.
260. Fuentes JJ, Genescà L, Kingsbury TJ, Cunningham KW, Pérez-Riba M, Estivill X, et al. DSCR1, overexpressed in Down syndrome, is an inhibitor of calcineurin-mediated signaling pathways. Hum Mol Genet. 2000;9(11):1681–90.
261. Rothermel B, Vega RB, Yang J, Wu H, Bassel-Duby R, Williams RS. A protein encoded within the Down syndrome critical region is enriched in striated muscles and inhibits calcineurin signaling. J Biol Chem. 2000;275(12):8719–25.
262. Yang J, Rothermel B, Vega RB, Frey N, McKinsey TA, Olson EN, et al. Independent signals control expression of the calcineurin inhibitory proteins MCIP1 and MCIP2 in striated muscles. Circ Res. 2000;87(12).
263. Beals CR, Sheridan CM, Turck CW, Gardner P, Crabtree GR. Nuclear export of NF-ATc enhanced by glycogen synthase kinase-3. Science (80-). 1997;275(5308):1930–3.
264. Zhu J, Shibasaki F, Price R, Guillemot JC, Yano T, Dötsch V, et al. Intramolecular masking of nuclear import signal on NF-AT4 by casein kinase I and MEKK1. Cell. 1998;93(5):851–61.
265. Schwartz N, Schohl A, Ruthazer ES. Neural Activity Regulates Synaptic Properties and Dendritic Structure In Vivo through Calcineurin/NFAT Signaling. Neuron [Internet]. 2009;62(5):655–69. Available from: http://dx.doi.org/10.1016/j.neuron.2009.05.007
266. Graef IA, Mermelstein PG, Stankunas K, Hellson JR, Delsseroth K, Tsien RW, et al. L-type calcium channels and GSK-3 regulate the activity of NF-ATc4 in hippocampal neurons. Nature. 1999;401(6754):703–8.
267. Trama J, Lu Q, Hawley RG, Ho SN. The NFAT-Related Protein NFATL1 (TonEBP/NFAT5) Is Induced Upon T Cell Activation in a Calcineurin-Dependent Manner. J Immunol. 2000;165(9):4884–94.
268. Miyakawa H, Woo SK, Dahl SC, Handler JS, Kwon HM. Tonicity-responsive enhancer binding protein, a Rel-like protein that stimulates transcription in response to hypertonicity. Proc Natl Acad Sci U S A. 1999;96(5):2538–42.

269. Stroud JC, Lopez-Rodriguez C, Rao A, Chen L. Structure of a tonebp-dna complex reveals dna encircled by a transcription factor. Nat Struct Biol. 2002;9(2):90–4.
270. López-Rodríguez C, Antos CL, Shelton JM, Richardson JA, Lin F, Novobrantseva TI, et al. Loss of NFAT5 results in renal atrophy and lack of tonicity-responsive gene expression. Proc Natl Acad Sci U S A. 2004;101(8):2392–7.
271. Christoph Kuper, Franz-X. Beck, Wolfgang Neuhofer. Osmoadaptation of Mammalian Cells - An Orchestrated Network of Protective Genes. Curr Genomics. 2007;8(4):209–18.
272. Neuhofer W, Beck FX. Cell survival in the hostile environment of the renal medulla. Annu Rev Physiol. 2005;67:531–55.
273. Miyakawa H, Woo SK, Chen CP, Dahl SC, Handler JS, Kwon HM. Cis- and trans-acting factors regulating transcription of the BGT1 gene in response to hypertonicity. Am J Physiol - Ren Physiol. 1998;274(4 43-4).
274. Loyher ML, Mutin M, Woo SK, Kwon HM, Tappaz ML. Transcription factor tonicity-responsive enhancer-binding protein (tonebp) which transactivates osmoprotective genes is expressed and upregulated following acute systemic hypertonicity in neurons in brain. Neuroscience. 2004;124(1):89–104.
275. Dalski A, Wagner HJ, Schwinger E, Zühlke C. Quantitative PCR analysis of different splice forms of NFAT5 revealed specific gene expression in fetal and adult brain. Mol Brain Res. 2000;83(1–2):125–7.
276. Maouyo D, Kim JY, Lee SD, Wu Y, Woo SK, Kwon HM. Mouse TonEBP-NFAT5: Expression in early development and alternative splicing. Am J Physiol - Ren Physiol. 2002;282(5 51-5):802–9.
277. Aramburu J, Drews-Elger K, Estrada-Gelonch A, Minguillón J, Morancho B, Santiago V, et al. Regulation of the hypertonic stress response and other cellular functions by the Rel-like transcription factor NFAT5. Biochem Pharmacol. 2006;72(11):1597–604.
278. Yi MH, Lee YS, Kang JW, Kim SJ, Oh SH, Kim YM, et al. NFAT5-dependent expression of AQP4 in astrocytes. Cell Mol Neurobiol. 2013;33(2):223–32.
279. Mak KMC, Lo ACY, Lam AKM, Yeung PKK, Ko BCB, Chung SSM, et al. Nuclear factor of activated T cells 5 deficiency increases the severity of neuronal cell death in ischemic injury. NeuroSignals. 2012;20(4):237–51.
280. Shaterian A, Borboa A, Coimbra R, Baird A, Eliceiri BP. Non-invasive detection of spatio-temporal activation of SBE and NFAT5 promoters in transgenic reporter mice following stroke. Neuropathology. 2012;32(2):118–23.
281. Jeong GR, Im SK, Bae YH, Park ES, Jin BK, Kwon HM, et al. Inflammatory signals induce the expression of tonicity-responsive enhancer binding protein (TonEBP) in microglia. J Neuroimmunol [Internet]. 2016;295–296:21–9. Available from: http://dx.doi.org/10.1016/j.jneuroim.2016.04.009
282. Yang XL, Wang X, Peng BW. NFAT5 Has a job in the brain. Dev Neurosci. 2018;40(4):289–300.
283. Irarrazabal CE, Liu JC, Burg MS, Ferraris JD. ATM, a DNA damage-inducible kinase, contributes to activation by high NaCl of the transcription factor TonEBP/OREBP. Proc Natl Acad Sci U S A. 2004;101(23):8809–14.
284. Zhou X, Wang H, Burg MB, Ferraris JD. Inhibitory phosphorylation of GSK-3β by AKT, PKA, and PI3K contributes to high NaCl-induced activation of the transcription factor NFAT5 (TonEBP/OREBP). Am J Physiol - Ren Physiol. 2013;304(7):908–17.
285. Gallazzini M, Heussler GE, Kunin M, Izumi Y, Burg MB, Ferraris JD. High NaCl-induced activation of CDK5 increases phosphorylation of the osmoprotective transcription factor TonEBP/OREBP at threonine 135, which contributes to its rapid nuclear localization. Mol Biol Cell. 2011;22(5):703–14.
286. Xu SX, Wong CCL, Tong EHY, Chung SSM, Yates JR, Yin YB, et al. Phosphorylation by casein kinase 1 regulates tonicity-induced osmotic response element-binding

protein/tonicity enhancer-binding protein nucleocytoplasmic trafficking. J Biol Chem. 2008;283(25):17624–34.
287. Burg MB, Ferraris JD, Dmitrieva NI. Cellular response to hyperosmotic stresses. Physiol Rev. 2007;87(4):1441–74.
288. Irarrazabal CE, Gallazzini M, Schnetz MP, Kunin M, Simons BL, Williams CK, et al. Phospholipase C-γ1 is involved in signaling the activation by high NaCl of the osmoprotective transcription factor TonEBP/OREBP. Proc Natl Acad Sci U S A. 2010;107(2):906–11.
289. Zhou X, Gallazzini M, Burg MB, Ferraris JD. Contribution of SHP-1 protein tyrosine phosphatase to osmotic regulation of the transcription factor TonEBP/OREBP. Proc Natl Acad Sci U S A. 2010;107(15):7072–7.
290. Gallazzini M, Yu M, Gunaratne R, Burg MB, Ferraris JD. c-Abl mediates high NaCl-induced phosphorylation and activation of the transcription factor TonEBP/OREBP. FASEB J. 2010;24(11):4325–35.
291. Woo SK, Dahl SC, Handler JS, Kwon HM. Bidirectional regulation of tonicity-responsive enhancer binding protein in response to changes in tonicity. Am J Physiol - Ren Physiol. 2000;278(6 47-6):1006–12.
292. Jantsch J, Schatz V, Friedrich D, Schröder A, Kopp C, Siegert I, et al. Cutaneous Na+ storage strengthens the antimicrobial barrier function of the skin and boosts macrophage-driven host defense. Cell Metab. 2015;21(3):493–501.
293. Lee N, Kim D, Kim WU. Role of NFAT5 in the immune sustem and pathogenisis of autoimmune disease. Front Immunol. 2019;10(FEB):1–10.
294. Lee KM, Danuser R, Stein J V, Graham D, Nibbs RJ, Graham GJ. The chemokine receptors ACKR 2 and CCR 2 reciprocally regulate lymphatic vessel density . EMBO J. 2014;33(21):2564–80.
295. Graef IA, Wang F, Charron F, Chen L, Neilson J, Tessier-lavigne M, et al. Neurotrophins and Netrins Require Calcineurin / NFAT Signaling to Stimulate Outgrowth of Embryonic Axons. 2003;113:657–70.
296. Delmas P, Brown DA. Pathways modulating neural KCNQ/M (Kv7) potassium channels. Nat Rev Neurosci. 2005;6(11):850–62.
297. Manuscript A. Sympathetic Ganglion Neurons During Repetitive Action Potentials. 2011;41(6):559–71.
298. Wibrand K, Messaoudi E, Håvik B, Steenslid V, Løvlie R, Steen VM, et al. Identification of genes co-upregulated with Arc during BDNF-induced long-term potentiation in adult rat dentate gyrus in vivo. Eur J Neurosci. 2006;23(6):1501–11.
299. Yao J, Zhao Q, Liu D, Chow C, Mei Y. Neuritin Up-regulates Kv4 . 2 ⌴ -Subunit of Potassium Channel Expression and Affects Neuronal Excitability by Regulating the Calcium-Calcineurin-NFATc4 Signaling Pathway *. 2016;291(33):17369–81.
300. Amberg GC, Rossow CF, Navedo MF, Santana LF. NFATc3 regulates Kv2.1 expression in arterial smooth muscle. J Biol Chem. 2004;279(45):47326–34.
301. Nieves-Cintrón M, Amberg GC, Nichols CB, Molkentin JD, Santana LF. Activation of NFATc3 down-regulates the β1 subunit of large conductance, calcium-activated K+ channels in arterial smooth muscle and contributes to hypertension. J Biol Chem. 2007;282(5):3231–40.
302. Rossow CF, Minami E, Chase EG, Murry CE, Santana LF. NFATc3-induced reductions in voltage-gated K+ currents after myocardial infarction. Circ Res. 2004;94(10):1340–50.
303. Gong N, Bodi I, Zobel C, Schwartz A, Molkentin JD, Backx PH. Calcineurin increases cardiac transient outward K+ currents via transcriptional up-regulation of Kv4.2 channel subunits. J Biol Chem. 2006;281(50):38498–506.
304. Rossow CF, Dilly KW, Santana LF. Differential calcineurin/NFATc3 activity contributes to the Ito transmural gradient in the mouse heart. Circ Res. 2006;98(10):1306–13.

305. Keyser P, Borge-Renberg K, Hultmark D. The Drosophila NFAT homolog is involved in salt stress tolerance. Insect Biochem Mol Biol. 2007;37(4):356–62.
306. Vanschoiack LR, Shubayev VI, Myers RR, Sheets CG, Earthman JC. NIH Public Access. 2014;28(5):1286–92.
307. Livak KJ, Schmittgen TD. Analysis of Relative Gene Expression Data Using Real-Time Quantitative PCR and the 2−ΔΔCT Method. Methods [Internet]. 2001;25(4):402–8. Available from: http://linkinghub.elsevier.com/retrieve/pii/S1046202301912629
308. Quan PL, Sauzade M, Brouzes E. DPCR: A technology review. Sensors (Switzerland). 2018;18(4).
309. Wondolowski J, Dickman D. Emerging links between homeostatic synaptic plasticity and neurological disease. Front Cell Neurosci. 2013;7(NOV):1–9.
310. Small DH, Fodero LR. Cholinergic regulation of synaptic plasticity as a therapeutic target in Alzheimer's disease. J Alzheimer's Dis. 2002;4(5):349–55.
311. Dekosky ST, Ikonomovic MD, Styren SD, Beckett L, Wisniewski S, Bennett DA, et al. Upregulation of choline acetyltransferase activity in hippocampus and frontal cortex of elderly subjects with mild cognitive impairment. Ann Neurol. 2002;51(2):145–55.
312. Liu Q, Xie X, Lukas RJ, St.John PA, Wu J. A novel nicotinic mechanism underlies β-amyloid-induced neuronal hyperexcitation. J Neurosci. 2013;33(17):7253–63.
313. Dineley KT, Xia X, Bui D, David Sweatt J, Zheng H. Accelerated plaque accumulation, associative learning deficits, and up-regulation of α7 nicotinic receptor protein in transgenic mice co-expressing mutant human presenilin 1 and amyloid precursor proteins. J Biol Chem. 2002;277(25):22768–80.
314. Eadaim A, Hahm ET, Justice ED, Tsunoda S. Cholinergic Synaptic Homeostasis Is Tuned by an NFAT-Mediated α7 nAChR-Kv4/Shal Coupled Regulatory System. Cell Rep [Internet]. 2020;32(10):108119. Available from: https://doi.org/10.1016/j.celrep.2020.108119
315. Ping Y, Waro G, Licursi A, Smith S, Vo-Ba DA, Tsunoda S. Shal/Kv4 channels are required for maintaining excitability during repetitive firing and normal locomotion in Drosophila. PLoS One. 2011;6(1):15–20.
316. Chen X, Yuan LL, Zhao C, Birnbaum SG, Frick A, Jung WE, et al. Deletion of Kv4.2 gene eliminates dendritic A-type K+ current and enhances induction of long-term potentiation in hippocampal CA1 pyramidal neurons. J Neurosci. 2006;26(47):12143–51.
317. Kim J, Jung S, Clemens AM, Petralia RS, Dax A. neurons. 2008;54(6):933–47.
318. Jung SC, Hoffman DA. Biphasic somatic A-type K+ channel downregulation mediates intrinsic plasticity in hippocampal CA1 pyramidal neurons. PLoS One. 2009;4(8).
319. Sweeney ST, Broadie K, Keane J, Niemann H, O'Kane CJ. Targeted expression of tetanus toxin light chain in Drosophila specifically eliminates synaptic transmission and causes behavioral defects. Neuron. 1995;14(2):341–51.
320. Dertcher DL, Ueda A, Stewart BA, Burgess RW, Kidokoro Y, Schwarz TL. Distinct requirements for evoked and spontaneous release of neurotransmitter are revealed by mutations in the Drosophila gene neuronal- synaptobrevin. J Neurosci. 1998;18(6):2028–39.
321. Vazquez J, Pauli D, Tissières A. Transcriptional regulation in Drosophila during heat shock: A nuclear run-on analysis. Chromosoma. 1993;102(4):233–48.
322. Macián F, López-Rodríguez C, Rao A. Partners in transcription: NFAT and AP-1. Oncogene. 2001;20(19 REV. ISS. 2):2476–89.
323. Kim J, Kwon J, Kim M, Do J, Lee D, Han H. Low-dielectric-constant polyimide aerogel composite films with low water uptake. Polym J. 2016;48(7):829–34.
324. Rao A, Luo C, Hogan PG. Transcription factors of the NFAT family: Regulation and function. Annu Rev Immunol. 1997;15:707–47.
325. Masuyama K, Zhang Y, Rao Y, Wang JW. Mapping neural circuits with activity-

dependent nuclear import of a transcription factor. J Neurogenet. 2012;26(1):89–102.
326. Lonze BE, Ginty DD. Function and regulation of CREB family transcription factors in the nervous system. Neuron. 2002;35(4):605–23.
327. Solanyk E, Farmer J, Mosely N, Loving K, Kunapuli C. a Pulsed Plasma Thruster Gateway To Space Spring 2006 Design Document. Physiol Rev [Internet]. 2009;89(1):121–45. Available from: http://www.ncbi.nlm.nih.gov/pubmed/19126756%0Ahttp://www.pubmedcentral.nih.gov/articlerender.fcgi?artid=PMC3883056%0Ahttp://spacegrant.colorado.edu/COSGC_Projects/space/downloads_S06/Teams/DD_C/MASA_DDC.PDF
328. Kahl G. T ranscription f actor II E (TFIIE) . Dict Genomics, Transcr Proteomics. 2015;1–1.
329. Dyson HJ, Wright PE. Role of intrinsic protein disorder in the function and interactions of the transcriptional coactivators CREB-binding Protein (CBP) and p300. J Biol Chem. 2016;291(13):6714–22.
330. Bartel DP, Sheng M, Lau LF, Greenberg ME. Growth factors and membrane depolarization activate distinct programs of early response gene expression: dissociation of fos and jun induction. Genes Dev. 1989;3(3):304–13.
331. Sheng M, Thompson MA, Greenberg ME. CREB : A Ca $^ { 2 + } $ -Regulated Transcription Factor Phosphorylated by Calmodulin- Dependent Kinases Published by : American Association for the Advancement of Science Stable URL : https://www.jstor.org/stable/2875923 American Association for the Adva. 1991;252(5011):1427–30.
332. Dash PK, Karl KA, Colicos MA, Prywes R, Kandel ER. cAMP response element-binding protein is activated by Ca2+/calmodulin- as well as cAMP-dependent protein kinase. Proc Natl Acad Sci U S A. 1991;88(11):5061–5.
333. Yin JCP, Del Vecchio M, Zhou H, Tully T. CREB as a Memory Modulator: induced expression of a dCREB2 activator isoform enhances long-term memory in drosophila. Cell. 1995;81(1):107–15.
334. Tan P. Drug tolerance. Nurs Stand. 2002;16(30):21.
335. Kamenetz F, Tomita T, Hsieh H, Seabrook G, Borchelt D, Iwatsubo T, et al. APP Processing and Synaptic Function State University of New York at Stony Brook. Neuron. 2003;37:925–37.
336. Francisco S, Jolla L, Pharmaceuticals E, San S. Plaque-independent disruption of neural circuits in Alzheimer ' s. Neurobiology. 1999;96(March):3228–33.
337. Hsieh H, Boehm J, Sato C, Iwatsubo T, Tomita T, Sisodia S, et al. AMPAR Removal Underlies Aβ-Induced Synaptic Depression and Dendritic Spine Loss. Neuron. 2006;52(5):831–43.
338. Oddo S, Caccamo A, Shepherd JD, Murphy MP, Golde TE, Kayed R, et al. Triple-transgenic model of Alzheimer's Disease with plaques and tangles: Intracellular Aβ and synaptic dysfunction. Neuron. 2003;39(3):409–21.
339. Verderio C, Coco S, Bacci A, Rossetto O, De Camilli P, Montecucco C, et al. Tetanus toxin blocks the exocytosis of synaptic vesicles clustered at synapses but not of synaptic vesicles in isolated axons. J Neurosci. 1999;19(16):6723–32.
340. Duerkop. 基因的改变NIH Public Access. Bone. 2008;23(1):1–7.
341. Wang X, Michael McIntosh J, Rich MM. Muscle nicotinic acetylcholine receptors may mediate trans-synaptic signaling at the mouse neuromuscular junction. J Neurosci. 2018;38(7):1725–36.
342. Aizenman CD, Linden DJ. Rapid, synaptically driven increases in the intrinsic excitability of cerebellar deep nuclear neurons. Nat Neurosci. 2000;3(2):109–11.
343. Lee D, O'Dowd DK. Fast excitatory synaptic transmission mediated by nicotinic acetylcholine receptors in Drosophila neurons. J Neurosci. 1999;19(13):5311–21.

344. Alexander JK, Sagher D, Krivoshein A V., Criado M, Jefford G, Green WN. Ric-3 promotes α7 nicotinic receptor assembly and trafficking through the ER subcompartment of dendrites. J Neurosci. 2010;30(30):10112–26.
345. Lansdell SJ, Collins T, Yabe A, Gee VJ, Gibb AJ, Millar NS. Host-cell specific effects of the nicotinic acetylcholine receptor chaperone RIC-3 revealed by a comparison of human and Drosophila RIC-3 homologues. J Neurochem. 2008;105(5):1573–81.
346. Lansdell SJ, Collins T, Goodchild J, Millar NS. The Drosophila nicotinic acetylcholine receptor subunits Dα5 and Dα7 form functional homomeric and heteromeric ion channels. BMC Neurosci. 2012;13(1):1–11.
347. Keyser P, Borge-renberg K, Ã DH. The Drosophila NFAT homolog is involved in salt stress tolerance. 2007;
348. Freeman A, Franciscovich A, Bowers M, Sandstrom DJ, Sanyal S. NFAT regulates pre-synaptic development and activity-dependent plasticity in Drosophila. Mol Cell Neurosci [Internet]. 2011;46(2):535–47. Available from: http://dx.doi.org/10.1016/j.mcn.2010.12.010
349. Kojima R, Taniguchi H, Tsuzuki A, Nakamura K, Sakakura Y, Ito M. Hypertonicity-Induced Expression of Monocyte Chemoattractant Protein-1 through a Novel Cis -Acting Element and MAPK Signaling Pathways . J Immunol. 2010;184(9):5253–62.
350. Kleinewietfeld M, Manzel A, Titze J, Kvakan H, Yosef N, Linker RA, et al. Sodium chloride drives autoimmune disease by the induction of pathogenic TH 17 cells. Nature [Internet]. 2013;496(7446):518–22. Available from: http://dx.doi.org/10.1038/nature11868
351. Tubon TC, Zhang J, Friedman EL, Jin H, Gonzales ED, Zhou H, et al. dCREB2-Mediated Enhancement of Memory Formation. J Neurosci [Internet]. 2013;33(17):7475–87. Available from: http://www.jneurosci.org/cgi/doi/10.1523/JNEUROSCI.4387-12.2013
352. López-Rodríguez C, Aramburu J, Rakeman AS, Rao A. NFAT5, a constitutively nuclear NFAT protein that does not cooperate with Fos and Jun. Proc Natl Acad Sci U S A. 1999;96(13):7214–9.
353. Kel A, Kel-Margoulis O, Babenko V, Wingender E. Recognition of NFATp/AP-1 composite elements within genes induced upon the activation of immune cells. J Mol Biol. 1999;288(3):353–76.
354. Bartus, R. T., Dean, R. L., Beer, B., & Lippa, A. S. (1982). The cholinergic hypothesis OfGeriatricmemorydysfunction. *Science,217*(4558),408417. https://doi.org/10.1126/science.7046051
355. Davies P. (1983). The neurochemistry of Alzheimer's disease and senile dementia. *Medicinal research reviews*, *3*(3), 221–236. https://doi.org/10.1002/med.2610030302
356. Michael Gorczyca & Jeffrey C. Hall (1984) Identification of a Cholinergic Synapse in the Giant Fiber Pathway of *Drosophila* Using Conditional Mutations of Acetylcholine Synthesis, Journal of Neurogenetics, 1:4, 289-313, DOI: 10.3109/01677068409107093